[redacted]

Russian Original Vol. 35, No. 2, August, 1973

February, 1974

SATEAZ 35(2) 705–790 (1973)

SOVIET ATOMIC ENERGY

АТОМНАЯ ЭНЕРГИЯ

(ATOMNAYA ÉNERGIYA)

TRANSLATED FROM RUSSIAN

CONSULTANTS BUREAU, NEW YORK

SOVIET ATOMIC ENERGY

Soviet Atomic Energy is a cover-to-cover translation of *Atomnaya Énergiya*, a publication of the Academy of Sciences of the USSR.

An arrangement with Mezhdunarodnaya Kniga, the Soviet book export agency, makes available both advance copies of the Russian journal and original glossy photographs and artwork. This serves to decrease the necessary time lag between publication of the original and publication of the translation and helps to improve the quality of the latter. The translation began with the first issue of the Russian journal.

Consultants Bureau journals appear about six months after the publication of the original Russian issue. For bibliographic accuracy, the English issue published by Consultants Bureau carries the same number and date as the original Russian from which it was translated. For example, a Russian issue published in December will appear in a Consultants Bureau English translation about the following June, but the translation issue will carry the December date. When ordering any volume or particular issue of a Consultants Bureau journal, please specify the date and, where applicable, the volume and issue numbers of the original Russian. The material you will receive will be a translation of that Russian volume or issue.

Subscription
$80 per volume (6 Issues)
2 volumes per year
(Add $5 for orders outside the United States and Canada.)

Single Issue: $30
Single Article: $15

CONSULTANTS BUREAU, NEW YORK AND LONDON

227 West 17th Street
New York, New York 10011

Davis House
8 Scrubs Lane
Harlesden, NW10 6SE
England

Published monthly. Second-class postage paid at Jamaica, New York 11431.

Soviet Atomic Energy is abstracted or indexed in *Applied Mechanics Reviews, Chemical Abstracts, Engineering Index, INSPEC—Physics Abstracts and Electrical and Electronics Abstracts, Current Contents,* and *Nuclear Science Abstracts.*

SOVIET ATOMIC ENERGY

A translation of *Atomnaya Énergiya*
February, 1974

Volume 35, Number 2 August, 1973

CONTENTS

Declassified and Approved For Release 2013/01/22 : CIA-RDP10-02196R000400020002-7

CONTENTS

(continued)

The Russian press date (podpisano k pechati) of this issue was 7/20/1973. Publication therefore did not occur prior to this date, but must be assumed to have taken place reasonably soon thereafter.

DETERMINATION OF FISSION PRODUCTS IN THE WATER OF THE FIRST CIRCUIT BY GROUP CHROMATOGRAPHIC SEPARATION

L. N. Moskvin, V. S. Miroshnikov,
V. A. Mel'nikov, G. K. Slutskii,
and G. G. Leont'ev

UDC 621.039.534:543.343

One of the several possible ways of simplifying and increasing the sensitivity of radiochemical methods of monitoring the proportions of fission products in the water of the first circuit of nuclear reactions is that of chromatographic analysis. However, the choice of the best conditions for the chromatographic separation of such a mixture of elements in one sorbent is a very difficult matter. Moreover successive elutriation greatly extends the period of analysis and impedes the determination of isotopes with short half lives [1]. It is more promising to carry out a chromatographic separation in one medium using different selective sorbents. As medium for this purpose we may use dilute solutions of formic acid, in which it is easy to stabilize the ionic forms of most of the elements formed during fission [2].

This paper is devoted to studying the conditions of selectively extracting fission products from aqueous solutions and verifying the applicability of the method so developed to water samples from the first circuit of the VVR-M research reactor. As possible selective absorbents we used the following ion-exchange materials and extraction agents: anion exchange AV-17 in the HCOO' form, cation exchanger KU-2 in the $H^{\cdot}$ and $NH_4^{\cdot}$ forms, ammonium phosphoromolybdate (PMo), di-2-ethylhexylorthophosphoric acid (D2EHPA), and trioctylamine (TOA). Since the elutriation of the absorbed elements and the preparation of special sources for measuring the radioactivity would require additional time, and these operations would introduce additional errors in determining the chemical yield, we sought to prepare selective absorbents in such a form as would enable us to carry out chromatographic sorption from large volumes of solution and quantitative γ-spectrometric analysis at the same time.

Experimental Procedure

The chromatographic column consisted of several tablets of porous Teflon in series; on each of these the corresponding extraction agent or ion exchanger was deposited (Fig. 1). In order to prepare the tablets, polymerized Teflon powder was crushed to a loose state, poured into a mold, then subjected to a pressure of 350 kg/cm² for 5 min. The arrangement of the mold is shown in Fig. 2. The pressed (extruded) molding was extracted from the die, and the cavity so formed was filled with granulated Teflon having a grain size of 0.25-0.5 mm. The method of producing the granulated Teflon was described in [3]. The molding was annealed at 375-380° for 30-40 min. As a result of this annealing porous Teflon sintered to the sides of the extruded Teflon molding was formed in the cavity [4]. In order to eliminate internal stresses, the molding was held for a day at room temperature, after which the molding was machined on a lathe and tablets of the required diameter and height were produced. The internal volume of the tablets so created had a porosity of up to 60% and a low hydraulic resistance.

TABLE 1. Results of the Radiochemical Analysis of a Model Solution

Sorbent	Isotopes	Absolute activity, μCi	
		introduced	determined
TOA	I^{131}	4,51±0,62	4,81±0,69
	Mo^{99}	3,22±0,54	3,45±0,57
AV-17	—	—	—
D2EHPA	La^{140}	0,18±0,03	0,20±0,04
	Ce^{144}	0,35±0,05	0,39±0,06
PMo	Cs^{137}	1,20±0,14	1,06±0,11
KU-2	Ba^{140}	0,18±0,05	0,14±0,04

Translated from Atomnaya Énergiya, Vol. 35, No. 2, pp. 83-88, August, 1973. Original article submitted October 17, 1972.

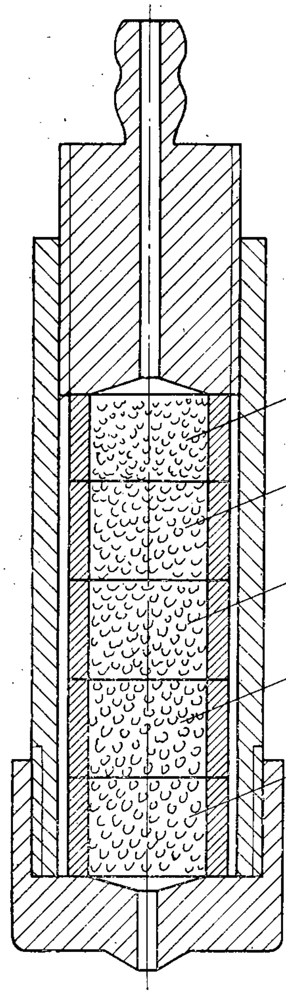

Fig. 1

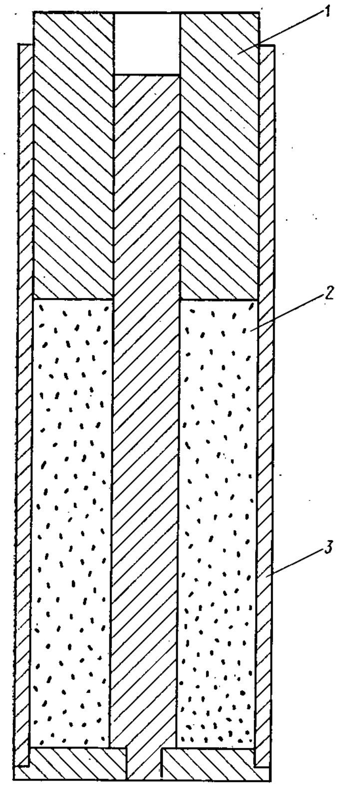

Fig. 2

Fig. 1. Arrangement of the chromatographic column with the tablets: 1) TOA; 2) AV-17; 3) D2EHPA; 4) PMo; 5) KU-2.

Fig. 2. Arrangement of mold: 1) plunger; 2) loose powder; 3) die.

The stationary organic phase was introduced into the tablets by successively washing them with the extraction agent to be employed and an aqueous solution. The volume of the retained organic phase applied to the tablet was 40% of the volume of the pores in the tablet. In order to impregnate the tablet with the solid ion exchangers, a finely-dispersed suspension (1-5 μ) of the sorbent in water was passed through it under pressure so as to create a flow rate of 50-70 ml/min$\cdot$cm^2. Filtration of the suspension was repeated two or three times until equilibrium saturation of the tablet had been achieved. In order to remove excess of sorbent the tablet was further washed with water. In order to verify the uniformity of the sorbent distribution over the height of the tablet the latter was extracted from the column and cut into layers 2-5 mm thick. The volume concentration of the ion exchange distributed in the filler was determined from the volumetric capacity of individual layers. It was found that the capacity remained almost constant over the height of the tablet. In a tablet saturated with KU-2 20 mm in height and 11.5 mm in diameter up to 0.04 g of resin was deposited.

In order to find the optimum disposition of the tablets in the chromatographic column, we determined the static distribution coefficients of I^{131}, Sr^{89}, Ba^{140}, Ce^{144}, Cs^{137}, and Mo^{99} in the system formed by the 0.1 M HCOOH and the sorbents chosen. On the basis of the resultant data we decided on the following order of disposition of the tablets in the chromatographic column with respect to the direction of flow of the solution under analysis: 1) TOA for separating iodine and molybdenum; 2) AV-17 for absorbing the unextracted anionic forms of molybdenum; 3) D2EHPA for absorbing the rare-earth elements; 4) PMo for the sorption of the heavy alkali metals; 5) KU-2 for extracting the alkaline-earth elements. The relatively

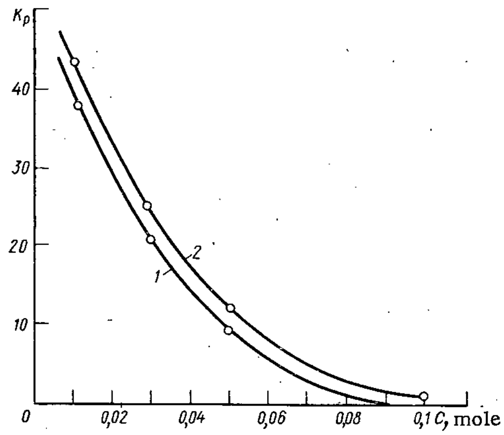

Fig. 3

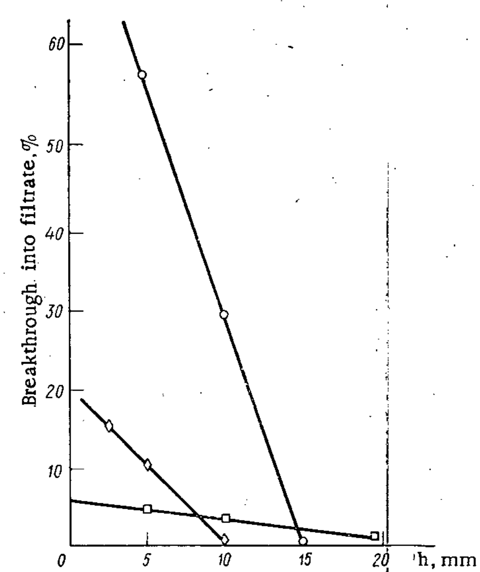

Fig. 4

Fig. 3. Relationship between the distribution coefficients K_p of strontium (1) and barium (2) in a 0.1 M HCOOH solution in ammonium phosphoromolybdate and the NH_4Cl concentration.

Fig. 4. Relationship between the breakthrough (as a percentage of the content in the original solution) and the height of the tablets h: ○) cesium in PMo; ◇) cerium in D2EHPA; □) strontium in KU-2. Solution velocity 10 ml/min · cm^2; volume of solution passed 100 ml.

TABLE 2. Results of the Radiochemical Analysis of the Water in the First Circuit of the VVR-M

Sorbent	Isotopes	Half life	Energy of ν quanta,* MeV	Yield of ν quanta,* %	Specific activity of the isotope 2 h from the moment of taking the sample, Ci/liter
TOA	I^{131}	8,14 days	0,364	78,4	$1,4\cdot10^{-6}$
	I^{132}	2,3 h	0,773	86	$7,4\cdot10^{-7}$
	I^{233}	20,7 h	0,529	94,5	$2,2\cdot10^{-6}$
	I^{135}	6,7 h	1,28	34	$2,6\cdot10^{-6}$
	Mo^{99}	66 h	0,141†	89 †	$7,5\cdot10^{-7}$
D2EHPA	Ce^{141}	33,1 days	0,145	67	$6,0\cdot10^{-8}$
	Ce^{143}	33 h	0,29	23	$5,5\cdot10^{-6}$
	La^{140}	40,2 h	1,6	95	$4,4\cdot10^{-7}$
PMo	Cs^{134}	2,04 years	0,605	98	$4,5\cdot10^{-9}$
	Cs^{137}	30 years	0,662	86	$1,1\cdot10^{-8}$
KU-2	Sr^{91}	9,67 h	0,748	27	$7,7\cdot10^{-6}$
	Sr^{92}	2,7 h	1,37	9	$2,6\cdot10^{-6}$
	Ba^{139}	82,9 min	0,167	23	$1,6\cdot10^{-5}$
	Ba^{140}	12,8 days	0,537	25	$5,2\cdot10^{-7}$

*Energy and yield per decay of the ν quanta from which the activity of the isotope was calculated.
†For Tc^{99m}.

high distribution coefficients of the alkaline-earth elements in PMo excludes the production of pure cesium specimens under the conditions of separation chosen. It is well known that the sorption of barium and strontium on PMo is weakened if ammonium salts are introduced into the original solution [5]. The relationship between the distribution coefficients of Ba^{140} and Sr^{89} and the ammonium chloride concentration obtained for PMo combined with porous Teflon (Fig. 3) shows that for an NH_4 content of 0.1 M the alkaline-earth elements are not retained in the PMo; the ammonium chloride has hardly any effect on the sorption of the other elements to be separated. It should be noted that formic acid does not guarantee the stabilization of molybdenum in a single ionic form, so that its partial passage through the TOA cannot be excluded.

The extent to which the zone containing trace amounts of the elements spreads through the layer of sorbent depends on the granular characteristics of the latter, the dimensions of the column, and the rate of flow of the solution. The use of a finely divided sorbent creates favorable conditions for absorption at higher rates of flow, since the rate of establishing equilibrium increases with diminishing particle size. The effect of the rate of flow of the solution on the breakthrough was checked for tablets 20 mm high saturated with KU-2 and PMo. In the KU-2 tablet, breakthrough started at rates above 12 ml/min · cm^2, while in the PMo tablet none was detected until reaching 50 ml/min · cm^2.

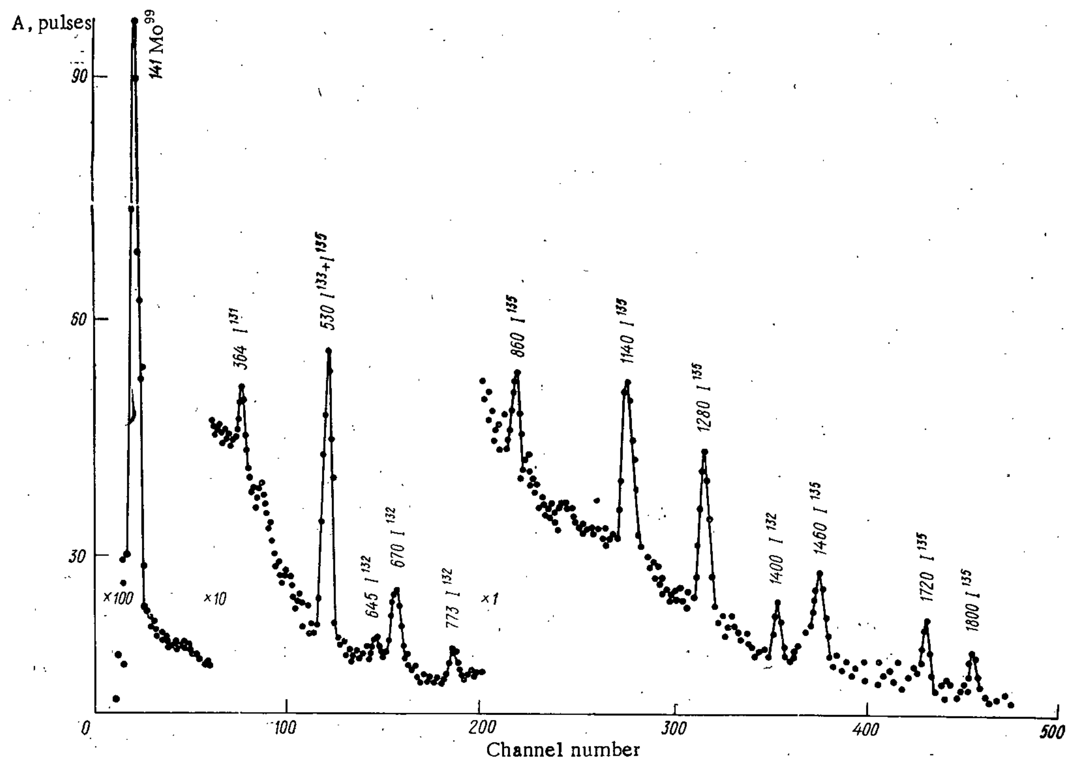

Fig. 5. Gamma spectrum of the tablet with TOA.

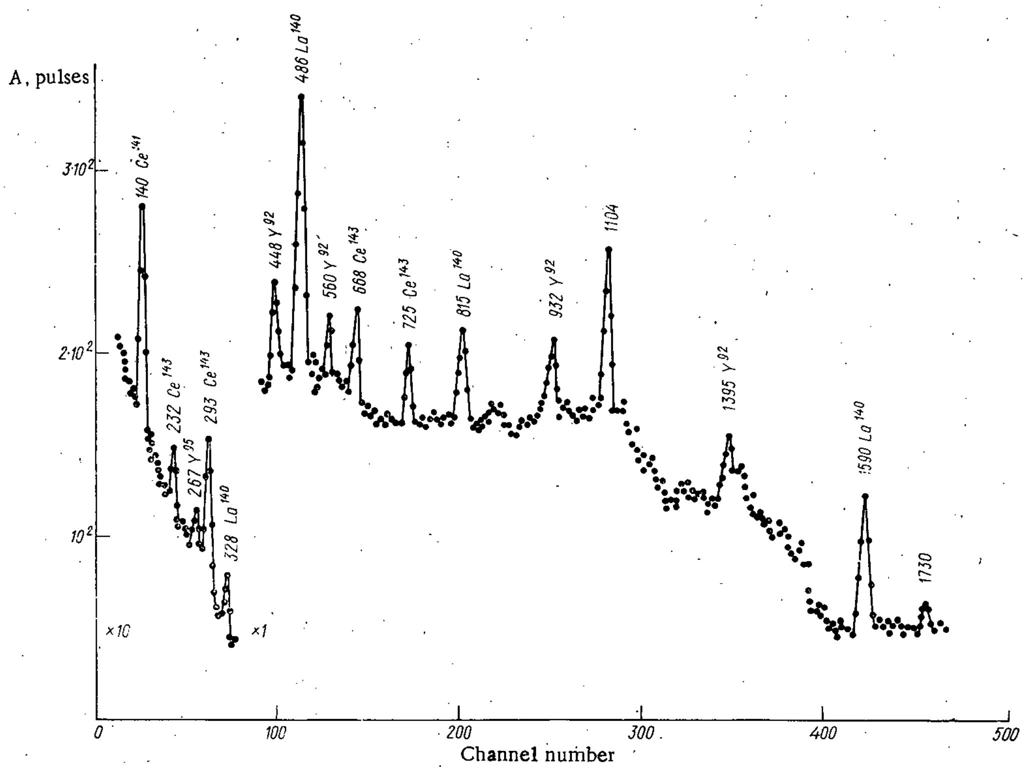

Fig. 6. Gamma spectrum of the tablet with D2EHPA.

Figure 4 shows the relation between the breakthrough and the height of the tablet; this enables us to make a direct determination of the minimum tablet dimensions required for the quantitative absorption of the element under analysis at specified rates of flow. On the basis of the data so presented we established the volume of solution to be analyzed (100 ml) and the rate of flow (10 ml/min·cm^2) for a tablet height of 20 mm and an internal diameter of 10 mm.

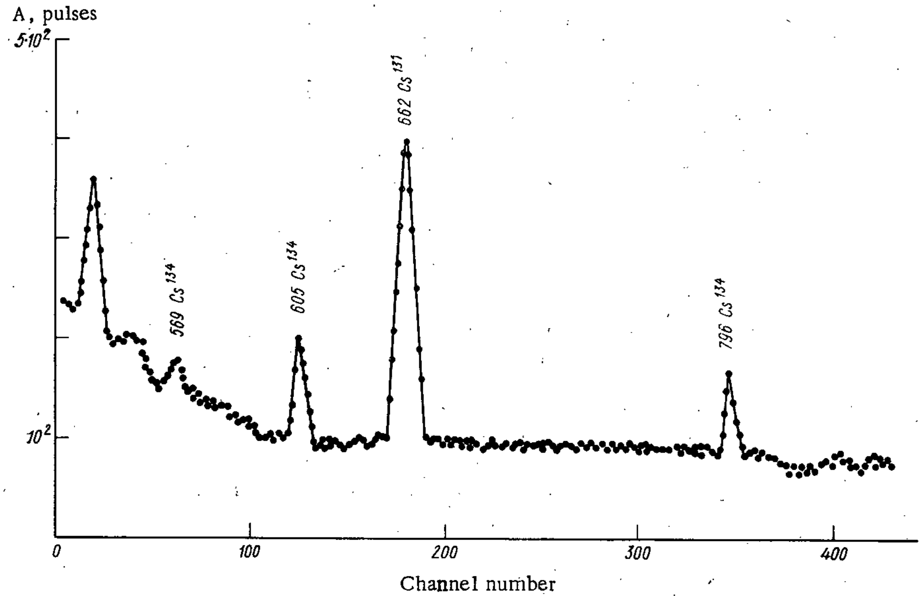

Fig. 7. Gamma spectrum of the tablet with PMo.

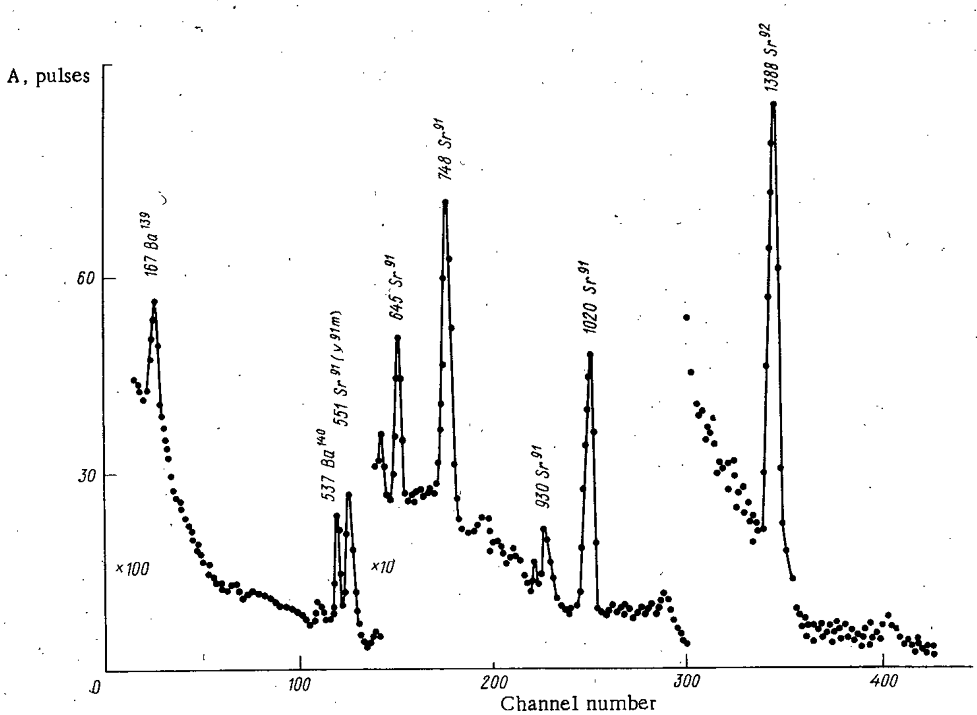

Fig. 8. Gamma spectrum of the tablet with KU-2.

The possibility of separating fission-fragment elements was verified for a model aqueous solution containing indicator quantities of I^{131}, Mo^{99}, Ba^{140}, Ce^{144}, Na^{22}, the activity of the last-named being 100 times greater than that of the other isotopes. Into the original water sample we introduced formic acid and ammonium chloride up to a concentration of 0.1 M, passed the resultant solution through the tablet-containing column, washed it with a solution of 0.1 M HCOOH + 0.1 M NH_4Cl (50 ml), and passed air through to remove the washing solution. The tablets extracted from the column were hermetically sealed and measured in a Ge(Li) γ-spectrometer using rigorous geometry. Preliminary calibration of the spectrometer with respect to efficiency was carried out on tablets having a known content of the isotopes under analysis. The results of the γ-spectrometric analysis of the individual tablets are presented in Table 1. Only Na^{22} was found in the filtrate.

The method was tested under practical conditions using water samples from the first circuit of the water-cooled, water-moderated VVR-M reactor. The analysis was conducted 6 h after taking the samples. The specific activity of the water at the moment of analysis was 10^{-4} Ci/liter. Direct γ-spectrometric identification of the isotopes of present interest was impossible since their concentrations in the samples were not mutually compatible. The results of the analyses are presented in Table 2. The data obtained in the tablet containing the AV-17 anion exchanger were not processed in view of their extremely low activity. The purity of the remaining fractions of the isotopes may be judged from their γ-spectra presented in Figs. 5-8. The analysis lasted 15-20 min from the beginning of separation to measurement. The error in the determination varied according to the energy and intensity of the characteristic photopeak; it never exceeded ±20% (relative).

The advantages of the method include its use of absorbing tablets as radiation sources of strictly specified geometry. As a result of the uncomplicated apparatus, the simplicity of the separation arrangements, and the use of readily available sorbents, this method may be employed in mass radiochemical analyses.

The authors wish to thank Yu. P. Saikov, V. A. Kochevanov, and I. S. Orlenkov most sincerely for help in this work.

LITERATURE CITED

1. Yu. N. Saikov, At. Énerg., 20, 123 (1966).
2. L. N. Moskvin and N. N. Kalinin, At. Énerg., 29, 458 (1970).
3. B. K. Preobrazhenskii and L. N. Moskvin, Radiokhimiya, 10, 373 (1968).
4. L. N. Moskvin and L. G. Tsaritsyna, Radiokhimiya, 12, 737 (1970).
5. C. Amflett, Inorganic Sorbents [Russian translation], Mir, Moscow (1966).

ITERATIVE SYNTHESIS OF SOLUTIONS OF THE NEUTRON TRANSPORT EQUATIONS

V. V. Khromov, A. M. Sirotkin, and V. A. Apsé

UDC 539.125.52:621.039.51.12

Methods for synthesizing neutron distributions based on an idea by Kantorovich [1] of reducing partial differential equations to ordinary differential equations were developed in the hope of avoiding the expenditure of large amounts of machine time and overloading the computer memory in solving multidimensional problems in neutron transport theory. A rather complete summary of the application of synthesis methods to various neutron transport problems is given in [2, 3]. In spite of important advantages synthesis methods have the disadvantage that their accuracy depends on how well intuition and experience suggest to the investigator an a priori choice of functions from which the neutron distributions in the reactor are synthesized. In addition, synthesis methods require preliminary calculations of these functions. In this sense the algorithms of synthesis methods given in [2, 3] are open. We discuss below iterative synthesis methods with closed algorithms.

Iterative Synthesis in the Class of Continuous Functions

We consider the operator form of the reactor equation:

$$\hat{L}\Phi(x, y)-\frac{1}{K_{\text{eff}}}\hat{Q}\Phi(x, y)=0, \tag{1}$$

where $\hat{L}$ is a differential operator describing neutron transport, absorption, and scattering; $\hat{Q}$ is an operator characterizing the secondary neutron sources. Let $0 \le x \le 1$ and $0 \le y \le 1$ be the range of the arguments x and y; the neutron flux must vanish on the boundary of this region.

We seek a solution of Eq. (1) in the form

$$\Phi(x, y)=\sum_{n=1}^{N}\lambda_n X_n(x)\, Y_n(y), \tag{2}$$

where $X_n(x)$ and $Y_n(y)$ are orthonormal functions which are continuous in the range of the arguments. The orthogonality and normalization conditions are

$$\begin{gathered}\{X_m(x)\, X_n(x)\}_x=\delta_{m,\,n};\\ \{Y_m(y)\, Y_n(y)\}_y=\delta_{m,\,n}.\end{gathered} \tag{3}$$

Here $\delta_{m,n}$ is the Kronecker symbol and the braces denote integration over the range of the variables x and y. We substitute (2) into (1) and weight the residual, using for simplicity the required functions $X_n(x)$ and $Y_n(y)$ as weighting functions (the Bubnov–Galerkin method). This leads to the equations

$$\sum_{n=1}^{N}\lambda_n\left[\{Y_k\hat{L}Y_n\}_y X_n(x)-\frac{1}{K_{\text{eff}}}\{Y_k\hat{Q}Y_n\}_y X_n(x)\right]=0; \tag{4}$$

$$\sum_{n=1}^{N}\lambda_n\left[\{X_k\hat{L}X_n\}_x Y_n-\frac{1}{K_{\text{eff}}}\{X_k\hat{Q}X_n\}_x Y_n(y)\right]=0. \tag{4a}$$

Translated from Atomnaya Énergiya, Vol. 35, No. 2, pp. 89–93, August, 1973. Original article submitted July 21, 1972.

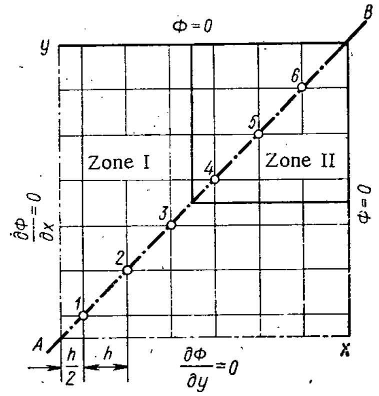

Fig. 1

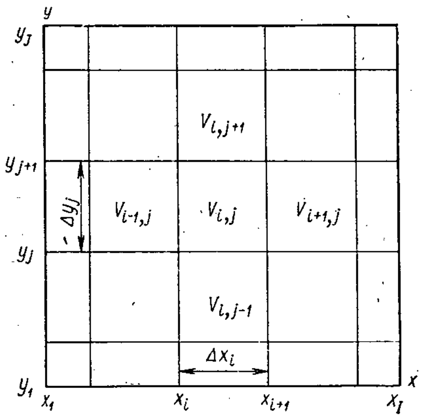

Fig. 2

Fig. 1. Finite-difference mesh for a reactor with a cross-shaped core.

Fig. 2. Scheme for dividing a reactor into subregions when the variables are separable.

We solve Eqs. (4) and (4a) subject to the boundary conditions

$$X_n(0) = X_n(1) = 0; \quad Y_n(0) = Y_n(1) = 0; \\ n = 1, 2, \ldots, N. \tag{5}$$

We consider an iterative method for solving Eqs. (4) and (4a). We choose N linear independent functions $Y_n^{(0)}$ and construct the operators of Eq. (4). We solve this equation for the functions $\xi_n^{(0)} = \lambda_n^{(0)} X_n^{(0)}$ corresponding to the largest eigenvalue $K_{eff}^{(1)}$. This gives the first approximation $\Phi^{(1)}(x, y)$ for the neutron flux

$$\Phi^{(1)}(x, y) = \sum_{n=1}^{N} \xi_n^{(0)}(x) Y_n^{(0)}(y), \tag{6}$$

where the $\xi_n^{(0)}(x)$ are not necessarily orthonormal functions. We transform Eq. (6) to the form

$$\Phi^{(1)}(x, y) = \sum_{n=1}^{N} \lambda_n^{(1)} X_n^{(1)}(x) Y_n^{(1)}(y), \tag{7}$$

where the $X_n^{(1)}(x)$ and $Y_n^{(1)}(y)$ are sets of orthonormal functions. It can be shown that this transformation is possible and the functions $X_n^{(1)}(x)$ and $Y_n^{(1)}(y)$ can be expressed in terms of the $Y_n^{(0)}(y)$ and $\xi_n^{(0)}(x)$ by the equations

$$X_n^{(1)}(x) = \frac{1}{\lambda_n^{(1)}} \sum_{k=1}^{N} a_{k,n} \xi_k^{(0)}; \\ Y_n^{(1)}(y) = \sum_{k=1}^{N} a_{k,n} Y_k^{(0)}, \tag{8}$$

where the $a_{k,n}$ are the components of the orthonormal eigenvectors a_n of the symmetric matrix A the components A_{ij} of which are given by

$$A_{ij} = \{\xi_i^{(0)}(x)\, \xi_j^{(0)}(x)\}_x; \quad i, j = 1, 2, \ldots, N. \tag{9}$$

The numbers $(\lambda_n^{(1)})^2$ are the eigenvalues of matrix A. Using the values found for the $X_n^{(1)}(x)$ we construct the operators of Eq. (4a) and solve it for $\eta_n(y) = \lambda_n Y_n(y)$ to find the second approximation for the effective multiplication factor $K_{eff}^{(2)}$ and the neutron flux $\Phi^{(2)}(x, y)$ in the form

$$\Phi^{(2)}(x, y) = \sum_{n=1} X_n^{(1)}(x) \eta_n^{(1)}(y). \tag{10}$$

Using the method described above we transform Eq. (10) to the form (2) etc.

As an example of the iterative algorithm described above, we consider a calculation in the one-group diffusion approximation of a reactor with a cross-shaped core. A schematic diagram of one quarter of this reactor is shown in Fig. 1. This method was applied to the finite-difference analog of the diffusion equation

TABLE 1. Values of K_{eff} and the Neutron Flux Φ_i along the Diagonal AB of a Cross-Shaped Reactor

Calculation	K_{eff}	Value of Φ_i for i equal to					
		1	2	3	4	5	6
For $N=1$	0,8969	1,000	0,796	0,473	0,167	0,052	0,010
For $N=2$	0,9996	1,000	0,844	0,561	0,110	0,014	0,001
Exact	1,0000	1,000	0,847	0,558	0,110	0,014	0,001

TABLE 2. Properties of a Five-Zone Slab Reactor

Properties	Zone No.		
	I, V	II, IV	III
Σ_1	1,0	1,0	5,0
Σ_2	0,5	4,0	0,0
Thickness, cm	0,5	0,14	0,1

with 6 × 6 internal points for a constant pitch h = 1.549. The parameters of core zone I ($D = 1$, $\Sigma_{c,f} = 0.5$, $\nu_f\Sigma_f = 0.1137$) and reflector zone II ($D = 1$, $\Sigma_{c,f} = 1.5$, $\nu_f\Sigma_f = 0$) were chosen so that $K_{eff} = 1$ for the exact solution of the finite difference analog of the diffusion equation. Table 1 shows the results of the calculation of this reactor by the method of iterative synthesis for one and two terms in Eq. (2).

As is shown in Table 1, for N = 2 the results obtained by iterative synthesis hardly differ from the exact results. The iterative synthesis method proposed is free of a fault inherent in the method discussed in [4, 5]: the iterative process used in those papers can become unstable and lead to a linear dependence in the systems of functions $X_n(x)$ and $Y_n(y)$. In addition our method permits an estimate of the accuracy of the solution from the way that the numbers λ_n vary with n.

Iterative Synthesis in the Class of Discontinuous Functions

The iterative synthesis algorithm in the class of discontinuous functions is constructed in the following way. The range of the arguments of the neutron flux distribution function is divided into a series of nonoverlapping subregions. Discontinuities in the functions $X_n(x)$ and $Y_n(y)$ may occur at the bonding surfaces of these subregions. The accuracy of the solution can be improved either by increasing the number N of terms in series (2) or by increasing the number of subregions for a fixed N.

We discuss two examples of iterative synthesis methods in the class of discontinuous functions.

Iterative Synthesis when the Variables are Separable. The iterative synthesis algorithm is simplest when only one term of series (2) is retained in each subregion and the neutron flux is written in the form

$$\Phi(x, y) = X(x)\,Y(y).$$

Closed iterative algorithms for the synthesis of the spatial, angular, and energy distributions of neutrons, based on the separation of variables in the neutron flux function in the various subregions of the arguments of this function, have been proposed in [6-8].

As an example of the algorithm of the synthesis method in the class of discontinuous functions we discuss the calculation of the distribution of the flux and importance of the neutrons in a two-dimensional reactor. We divide the reactor volume $V(0 \le x \le 1,\ 0 \le y \le 1)$ into zones $V_{ij} = \Delta x_i y_j$ ($V = \sum_i \sum_j V_{ij}$) by the coordinate surfaces $x = x_i$, $y = y_j$ ($i = 1, 2, \ldots, I$; $j = 1, 2, \ldots, J$) in accord with the scheme shown in Fig. 2. In each zone V_{ij} we represent the neutron flux $\Phi(x, y)$ and the importance $\Phi^+(x, y)$ in the form

$$\Phi_{ij}(x, y) = X_{ij}(x)\,Y_{ij}(y);\quad \Phi^+_{ij}(x, y) = X^+_{ij}(x)\,Y^+_{ij}(y);\quad i = 1, 2, \ldots, I+1;\quad j = 1, 2, \ldots, J+1. \tag{11}$$

When the variables are separable it is convenient to derive the equations for the functions X_{ij}, Y_{ij}, X^+_{ij}, and Y^+_{ij} and the continuity conditions at the zone boundaries from a variational formulation of the problem, by requiring a certain functional to remain stationary when the functions $\Phi(x, y)$ and $\Phi^+(x, y)$ are varied. This functional is generally formed by using Lagrangian multipliers to add to the functional determining the K_{eff} of the reactor the conditions for joining the solutions for the neutron flux and importance at the zone boundaries when the variables are separable. By substituting trial functions in the form (11) into the functional and requiring it to be stationary when the functions $X(x)$, $Y(y)$, $X^+(x)$, and $Y^+(y)$ are varied, we obtain a complete set of equations

$$\hat{l}_{ij}X_{ij} - \frac{1}{K_{eff}}\hat{q}_{ij}X_{ij} - \hat{\alpha}_{ij}X_{i,\,j-1} - \hat{\beta}_{ij}X_{i,\,j+1} = 0; \tag{12a}$$

$$\hat{p}_{ij}Y_{ij} - \frac{1}{K_{eff}}\hat{r}_{ij}Y_{ij} - \hat{\mu}_{ij}Y_{i-1,\,j} - \hat{\nu}_{ij}Y_{i+1,\,j} = 0; \tag{12b}$$

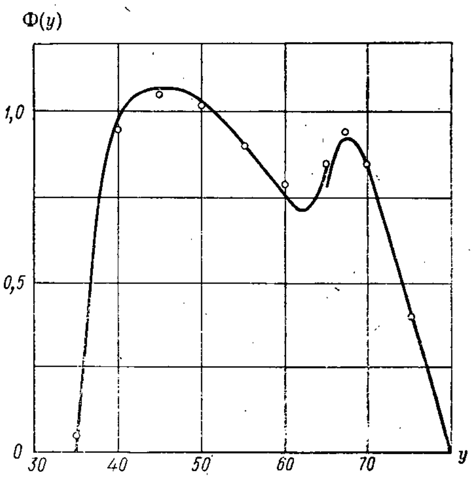

Fig. 3

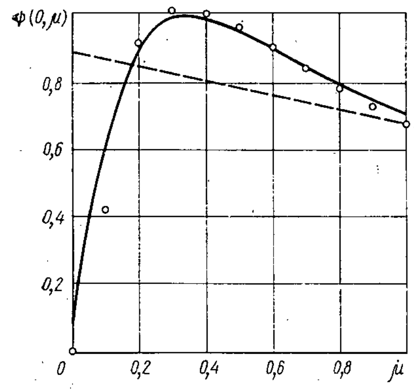

Fig. 4

Fig. 3. Neutron flux distribution in a reactor [9] computed by an exact method (○) and by iterative synthesis (——).

Fig. 4. Angular distribution of neutrons at the center of a slab reactor in various approximations: – – –) DP_1 approximation; ○) DP_9 approximation (exact); ——) iterative synthesis method.

$$\hat{l}^+_{ij}X^+_{ij} - \frac{1}{K_{eff}}\hat{q}^+_{ij}X^+_{ij} - \hat{\alpha}^+_{ij}X^+_{i,\,j-1} - \hat{\beta}^+_{ij}X^+_{i,\,j+1} = 0; \quad (12c)$$

$$\hat{p}^+_{ij}Y^+_{ij} - \frac{1}{K_{eff}}\hat{r}^+_{ij}Y^+_{ij} - \hat{\mu}^+_{ij}Y^+_{i-1,\,j} - \hat{\nu}^+_{ij}Y^+_{i+1,\,j} = 0. \quad (12d)$$

Here the operators $\hat{l}$, $\hat{q}$, $\hat{\alpha}$, and $\hat{\beta}$ ($\hat{l}^+$, $\hat{q}^+$, $\hat{\alpha}^+$, and $\hat{\beta}^+$) are bilinear functionals of Y and Y^+, and the operators $\hat{p}$, $\hat{r}$, $\hat{\mu}$, and $\hat{\nu}$ ($\hat{p}^+$, $\hat{r}^+$, $\hat{\mu}^+$, and $\hat{\nu}^+$) are bilinear functionals of X and X^+, where $\hat{l}$ and $\hat{l}^+$ are differential operators with respect to x, and $\hat{p}$ and $\hat{p}^+$ with respect to y. The conditions for the joining of the solutions of Eqs. (12a) and (12c) at $x = x_i$, and Eqs. (12b) and (12d) at $y = y_j$ also follow from the requirement that the functional be stationary. It should be noted that in the variational formulation of Eqs. (12) the choice of the Lagrangian multipliers in the initial functional is indeterminate [3]. In the iterative synthesis algorithm these multipliers are chosen so as to ensure that the operators $\hat{\alpha}$, $\hat{\beta}$ ($\hat{\alpha}^+$, $\hat{\beta}^+$) and $\hat{\mu}$, $\hat{\nu}$ ($\hat{\mu}^+$, $\hat{\nu}^+$) describing the exchange of neutrons between adjacent zones are positive definite. In this way the solutions of Eqs. (11) turn out to be positive.* The iterative process of solving Eqs. (12) results in a sequence of solutions of the equations of this system. At each step of the iteration the operators of Eqs. (12) are recalculated.

Based on the algorithm described above a program called RADAR was written in FORTRAN for a BÉSM-6 computer. This program permits the calculation of the neutron flux and importance in a two-dimensional reactor in the multigroup diffusion approximation. The main features of the program are the following: there can be up to 26 energy groups; there can be up to 100 nodes in the finite-difference mesh for solving Eqs. (12); there can be no more than 36 zones with separable variables.

As an illustration of the method, we consider the previous example of the calculation of the two-dimensional reactor referred to in [9]. The effective neutron multiplication factor of this reactor K_{eff} calculated by the RADAR program turned out to be 1.02, which agrees with the value obtained with the two-dimensional finite-difference mesh with 40 × 40 nodes. Figure 3 shows the thermal neutron flux distribution at x = 21 cm (cf. [9]) obtained by solving the two-dimensional finite-difference equation and by iterative syntheses with 3 × 3 zones with separable variables. In spite of the discontinuities in the neutron flux obtained by iterative synthesis the integral characteristics of the neutron distribution are calculated with high accuracy in all reactor zones.

Calculation of the Spatial–Angular Distribution of Neutrons. We illustrate the method of iterative synthesis by solving the transport equation in a five-zone slab reactor with the zone properties listed in

* The explicit form of the operators of Eqs. (12) and the method of choosing the multipliers are discussed in [8] by calculating a two-dimensional reactor in the diffusion approximation.

Table 2:

$$\mu \frac{\partial \Phi(x, \mu)}{\partial x} + \Sigma_1 \Phi(x, \mu) = \frac{1}{K} \Sigma_2 \int_{-1}^{1} d\mu' \Phi(x, \mu'). \tag{13}$$

We divide the range of the angular variable $-1 \leq \mu \leq 1$ into two subregions $-1 \leq \mu < 0$ and $0 < \mu \leq 1$ and consider the case when the neutron flux $\Phi(x, \mu)$ in each reactor zone and in each subregion of μ can be represented by two terms $(N = 2)$ of series (2), where $y \equiv \mu$.

The equations of the iterative synthesis method and the joining conditions for the solutions were obtained from the condition that the functional determining the eigenvalue K of the problem remain stationary. Trial functions for the neutron importance $\Phi^+(x, \mu)$ were chosen in each zone and each subregion of μ in the form

$$\Phi^+(x, \mu) = X_1^+(x) + \mu X_2^+(x) + Y_1^+(\mu) + x Y_2^+(\mu).$$

The equations for the functions $X_1(x)$, $X_2(x)$, $Y_1(\mu)$, and $Y_2(\mu)$ and the joining conditions for the functions $X_1(x)$ and $X_2(x)$ at the zone boundaries where the trial function has a discontinuity were obtained from the condition that the functional be stationary for variations of the functions $X_1^+(x)$, $X_2^+(x)$, $Y_1^+(\mu)$, and $Y_2^+(\mu)$. Solving the equations by the iterative method, we find the spatial distribution of neutrons in the reactor and the parameter K. We list below the values of K for the five-zone slab reactor:

Approximation	Value of K
DP_1	0.9198
DP_9	1.0243
Synthesis	1.0203
Exact	1.0227

Figure 4 shows the angular distribution of the neutron flux at the center of the zone III for $0 < \mu \leq 1$ obtained by the synthesis method and by solving Eq. (13) in the DP_1 and DP_9 approximations.

Analysis of the results shows that the iterative synthesis method gives high accuracy in comparison with the DP_1 approximation and is close to the DP_9 method for 200 spatial nodes. The DP_9 results are taken as exact.

In conclusion we note that the iterations of the iterative synthesis method as a rule converge rather rapidly and agree with the source iterations used to determine K_{eff}. In this way iterative synthesis methods shorten the calculation time by a factor of about five, depending on the kind of problem being solved, and decrease the load on the computer memory in comparison with finite-difference methods of solving multidimensional problems.

LITERATURE CITED

1. L. V. Kantorovich and V. I. Krylov, Approximate Methods of Higher Analysis [in Russian], Fizmatgiz, Moscow (1962).
2. S. Kaplan, "Synthesis method in reactor analysis," in: Advances in Nuclear Science and Technology (1966), p. 233.
3. S. Kaplan, ibid. (1969), p. 183.
4. I. Toivanen, J. Nucl. Energy, 22, 283 (1968).
5. M. Lansfield, Nucl. Sci. and Engng., 37, 423 (1969).
6. V. V. Khromov and A. M. Kuz'min, Atomnaya Énergiya, 21, 406 (1966).
7. V. V. Khromov and I. S. Slesarev, Atomnaya Énergiya, 19, 540 (1971).
8. V. V. Khromov and I. S. Slesarev, Atomnaya Énergiya, 30, 296 (1971).
9. S. Kaplan, Nucl. Sci. and Engng., 13, 22 (1962).

ESTIMATE OF THE APPLICABILITY OF THEORY TO THE PROBLEM OF THE PENETRATION OF A CHARGED PARTICLE THROUGH A LAYER

A. A. Belyaev and A. I. Krupman

UDC 539.124.17

Ordinarily the measurable spectral characteristics of the flux of charged particles scattered in a layer are interpreted and estimated by using distributions obtained along the path of the particle in an infinite medium [1-6]. The use of these distributions is proper for sufficiently high energies E and for thicknesses t permitting the use of the small-angle approximation in the theory of multiple scattering [2, 4, 7]:

$$10^2 T(T+2) > \frac{t}{\lambda} > 20, \tag{1}$$

where $T = E/mc^2$ and λ is the mean free path between elastic collisions.

For $T \leq 0.2$ and $t \approx 100\lambda$ the condition for the applicability of the theory is no longer satisfied. Therefore the physical accuracy of the theory in this range is appropriately estimated by using the Monte Carlo method since it can take account of the effect of boundaries, large-angle scattering, and range straggling in the calculations of angular, radial, and energy distributions of particles which have penetrated the layer.

A calculational scheme was proposed in [8] for simulating individual collisions of a particle with a scattering center. In contrast with the broadly applicable schemes of the grouping of collisions [9-11], this scheme does not use the results of multiple scattering theory or the continuous slowing down approximation.

The systematic error in simulating the trajectory of a particle in the individual collisions scheme is determined solely by the differential interaction cross sections. In order to compare the experimental data with the results of theoretical calculations we estimate the limits of applicability of the theory in problems of electron transport through a layer. We present an algorithm for the simulation of an electron trajectory and discuss the results obtained.

The Monte Carlo Algorithm

In the energy range under consideration, the total cross section for the interaction of electrons with atoms of the scatterer is

$$\sigma_t = \sigma_{el} + \sigma_{inel}, \tag{2}$$

where σ_{el} is the elastic scattering cross section; σ_{inel}, the inelastic scattering cross section, is equal to the sum of the excitation cross section σ_{ex} and the ionization cross section σ_i. The elastic scattering differential cross section $d\sigma_{el}/d\Omega$, where Ω is the solid angle, is taken as the Rutherford cross section with Molière screening [2] or with screening obtained from experimental data [12]. The differential ionization cross section $d\sigma_i/d\varepsilon$ is taken as the Mott expression [13]:

$$\frac{d\sigma_i}{d\varepsilon} = \frac{2\pi e^4 EZ}{mv^2}\left[\frac{1}{\varepsilon^2} + \frac{1}{(E-\varepsilon)^2} - \frac{1}{\varepsilon(E-\varepsilon)}\right], \tag{3}$$

where ε is the loss of energy of the outgoing electron with energy E, $\varepsilon_1 \leq \varepsilon \leq E/2$; ε_1 is the value of the average ionization potential I; e, m, and v are respectively the charge, mass, and velocity of the electron.

σ_{inel} has been measured in our energy range for a number of elements [12, 14]. In the absence of experimental data, the expression for σ_{inel} obtained from the Thomas–Fermi model [15] can be used. The value of σ_{ex} is uniquely determined from σ_{inel} and σ_i.

Translated from Atomnaya Énergiya, Vol. 35, No. 2, pp. 95-100, August, 1973. Original article submitted October 2, 1972.

Taking into account that, in collisions with the excitation of atoms, electrons are scattered through an angle θ_{ex} which is small in comparison with the scattering angles in elastic collisions [16] and lose energy $\Delta E_{ex} \ll E$, it can be assumed in the proposed model that

$$\theta_{ex} = \langle\theta^2\rangle^{1/2}, \tag{4}$$

where $\langle\theta^2\rangle$ is the mean square scattering angle in collisions with excitation, selected from experimental data or on the basis of calculations in [15].

The value of ΔE_{ex} is assumed equal to

$$\Delta E_{ex} = \left(\frac{dE}{dx}\right)_{\varepsilon<\varepsilon_1} \Big/ N\sigma_{ex}, \tag{5}$$

where

$$\left(\frac{dE}{dx}\right)_{\varepsilon<\varepsilon_1} NZ\frac{2\pi e^4}{mv^2}\left[\ln\frac{4mc^2E}{I^2} + \ln(1-\tau)^2\tau + \frac{\tau}{1-\tau}\right] \tag{6}$$

is the average rate of loss to excitation; $\tau = \varepsilon/E$; N is the number of atoms per unit volume. The limits of applicability of the model in question are discussed below.

Collisions of electrons with atoms of an amorphous scatterer are statistically independent, the probability of their occurrence being proportional to the path length. Therefore the trajectory of a particle can be chosen in the following order.

The path length l between collisions of an electron with atoms is chosen from a Poisson distribution $\exp(-lN\sigma_t)$. The probability that these collisions are elastic is σ_{el}/σ_t; the probability that they are inelastic is $1-\sigma_{el}/\sigma_t$. If the collision is elastic a scattering angle is chosen from the distribution $(d\sigma_{el}/d\Omega)/\sigma_{el}$ and the direction of motion of the electron is changed. In an inelastic collision, with probability $\sigma_{ex}/\sigma_{inel}$ the energy of the electron is decreased by ΔE_{ex} and the electron is changed in direction by $\langle\theta_{ex}\rangle$, or with probability σ_i/σ_{inel} the energy loss ε is chosen from the distribution $(d\sigma_i/d\varepsilon)/\sigma_i$ and the corresponding scattering angle θ ($\sin\theta = \sqrt{\varepsilon/E}$) is determined from the kinematics of the scattering process. This process is continued until the particle crosses the boundaries of the layer or is absorbed. The particle is considered absorbed if its energy is less than $E_{lim} \approx 10$ keV.

Organization of the Calculational Process

On the basis of the algorithm formulated a program of individual collisions was written in FORTRAN. The calculations were performed at the Latvian State University computing center. In various versions $(2\text{-}5)\cdot 10^3$ trajectories were simulated.

We note that the Monte Carlo method does not furnish the density of the distribution of a random quantity but its integral characteristics: the probability $P(0<\xi<x) = \int_0^x f(t)dt$, the moments of the distribution of a random quantity $\langle x^n\rangle = \int_0^\infty t^n f(t)dt$, the histogram $H(x_i<\xi<x_{i+1}) = \int_{x_i}^{x_{i+1}} f(t)dt$, etc. In our case, such quantities are the energy loss Δ in the layer, the angle of emergence θ with respect to the Z axis, and the transverse displacement ρ of the particle in the XOY plane. The coordinate system is chosen with its origin at a point monodirectional source and its Z axis in the direction of incidence of the electron beam on the scatterer. In certain cases, when accuracy permitted, the spectral characteristics were obtained by differentiating the integral curves P(x). In the remaining cases the integral curves and moments were used for comparison and analysis of the distributions.

The angular, energy, and radial distributions were calculated simultaneously for the layer and for a fixed path length equal to the layer thickness (~50 collisions). A correlated calculation permitted an increase in the accuracy of determining the relative changes in similar distributions for the layer and path length. These changes could be estimated by performing calculations only for normal incidence of the beam.

Analysis of the Stability of the Physical Model and Its Agreement with Theory

The main approximations of the model relate to the excitation cross section. We discuss how they limit the range of its applicability.

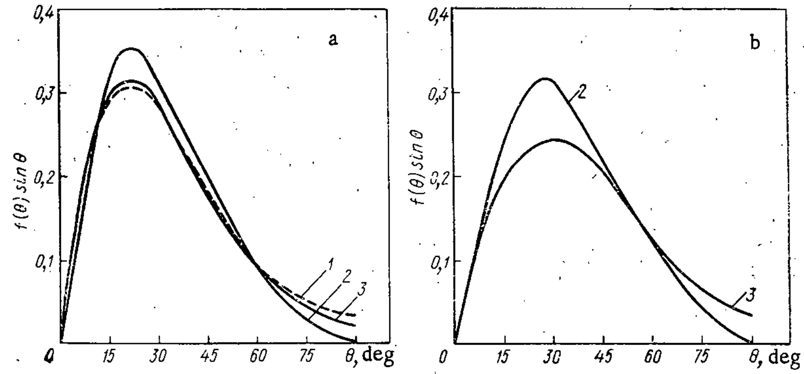

Fig. 1. Angular distributions of 62.5-keV electrons for: a) Z = 29; b) Z = 79. 1) Goudsmit–Sanderson distribution A(θ, s) · sin θ; 2, 3) the distributions A(θ, t) sin θ and A(θ, s) sin θ, respectively, obtained in the individual collision model.

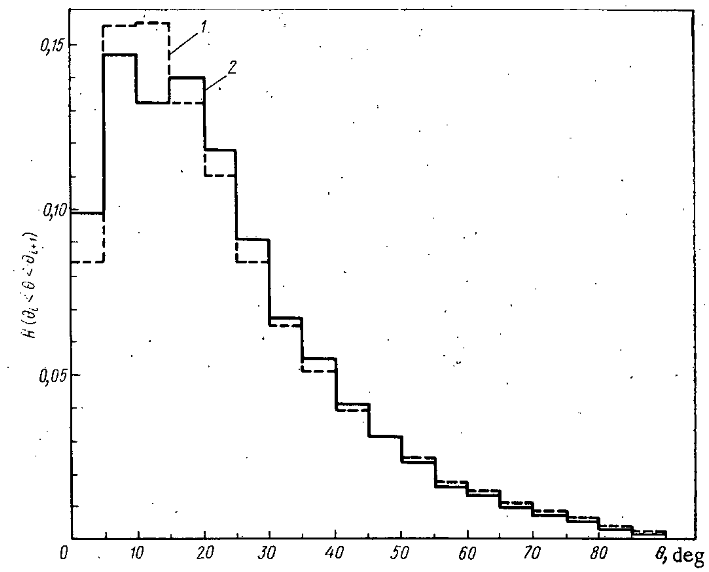

Fig. 2. Histogram of the angular distributions of 20-keV electrons. 1) Histogram constructed from experimental data of [18]; 2) calculated histogram [8].

The angular distribution of multiply scattered electrons is insensitive to the behavior of the scattering cross section in the range of small angles ($\leq 10^{-3}$ rad) [3], and varies slowly with energy [3, 4]. Therefore use of the assumption of a constant scattering angle θ_{ex} in excitation and a fixed energy loss ΔE_{ex} is justified when $\theta_{ex} \ll 1$ and $\Delta E_{ex}/E \ll 1$. Consequently the effect of fluctuations of θ_{ex} and ΔE_{ex} on the angular distribution can be neglected.

It is clear from Fig. 1 that, within the limits of error of the calculation, the simulated angular distribution of electrons which have traversed a path length s is in good agreement with the corresponding Goudsmit–Saunderson distribution calculated by the method given in [17].

Figure 2 compares the angular distribution obtained experimentally by Cosslett and Thomas [18] with that calculated by our method. These distributions agree within the limits of statistical error.

As regards the energy loss distribution Δ, the restrictions on the magnitude of the fluctuation of ΔE_{ex} becomes important as the foil thickness (path length) decreases, since excitation losses then contribute more to the energy loss spectrum. Since Landau [5] made this same assumption about ΔE_{ex} we can use his estimate of the minimum path length s_{min} for which the fluctuation of the excitation losses can be neglected in comparison with the ionization losses

$$s_{min} = 6.5 \frac{IA}{Z} \cdot \frac{\beta^2}{\rho},$$

where ρ is the density, g/cm^3; and I is the ionization potential, MeV.

TABLE 1. Moments of the Energy M_E^i, Angular M_A^i, and Radial M_ρ^i Distributions along a Path s and for the Penetration of Particles through a Layer of Thickness t

Moment i	t						s					
	Cu			Au			Cu			Au		
	M_E^i	M_A^i	M_ρ^i	M_E^i	M_A^i	M_ρ^i	M_E^i	M_A^i	M_ρ^i	M_E^i	M_A^i	M_ρ^i
1	$0{,}530 \times 10^{-2}$	0,821	0,132	$0{,}103 \times 10^{-1}$	0,770	$0{,}829 \times 10^{-1}$	$0{,}472 \times 10^{-2}$	0,739	0,242	0,789	0,633	0,290
2	$0{,}332 \times 10^{-4}$	0,704	$0{,}279 \times 10^{-1}$	$0{,}134 \times 10^{-3}$	0,634	$0{,}108 \times 10^{-1}$	$0{,}275 \times 10^{-4}$	0,652	$0{,}862 \times 10^{-1}$	$0{,}703 \times 10^{-4}$	0,548	0,117
3	$0{,}331 \times 10^{-6}$	0,620	$0{,}789 \times 10^{-2}$	$0{,}231 \times 10^{-5}$	0,542	$0{,}185 \times 10^{-2}$	$0{,}316 \times 10^{-6}$	0,553	$0{,}388 \times 10^{-1}$	$0{,}830 \times 10^{-6}$	0,440	$0{,}577 \times 10^{-1}$
4	$0{,}770 \times 10^{-8}$	0,555	$0{,}267 \times 10^{-2}$	$0{,}543 \times 10^{-7}$	0,476	$0{,}384 \times 10^{-3}$	$0{,}915 \times 10^{-8}$	0,506	$0{,}204 \times 10^{-1}$	$0{,}170 \times 10^{-7}$	0,400	$0{,}323 \times 10^{-1}$

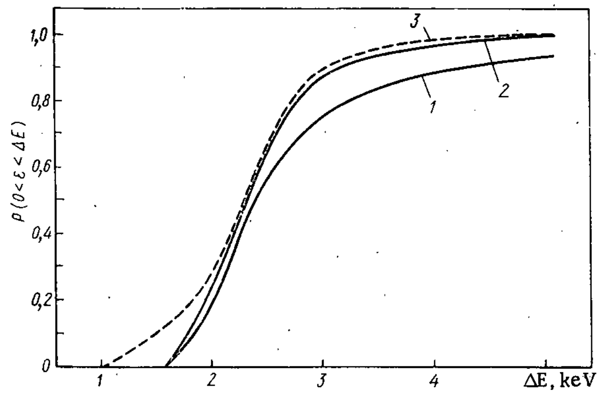

Fig. 3. Integral curves for electrons with E = 62.5 keV. 1) Curve calculated by Landau [5]; 2) curve calculated by Symon [6]; 3) our curve.

In order to make a proper comparison with the Landau distribution of energy losses further restrictions must be introduced: 1) the probability of an energy loss ε per unit length of path $w(E, \varepsilon) = w(E_0, \varepsilon)$, where E_0 is the initial energy of the particle; 2) the distribution of ionization energy losses is described by the classical formula $w \sim 1/\varepsilon^2$. Symon [6] performed a more accurate calculation without employing the first restriction. Our program permits the calculation of the energy loss distribution for a fixed path length, taking account of both restrictions, taking account only of the second, or taking account of neither.

Figure 3 compares the Monte Carlo integral curves with those of Landau (1) and Symon (2) for a path length longer than s_{min} for 62.5-keV electrons. Within the limits of statistical error our results agree with the corresponding theoretical curves. Taking account of the accurate cross section (3) increases the asymmetry of the distribution (cf. curve 3) in comparison with Symon's curve.

An estimate was made of the sensitivity of the angular and energy distributions to the parameters of the physical model used. To do this the quantities ε_1, σ_{ex}, characterizing the excitation loss (6), and the screening parameter η in the elastic scattering cross section (1) were varied. Changing σ_{ex} and η by an amount equal to the order of the experimental error (~30%) and changing ε_1 several hundred percent led to distributions which agreed within the limits of statistical error.

Analysis of the Results

Angular Distributions. Goudsmit and Saunderson [1] obtained angular distributions $A_{GS}(s, \theta)$ of scattered electrons along the path s in an infinite medium. In their method the presence of boundary conditions in general prevents the convolution of angular distributions after n successive collisions and the application of their result to the problem of the penetration of a particle through a layer. The effect of boundaries can be neglected only for sufficiently thin layers, when the small-angle approximation is valid, and for negligible range straggling.

Goudsmit and Saunderson proposed to take account of the spatial distribution of ranges by introducing the simple correction $t' = t/\langle\cos\theta\rangle$, where $\langle\cos\theta\rangle$ is the value of $\cos\theta$ averaged over the $A_{GS}(s = t, \theta)$ distribution.

Yakovlev and Girin [19] proposed an algorithm for calculating the angular distribution of particles by taking into account successively the distribution of ranges in the small-angle approximation.

Considerable mathematical difficulties prevented their taking into account large-angle scattering.

The angular distribution of particles penetrating a layer of thickness t can be written in the form

$$A_n(t, \theta) = \int_t^\infty \varphi(s, t) A(s, \theta)\, ds,$$

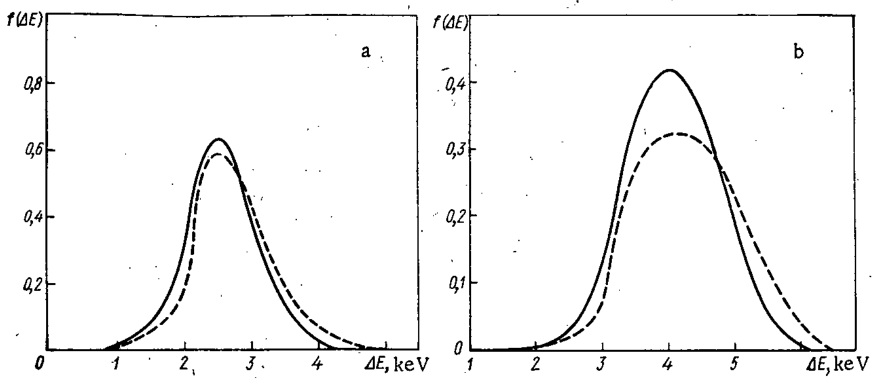

Fig. 4. Distribution of energy losses for electrons with E = 62.5 keV for: a) copper; b) gold. ——) $f(\Delta E, s)$; – – –) $f(\Delta E, t)$.

where $\varphi(s, t)$ is the distribution of ranges in the layer; $A(s, \theta)$ is the angular distribution of particles traversing a path length s and emerging from the layer. This distribution is narrower than the corresponding $A_{GS}(s, \theta)$ distribution since $A(s, \theta)$ can be obtained by the convolution of the angular distributions in successive collisions along paths corresponding to particles leaving the layer. It can be seen from (7) that the effect of boundaries is manifested in two competing factors: in the broadening of the $A_n(t, \theta)$ distribution in comparison with $A_{GS}(s, \theta)$ due to range straggling, and in the narrowing of the distribution as a consequence of the decrease in the domain of integration in the convolution. This is confirmed by the behavior of curve 2 in Fig. 1. The result obtained shows the inadequacy of the correction $t' = t/\langle\cos\theta\rangle$ which does not take account of the completeness of the correlation between the angular distribution and the thickness of the layer, and uses the value of $\langle\cos\theta\rangle$ from the $A_{GS}(t = s, \theta)$ distribution.

Radial Distribution. In [20] Fermi showed that the radial distribution of electrons is Gaussian in the small-angle approximation. Table 1 lists the moments of the radial distribution. The nonvanishing of the third moment of the radial distribution shows that the shape of the distribution in the layer is not Gaussian.

Spectrum of Energy Losses. For the distribution of energy losses in the layer it is important to take account only of range straggling

$$F(\Delta, t) = \int_t^\infty f(\Delta, s)\,\varphi(s, t)\,ds, \tag{8}$$

where $f(\Delta, s)$ is the distribution of energy losses Δ along the path s. It was assumed in [5, 6] that $\varphi(s, t)$ has the form $\delta(s - t)$, and consequently

$$F(\Delta, t) = f(\Delta, s = t). \tag{8'}$$

Yang [21] proposed to take account of the distribution of ranges by introducing the effective thickness

$$t_{\text{eff}} = t\left(1 + \frac{\langle\theta^2\rangle_t}{2}\right), \tag{9}$$

where $\langle\theta^2\rangle_t$ is the mean square angle of scattering at the end of the path s = t. We note that (9) is equivalent to the correction $(t' = t/\langle\cos\theta\rangle)$.

The results (Fig. 4) show that condition (8') is violated in successively taking into account range straggling. In this case the asymmetry of the distribution is increased because of the increase in the probability of large energy losses. The change in shape of the spectrum is illustrated by the values of the moments listed in Table 1.

CONCLUSIONS

By using our method of simulating an electron trajectory we have investigated the effect of boundaries on the spectral characteristics of electron fluxes penetrating a layer. The following results have been obtained:

1. It has been shown to be possible to use the Monte Carlo method to estimate physical information obtainable by using approximate solutions of the kinetic equations in problems of charged particle transport.

2. An algorithm has been formulated for simulating individual interactions of an electron with a scattering atom in a simple physical model which permits an estimate of the effect of boundaries and range straggling on the spectral characteristics of fluxes penetrating a layer of material.

3. Taking boundary conditions successively into account appreciably deforms the angular distribution of electrons penetrating a layer in comparison with the Goudsmit–Saunderson distribution. It is shown that the small-angle correction is not correct in this case.

4. Calculations of the moments of the radial distribution show that the commonly used assumption of a Gaussian distribution in the energy range under consideration (20-60 keV) is not realized.

5. Taking account of range straggling in the penetration of a charged particle through a layer deforms the spectrum of energy losses in comparison with theory [5, 6] as a consequence of the increase in the fraction of large losses.

All the results obtained, based on a simple physical model, are quite general and do not involve further assumptions of the nature of the model.

The authors thank T. I. Ovsyannikov for help with the calculations.

LITERATURE CITED

1. S. Goudsmit and J. Saunderssoñ, Phys. Rev., 57, 24 (1940); 58, 36 (1940).
2. G. Molière, Z. Naturforsch., 2a, 133 (1947); 3a, 78 (1948).
3. H. Bethe, Phys. Rev., 89, 1256 (1953).
4. H. Snyder and W. Scott, Phys. Rev., 76, 220 (1949); W. Scott, Rev. Mod. Phys., 36, 231 (1963).
5. L. D. Landau, J. Phys. USSR, 8, 204 (1944).
6. K. Symon, Thesis, Harvard University (1948).
7. E. Williams, Proc. Roy. Soc. (London), A169, 531 (1939); Phys. Rev., 58, 292 (1940).
8. A. A. Belyaev and A. I. Krupman, Atomnaya Énergiya, 25, 222 (1968).
9. M. Berger, Methods in Computational Physics, Vol. 1, Academic Press, New York (1963), p. 135.
10. D. Schneider and D. Cormack, Rad. Res., 11, 418 (1959).
11. H. Meister, Z. Naturforsch., 13a, 809 (1959).
12. W. Hilgner and J. Kessler, Z. Physik, 187, 119 (1965).
13. N. Mott, Proc. Camb. Phys. Soc., 27, 511 (1931).
14. A. Rauth and J. Simpson, Rad. Res., 22, 643 (1964).
15. L. Bewilogua, Physik. Z., 32, 740 (1931).
16. F. Lenz, Z. Naturforsch., 9a, 185 (1954).
17. L. Spencer, Phys. Rev., 98, 1597 (1955).
18. V. Cosslett and R. Thomas, Brit. J. Appl. Phys., 15, 883 (1964).
19. L. G. Yakovlev and I. A. Girin, Izv. Akad. Nauk SSSR, 30, 1986 (1966).
20. E. Fermi, Rev. Mod. Phys., 13, 241 (1941).
21. C. Yang, Phys. Rev., 84, 599 (1951).

NEW PROCEDURE AND EQUIPMENT FOR IN-PILE RESEARCH ON A SET OF PHYSICOMECHANICAL PROPERTIES OF A MATERIAL

Yu. V. Miloserdin, V. M. Baranov, A. V. Rimashevskii, and V. N. Kakurin

UDC 620.179.16:621.039.553

Measurements carried out directly in the reactor are of special interest in investigations of the effects of neutron radiation on the physicomechanical properties of reactor materials, because of the partial or total disappearance of the effects caused by the radiation after the exposure has been terminated [1, 2]. In most experiments involving the study of effects of neutron flux on materials, however, the properties of specimens before and after the radiation exposure are compared, in view of the technical difficulties attendant upon in-pile measurements. These difficulties can be overcome by resort to the method of ultrasonic spectroscopy of materials; the essentials of that method and different means of its implementation are discussed in [3-7]. The authors reported earlier [8] on the application of this method to an investigation of the elasticity and internal friction constants in in-pile irradiation. The procedure and the equipment described below make it possible to make measurements of the constants of elasticity, internal friction, and long-term static hardness of structural materials and fissionable materials in the core of a nuclear reactor. The temperature of the specimen is determined by the degree of heating up of the specimen when bombarded by radiation. The essence of the method for making the measurements consists in determining the spectrum of resonance frequencies of forced oscillations of the specimens and calculating the variables to be studied in terms of the characteristics of that spectrum. The resonance frequencies of the specimens are then used to find the elastic constants, and the internal friction constants are found from the width of the resonance peaks, while the shift in one of the resonance frequencies in response to indentation of the specimen by a hard-tipped indentor (Vickers pyramids) gives the hardness of the material.

The principles underlying the measurements are explained in Fig. 1. The specimen of test material 1, in the form of a thin round platelet (diameter ~20 mm, thickness ~3 mm) rests on three supports formed by sharp-tipped rods 2, 3, and 4. Rods 3 and 4 simultaneously serve as sound conductors transmitting ultrasonic vibrations. Excitation of vibrations in the specimen is achieved via the sound conductor 3 with the aid of the piezoelectric emitter 5, which is positioned outside the reactor core, and the vibrations are recorded via sound conductor 4 with the aid of a piezoelectric pickup device 6. The generator of high-frequency electrical oscillations 7, the frequency meter 8, the amplifier for electrical signals from the piezoelectric pickup 9, and the recording instrument (vacuum-tube voltmeter) 10 are kept in a laboratory room where normal operating conditions are maintained.

The effect of sound conductors on the results of the measurements has been studied by various authors [3-8]; it has been shown that errors caused by those conductors can be effectively minimized. Consequently, radiation-induced changes in the material comprising the sound conductors have no effects on the results of the measurements, and using the system in question it is possible to carry out measurements sufficiently precise for comparatively minor radiation effects on the specimen to be investigated.

The resonance frequencies of the specimen are found from the abrupt rise in the voltmeter readings. The width of the resonance curve is found by means of several measurements of the amplitude of the oscillations near the selected resonant frequency. The rod 1 tipped by the sapphire Vickers pyramid 12 is lowered to strike the specimen in order to determine the hardness of the specimen, and the change in

Translated from Atomnaya Énergiya, Vol. 35, No. 2, pp. 101-104, August, 1973. Original article submitted July 27, 1972; revision submitted Janaury 31, 1973.

TABLE 1. Coefficients for Calculating the Parameters of the Specimen Vibrations

σ	h/d	K	A	α	β	N_0
0,1	0,05	0,1802	−0,0234	4,485	4,349	0,2124
	0,10	0,3314	−0,0307	4,472	3,992	0,2061
	0,15	0,4459	−0,0428	4,457	3,537	0,1978
	0,20	0,5283	−0,0601	4,435	3,056	0,1890
0,2	0,05	0,1841	−0,0225	4,503	4,358	0,2120
	0,10	0,3378	−0,0297	4,495	3,984	0,2056
	0,15	0,4532	−0,0414	4,486	3,511	0,1974
	0,20	0,5357	−0,0582	4,471	3,015	0,1882
0,3	0,05	0,1900	−0,0218	4,520	4,363	0,2109
	0,10	0,3474	−0,0288	4,519	3,967	0,2045
	0,15	0,4641	−0,0405	4,516	3,470	0,1962
	0,20	0,5467	−0,0566	4,508	2,954	0,1880
0,4	0,05	0,1986	−0,0211	4,538	4,363	0,2103
	0,10	0,3609	−0,0283	4,542	3,936	0,2035
	0,15	0,4793	−0,0398	4,548	3,408	0,1951
	0,20	0,5620	−0,0550	4,546	2,867	0,1880

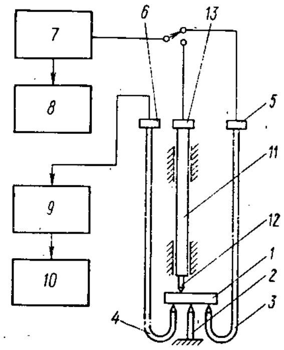

Fig. 1. Layout of experimental arrangement.

resonant frequency caused by the indentation of the pyramid is recorded. The excitation of the specimen is brought about by the piezoelectric transducer 13 working through the rod 11 and the Vickers pyramid 12.

The procedure developed for calculating the elastic constants from the resonant frequencies of specimens shaped as round platelets has been discussed in detail elsewhere [7]. Since the change in the elastic modulus E (or the change in the shear modulus G, which is practically the same) is of interest for in-pile measurements, it is sufficient to note that the elastic modulus E is proportional to the square of the resonant frequency f_{res}. And hence the values of E and f_{res} are related to the corresponding values of the variables prior to the irradiation, E_0 and f_{res0}, by the formula $E/E_0 = (f_{res}/f_{res0})^2$. The internal friction factor Q^{-1} is determined from the formula $Q^{-1} = \Delta f_{0.7}/f_{res}$, where $\Delta f_{0.7}$ is the width of the resonance curve at the level of the piezoelectric pickup signal, constituting $1/\sqrt{2} = 0.707$ of the maximum signal level when the instrument is tuned to resonance [9].

The procedure for determining hardness calls for a separate discussion. Methods of the theory of perturbations [10] have been used, showing that the change in the natural frequency of vibration of the platelet in flexural vibrations caused by contact with the sharp-tipped rods is expressed by the formula

$$\frac{\Delta f_{res}}{f_{res}} = \frac{1}{4\pi^2 \sqrt{\pi} N_0 \rho h f_{res}^2} \sum_{i=1}^{m} \frac{\sqrt{S_{ci}}\, w^2(r_i, \varphi_i)}{\left(\frac{1-\sigma^2}{E} + \frac{1-\sigma_{0i}^2}{E_{0i}}\right)}, \tag{1}$$

where Δf_{res} is the change in the natural (resonant) frequency; ρ, σ, E are the density, Poisson ratio, and elastic modulus of the material comprising the specimen; h is the thickness of the specimen; m is the number of points in contact; S_{ci} is the area of the projection of the surface of the i-th contact onto the flat face of the test specimen; r_i, φ_i are the polar coordinates of the point of contact reckoned from the center of the test specimen; σ_{0i}, E_{0i} are the Poisson ratio and elastic modulus of the rod material contacting the test specimen at the i-th point; $w(r, \varphi)$ is a function characterizing the distribution of vibrations over the surface of the platelet; $N_0 = \int_S w^2 dS$ (where S is the surface of the platelet).

If the supports are placed near the nodes of the vibrations, the effect of the supports on the resonant frequency and on the width of the resonance curve can be neglected [11]. The indentor, on the other hand, should be driven onto the specimen in an area corresponding to an antinode of the vibrations. Under these conditions, and recalling that the Vickers hardness HV is related to S_c by the formula $HV = F \sin\beta / S_c$ (where F is the applied load; and 2β is the angle at the apex of the pyramid), there is no difficulty in obtaining, from Eq. (1), the formula

$$HV = \frac{w^4(r, \varphi) F \sin\beta}{16\pi^5 N_0^2 \rho^2 h^2 f_{res}^2 \Delta f_{res}^2 \left(\frac{1-\sigma^2}{E} + \frac{1-\sigma_0^2}{E_0}\right)^2}. \tag{2}$$

The discussion of the distributions of amplitudes of vibrations for different resonant frequencies attests to the feasibility of using frequencies characterized by the presence of a single nodal circle to determine hardness. That frequency can be calculated on the basis of the formula

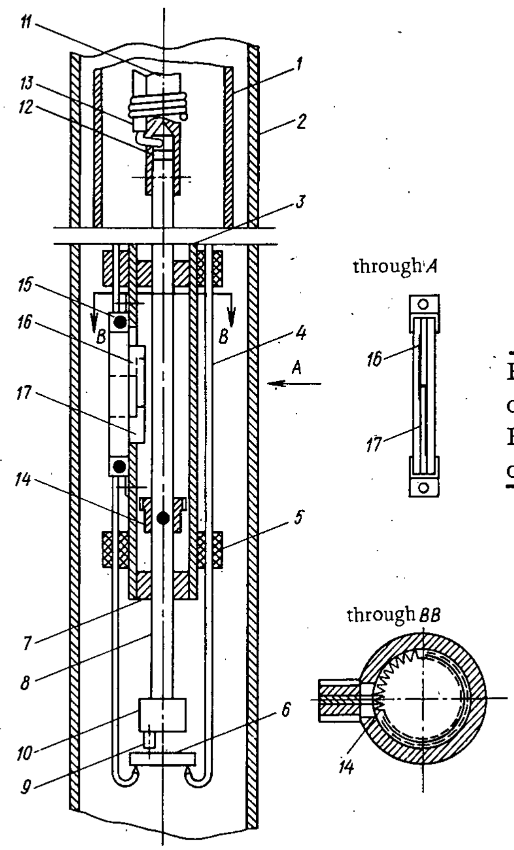

Fig. 2. Design of measuring assembly of arrangement (cross section through BB shown on scale enlarged by a factor of two).

$$f_{\mathrm{res}} = \frac{K}{d}\sqrt{\frac{E}{\rho}}, \tag{3}$$

where K is a numerical coefficient; and d is the diameter of the test specimen. The function $w(r, \varphi)$ exhibits the form

$$w(r, \varphi) = \left[J_1\left(\alpha \frac{r}{a}\right) + AI_1\left(\beta \frac{r}{a}\right)\right] \cos\varphi, \tag{4}$$

where J_1 and I_1 are first-order Bessel functions; α and β are coefficients; $a = d/2$ is the radius of the test specimen. In the arrangement described for exciting the specimen, $\cos\varphi = 1$, and all of the quantities figuring in Eq. (2) can be found with the aid of tabular data reflecting the results of calculations of the parameters A, α, β, K, and N_0 on an M-220 computer, using the most exact theory of flexural vibrations of round plates [7]. The results of calculations of the natural frequencies and of the distribution of the amplitude of vibration over the surface of the plate agree closely with available experimental data [11]. It turns out that the distribution is characterized by a smooth maximum at $r = 0.4a$, and by a nodal circle at $r = 0.78a$. This decides the choice of the position for the supports and indentor relative to the center of the test specimen.

The design of the measuring arrangement implementing the principles outlined was developed expressly for one of the research channels of the IRT-2000 reactor, with an internal diameter 52 mm, and to produce maximum neutron flux to $2 \cdot 10^{13}$ neutrons/cm^2 · sec. The arrangement is suspended from the bottom of a standard shielding plug positioned in the top of the channel. The electrical conductors are run through a groove in the plug, and on through the channel flange onto the top platform of the reactor. Before the measurements are started, the channel is evacuated and then filled with helium. The design of the capsule and specimen is shown in Fig. 2. The load-carrying part of the structure is the stainless steel tube 1 extending about 0.5 m in length and fastened to the top mounting flange of the arrangement (not shown in Fig. 2), which is suspended by a cable from the shielding plug 2 of the channel. Connection with the molybdenum tube 3, on which the measuring assembly is mounted, is made in the bottom via an adapter ring (not shown in Fig. 2). The molybdenum sound conductors, 2 mm in diameter, are held fast in fluorocarbon bushings 5, and the bottom ends of the sound conductors double as mountings for the test specimen 6. For simplicity, the third support is left out of Fig. 2. This support consists of a rod of the same sort as the sound conductors, though of shorter length. The test specimen does not rest directly on this support, but rather on the junction of a Chromel–Alumel thermocouple the insulating bushing of which is rigidly hinged to the support. As a result contact is made between the thermocouple and the test specimen without the introduction of any additional error into the results of the ultrasonic measurements. Wire limit stops are fitted onto the sound conductors in the immediate vicinity of the test specimen in order to keep the specimen in place and to prevent it from moving about. The length of the tube 3 and of the sound conductors 4 is about 1.5 m, which is adequate for the TsTs-19 piezoceramic transducers mounted on the top ends of the sound conductors, when conditions are close to normal. The piezoelectric transducers are 3 mm in diameter and 20 mm high. Centering bushings 7 in which the molybdenum rod 8 with pyramid 9 press-fitted in an adapter cylinder 10 moves back and forth are set in the tube 3. The rod 8, about 1.5 m in length, has its top part held fast in the steel rod 11, the top of which passes through a solenoid. The system is raised and lowered by adjusting the current flowing through the solenoid. The voltage is supplied to the piezoelectric emitter 12 via the high-frequency cable 13.

The indentor is moved relative to the test specimen by rotating the gear 14 with the aid of the part 15 set in a notch of tube 3, and shown separately; this facilitates action by the indentor striking the specimen at different specified points. The gear-rotating part contains flexible spring-loaded bronze plates 16 and 17, the stems of which are compressed between bolted-down gaskets. When the rod 8 is raised, one of the gearteeth falls between the plates and passes between them without rotating, so that the plate 17 is bent, since the top end of plate 16 exerts comparatively great resistance to bending because of the presence of the stem. When the rod is lowered, plates 16 and 17 are compressed together, as they lie between two teeth of the gear 15. Since the bottom end of plate 17 is sufficiently rigid in flexure, the geartooth follows the bend, thereby rotating the gear and the rod 8. In this way, the indentor moves on a circle 8 mm in diameter through an angle $(360/p)^\circ$, where $p = 32$, i.e., the number of teeth in the gear, as the rod is raised and lowered.

The accuracy with which the resonant frequencies are measured on the arrangement described here is about 0.03% over the entire range of working temperatures (up to 600°C); this has been confirmed by repeated measurements and by comparison of the results obtained with published data [12]. Consequently, changes in elastic modulus can be determined to within ~0.06%. The absolute values of the elastic modulus are calculated from results of measurements of the resonant frequencies accurate to within ~1%, and of the Poisson ratio accurate to within 4%. The accuracy with which internal friction is determined is equal to the accuracy with which the width of the resonance curve is measured, viz. 7-8%; the accuracy with which the temperature of the test specimen is determined is ±10°C.

Experimental verification of Eq. (2) on a scaled-up model of the arrangement, using specimens of materials 40 mm in diameter and 5 mm thick with precisely known properties and dimensions, showed that the predicted values (based on ultrasonic measurements data) and the experimental data (based on the dimensions of impressions) differ by not more than 3%. Similar investigations carried out on the facility described, over the entire range of working temperature (to 600°C), using specimens of M3 copper 20 mm in diameter and 3 mm in thickness, led to error values as great as 6%. Analysis of Eq. (2) shows that the principal components of the error are:

a) the error in the determination of the frequency increment under load Δf_{res}; when $\Delta f_{res} \approx$ 1-2 kHz, $f_{res} \approx 50$ kHz (the order of magnitude of the variables dealt with in the experiment) and the accuracy of the determination of the frequency (0.03%) runs from 0.75 to 1.5%, which yields a 1.5 to 3% contribution to the error;

b) the error in the determination of the elastic constants E and E_0 (~1%), which makes a contribution of about 4%;

c) the error due to the change in the point of penetration of the indentor relative to the center of the specimen; this error can be safely neglected for the selected frequency of measurements with the principal maximum of the distribution of amplitudes of vibrations.

The remaining errors make an insignificant contribution, amounting to about 1% when the specimens are fabricated with care. Consequently, the maximum error in the hardness determination is 6-8%, which is in agreement with the above error for copper. The error in the determination of the change in hardness relative to the initial value depends primarily on the accuracy with which Δf_{res} is measured, and amounts to 1.5-3%.

Prereactor investigations are being carried out with a view to obtaining more representative data on radiation effects on the material in this facility. The arrangement is suspended in a vacuum chamber made from a fragment of tube about 2 m long with a Nichrome heater in the bottom. Helium evaporated from a Dewar flask with liquefied gas blown through the tube after the preliminary evacuation. This permits measurements at a temperature of about −200°C. Then the supply of gas is gradually cut off, the temperature rises, the system heating the specimen is switched on as positive temperatures are attained, and measurements are carried out at higher temperatures.

A similar procedure makes it possible to carry out an impressive program of research on the physicomechanical properties of reactor materials on one facility, using specimens of small dimensions and simple configuration.

LITERATURE CITED

1. S. T. Konobeevskii, Effect of Radiation on Materials [in Russian], Atomizdat, Moscow (1967).
2. D. M. Skorov, Yu. F. Bychkov, A. I. Dashkovskii, and V. V. Chepkunov, Reactor Materials Studies [in Russian], Atomizdat, Moscow (1968).
3. V. M. Baranov, Sixth All-Union Acoustics Conference, Preprint CIV-3-4 [in Russian], Moscow (1968).
4. Yu. V. Miloserdin and V. M. Baranov, in: Methods for Investigating Refractory Materials [in Russian], Atomizdat, Moscow (1970), p. 61.
5. V. M. Baranov and Yu. V. Miloserdin, Inzh.-Fiz. Zh., 20, 737 (1971).
6. B. F. Anufriev, V. M. Baranov, and Yu. V. Miloserdin, Zavod. Lab., 37, 977 (1971).
7. V. M. Baranov, Zavod. Lab., 38, 1120 (1972).
8. V. M. Baranov and A. V. Rimashevskii, Seventh All-Union Acoustics Conference (Abstracts of Papers) [in Russian], Leningrad (1971), p. 204.
9. W. Mason (editor), Physical Acoustics. Vol. 1. Methods and Techniques in Ultrasonic Research [Russian translation], Part A, Mir, Moscow (1966), p. 363.
10. F. Morse and H. Feshback, Methods of Theoretical Physics [Russian translation], Vol. 1, IL, Moscow (1958).
11. V. M. Baranov, V. S. Vasil'kovskii, and Yu. V. Miloserdin, Seventh All-Union Acoustics Conference (Abstracts of Papers) [in Russian], Leningrad (1971), p. 99.
12. V. M. Baranov, O. S. Korostin, and Yu. V. Miloserdin, Zavod. Lab., 38, 1143 (1972).

TESTING NEW SORBENTS FOR THE PURIFICATION OF LIQUID WASTES WITH A LOW LEVEL OF RADIOACTIVITY

F. V. Rauzen and N. P. Trushkov

UDC 621.039.7:66.074.7

A method of purification of liquid wastes with a low level of radioactivity, based on the principle of complete desalting of the solutions, has been developed and introduced in the Soviet Union. Although solutions can be freed of radioactivity to the currently acceptable concentrations (CAC) with the aid of this method, it has a number of shortcomings; one of them is the need to reprocess a large volume of regeneration solutions if the content of salts in the initial solutions exceeds 0.5-1 g/liter.

At the last symposium of the International Atomic Energy Agency on the reprocessing of wastes with a low level of radioactivity (1970), Van de Voorde suggested the replacement of high-molecular synthetic ion-exchange resins by partially sulfurated bitumen and various inorganic sorbents [1].

In this work we verify the possibility of using partially sulfurated bitumen for the purification of solutions with a low level of radioactivity. A sorbent close in property to that proposed by Van de Voorde was prepared from brand BN-4 bitumen. The following solutions, simulating the compositions of liquid wastes, were freed of cesium and strontium radioisotopes on this sulforated bitumen: 1) waters of the Atomic Center in Mola (with which Van de Voorde worked), containing about 100 mg/liter of salts; 2) solutions from the Moscow Purification Station (MSO), containing about 0.7 g/liter; 3) solutions with a large salt content (up to 2 g/liter).

The results obtained are presented in Figs. 1 and 2 and in Table 1. From Fig. 1 it is evident that the volumes of the solutions described by us and by Van de Voorde were approximately the same. On our partially sulfurated bitumen there is a more complete purification from cesium and somewhat less complete purification from strontium than on the bitumen prepared by Van de Voorde. From the results presented in Fig. 2 and in Table 1, it is evident that the capacity of partially sulfurated bitumen is 0.9-1.2 meq/g. The duration of purification of the solution from isotopes of strontium, yttrium, and calcium ions is the same, while that from cesium isotopes is 10 times lower.

The coefficients of purification of the solutions from radioisotopes of strontium, yttrium, and cesium are 100 at the beginning of the filtration cycle, but then drop to 10.

For a final evaluation of the possibility of using partially sulfurated bitumen, we compared its sorption properties with the synthetic cation-exchange resin KU-2 in the Na-form. The bitumen sorbent can be used once, after which it should be melted into blocks with an addition of fresh bitumen. The cation-exchange resin KU-2 can be used repeatedly, and solutions of acids are used for desorption, while solutions of alkali or salts are used to regenerate its properties. It is suggested that the regenerates obtained in this case be evaporated, and the still residues bitumenized. The comparative volumes of waste products that can be obtained using partially sulfurated bitumen and the cation-exchange resin KU-2 are presented in Table 2. It is evident that the use of partially sulfurated bitumen in place of the cation-exchange resin KU-2 leads to an increase in the volume of wastes.

Comparative data on the purification of solutions on partially sulfurated bitumen and the cation-exchange resin KU-2 are cited in Fig. 3. They show that not only a more prolonged, but also a more profound purification of the solution from radioisotopes is achieved on the cation-exchange resin KU-2 than on partially sulfurated bitumen. Thus, purification using partially sulfurated bitumen does not lead to a reduction of the volume of wastes, causes a decrease in the purification of the solutions, and evidently will not be cheaper than purification on the cation-exchange resin KU-2.

Translated from Atomnaya Énergiya, Vol. 35, No. 2, pp. 105-108, August, 1973. Original article submitted July 21, 1972.

TABLE 1. Duration of Filtration Cycles and Coefficients of Purification of Solutions on Partially Sulfurated Bitumen

Experiment No.	Initial solution					Q	Filtrate				EC Ca, meq/g
	pH	concentration meq/liter		activity, counts/min · ml			activity, counts/min · ml		coefficient of purification from		
		Na	Ca	Sr	Cs		Sr	Cs	Sr	Cs	
1	6,9	—	1,4	2700	700	650	54	17	50	40	0,91
2	7,8	3,6	3,4	4000	—	350	270	—	15	—	1,19
2*	7,8	3,6	3,4	—	850	150	—	40	—	21	1,19
3*	7,2	12,7	—	1300	—	2 100	60	—	21	—	—
3*	7,2	12,7	—	—	760	200	—	42	—	18	—
4	8,1	20,0	1,5	3500	—	625	22	—	160	—	1,15
4*	8,1	20,0	1,5	—	1720	225	—	41	—	42	1,15

Note. The asterisks mark experiments in which filtration of the solution was continued until the coefficient of purification from isotopes was equal to 10; in other cases it was continued until the beginning of the appearance of calcium ions in solution; Q is the amount of solution that passed through 1 g (5 ml) of partially sulfurated bitumen. EC Ca is the fraction of the exchange capacity with respect to calcium.

TABLE 2. Volume of Wastes (% of volume of purified water)

Investigated solution*	Purification on sulfurated bitumen			Purification on the cation-exchange resin KU-2 in the sodium form		
	volume of purified solution†	volume of liquid wastes, %	volume of bitumen blocks	volume of purified solution†	volume of liquid wastes, %	volume of bitumen blocks
Atomic Center at Mola	130	0,77	1	1000	0,5	0,03
Moscow Purification Station	30	3,3	4,4	180	2,8	0,19
Burial Station at Zagorsk	45	2,2	2,9	330	1,5	0,1

*The solution simulated the composition of sewage at the indicated sites.
†In column volumes.

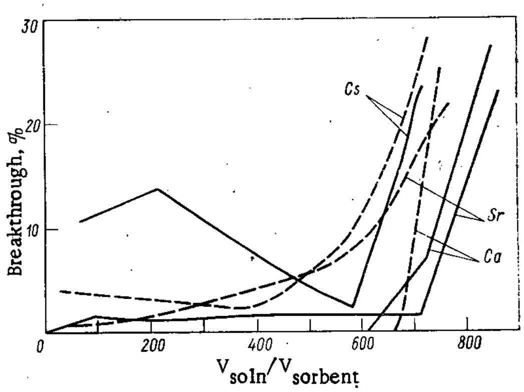

Fig. 1. Effluent curves of the sorption of Sr^{90}, Cs^{137}, and Ca^{2+} from waste solutions on various sulfurated bitumens: – – –) results of this work; ——) data of [1].

TABLE 3. Coefficients of Purification of the Solution from Cesium (the solution contains 2 g/liter of salts)

Brand of ion-exchange resin	pH = 7 ÷ 8	pH = 11,7 ÷ 11
KB-51X2	105	—
KB-51X5	226	260
KB-51X7	260	400
KB-51X10	—	300
KU-2	5,7	8
KU-2	7,0	130
KB-2	5,9	40
Wofatite CN	25	70

In our report at the conference of member countries of the Council of Economic Mutual Aid [2] at Dresden in 1967, it was shown that with increasing sodium-ion concentration in solution, the duration of the filtration cycle of purification of solutions from Cs^{137} on the cation-exchange resin KU-2 in the Na-form decreases. Moreover, the end of the purification from cesium isotopes far precedes the beginning of the appearance of calcium ions in the filtrate. Therefore, when the cation-exchange resin KU-2 is used in the Na-form for the purification of salt solutions containing cesium ions, a large volume of wastes is obtained.

In the United States, the phenol–carboxyl cation-exchange resin Duolite CS-100 is used for the removal of cesium radioisotopes from solutions containing 2 g/liter of salt. The soda–carbonate precipitation of calcium and magnesium ions is performed preliminarily. At pH = 12 the coefficient of separation

Declassified and Approved For Release 2013/01/22 : CIA-RDP10-02196R000400020002-7

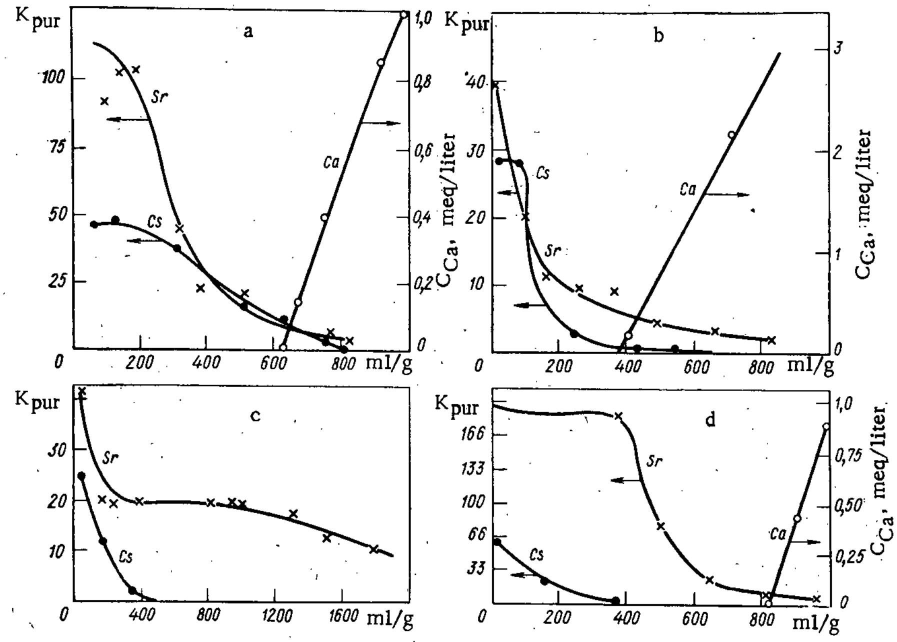

Fig. 2. Effluent curves and coefficients of purification of solutions on partially sulfurated bitumen in the Na-form: a) Ca^{2+} 1.5 meq/liter (Atomic Center at Mola); b) Ca^{2+} 2.8 meq/liter, Na^{+} 3.6 meq/liter (MSO); c) Na^{+} 12.7 meq/liter; d) Ca^{2+} 20 meq/liter (wash waters of the Burial Station at Zagorsk).

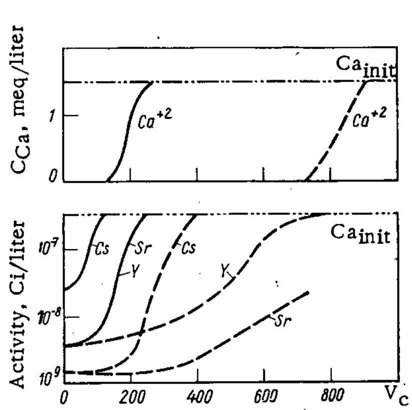

Fig. 3

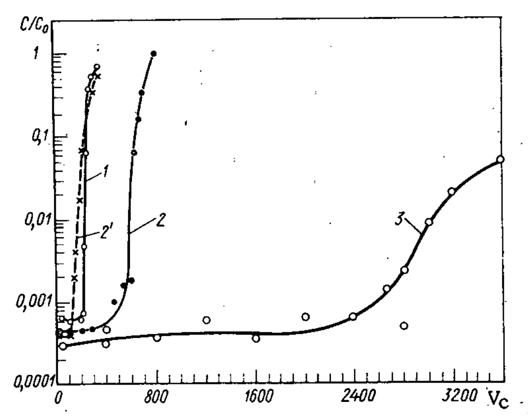

Fig. 4

Fig. 3. Effluent curves of the sorption of Sr^{90}, Y^{90}, Cs^{137}, and Ca^{2+} from sewage on the cation-exchange resin KU-2 (– – –) and sulfurated bitumen (——).

Fig. 4. Effluent curves of the sorption of Cs^{137} on the cation-exchange resins KB-51 × 7 and KU-2.

of sodium and cesium on the ion-exchange resin Duolite CS-100 is 160. We should note that this value is equal to three on the ion-exchange resin Dowex 50, as also on our cation-exchange resin KU-2.

Earlier we tested certain domestic industrial carboxyl resins, for example, KB-4, KB-2, etc. It was found that on these resins the same purification from cesium in the presence of sodium ions is achieved as on the cation-exchange resin KU-2. In searches for sorbent selective for cesium, we tested the phenol–carboxyl cation-exchange resin KB-51, synthesized and prepared at the Nizhnetagil'sk Laboratory of the State Scientific-Research Institute of Plastics (NIIPM) [3]. It was established that cesium can be extracted from solutions with a high sodium-ion concentration with the aid of this sorbent. The initial raw materials for this cation-exchange resin are salicyclic acid, phenol, and formalin. Resins containing 0.2, 0.5, 0.7, and 1 mole of phenol per mole of salicyclic acid were produced (these correspond to brands KB-51X2, KB-51X5, KB-51X7, and KB-41X10).

Table 3 presents the coefficients of purification of solutions from cesium isotopes on the carboxyl resins KB-51; the results obtained on other ion-exchange resins tested previously are cited for comparison.

Figure 4 presents the effluent curves obtained in filtration of solutions of three compositions through the cation-exchange resin KB-51X7: 1) the solution contained 10 meq/liter of sodium chloride, nitrate, and sulfate and 3 meq/liter of potassium nitrate, pH = 7 (curve 1); 2) the solution contained just as much of the sodium salts, but no potassium ions, pH = 7 (curve 2); 3) a solution analogous in composition to the preceding, but pH = 11.7 (curve 3).

The effluent curves obtained are shown in Fig. 4. It is evident that the cesium concentration in solution is lowered 1000-fold or more, despite the presence of sodium salts. When the pH is raised from 7-8 to 11.7-12, the capacity of the sorbent increases more than fivefold, while in the presence of calcium ions it is halved. From a comparison of the results of the sorption of cesium on the carboxyl phenol–salicyclic sorbent and the cation-exchange resin KU-2 in the Na-form (see Fig. 4, curves 2 and 2'), the clear advantages in the first case are evident. From a solution with pH = 11.7, the duration of the filtration cycle of purification from cesium exceeds 2500 column volumes. The same results were obtained in an analysis of sewage sent to the Moscow Purification Station. A cesium isotope was introduced into them to an activity of the solution equal to $1.1 \cdot 10^{-5}$ Ci/liter. Cesium was not detected in the filtrate; consequently, the coefficient of purification exceeded 3000-fold. No less than 1 m^3 of solution can be purified per liter of sorbent, after which cesium can be desorbed and the sorption properties of the ion-exchange resin regenerated using a solution of sodium hydroxide. The results obtained on the experimental setup show that if the cation-exchange resin KU in the Na-form, the anion-exchange resin also in salt form, and the carboxyl cation-exchange resin KB-51 are set up successively, the water of the Moscow Purification Station can be freed of all radioisotopes and the volume of the solutions to be evaporated can be reduced to half. The water sent to the MSO contains only 0.5-0.7 g/liter of salts. In the case of a larger salt content, the volumes of the solutions to be evaporated can be reduced even more.

LITERATURE CITED

1. N. Van de Voorde and K. Peeters, Management of Low- and Intermediate-Level Radioactive Wastes, IAEA, Vienna (1970), p. 669.
2. F. V. Rauzen et al., Collection of Reports of the Scientific and Technical Conference of Specialists of the Member Countries of the Council of Economic Mutual Aid (Dresden, September, 1967) [in Russian], SÉV, Moscow (1968).
3. V. P. Bogdanov and E. D. Kaverzneva, Izv. Akad. Nauk SSSR, Ser. Khim., No. 2, 469 (1969).

INFLUENCE OF THE HYDRATION OF AMINE SALTS ON THE EXTRACTION EQUILIBRIUM

Yu. G. Frolov, V. V. Sergievskii, and A. P. Zuev

UDC 542.61

For an understanding of the principles of the extraction of various rare and radioactive elements by solutions of substituted ammonium bases, detailed investigations of the extraction of acids by solutions of amines have been conducted [1-8]. Therefore, considerable efforts have been directed to establishing the cause of the substantial deviations from the ideal observed in amine systems, the nature of which has not yet been entirely elucidated [9-11].

Thus, it has been established in [12] that, in the description of the extraction of sulfuric acid by solutions of tri-n-octylamine (TOA) in benzene, the equilibrium constant of the reaction

$$nR_3N_{org} + H_nX_{aq} \rightleftarrows (R_3NH)_nX_{org}, \tag{1}$$

calculated without taking into account the activity coefficients of the components of the organic phase shows a substantial dependence on the concentration of TOA sulfate. It has been suggested that this is a consequence of "polymerization" of the salt. However, measurements of light scattering have shown that TOA sulfate in benzene is a monomer [13]. Later cryoscopic measurements of the extracts indicate a weak association of this salt [14, 15], due to the presence of water in the organic phase [15]. Such a lack of correspondence between the results of independent physicochemical measurements and the data on the distribution has also been noted for the extraction of monobasic acids by amines [8, 9, 16].

In the formulation of this work, the authors proceeded on the basis that water coextracted with acids should have a substantial influence on the activity of salts in the organic phase. This is confirmed by the increase in the solubility of trilaurylamine (TLA) chloride when water is introduced into the solutions [17].

That water has a substantial influence on the extraction of carboxylic acids was established long ago (see Lassettre's survey [18]). Subsequent studies [19] confirmed the significance of this effect. The method that is usually used for a consideration of the role of water in the distribution of carboxylic acids is not applicable to the systems investigated in this work. Actually, the stability constants of the hydrates of carboxylic acids are usually used in the calculations, but the results of an investigation of the distribution of water show [5] that in most cases the formation of hydrates of amine salts of constant composition is relatively improbable. Therefore, it seemed advisable to determine the activity of the components in ternary homogeneous solutions: solvent–amine salt–water. The authors know of no studies devoted to the determination of the influence of water on the activity of amine salts. Therefore, in conducting the present work a method of investigation was developed.

Theoretical Section

Methods of determination of the activity of components of solutions are based on the solution of the Gibbs–Duhem equation, which for a three-component mixture can be expressed in terms of the activities of the components:

$$n_1 d\ln a_1 + n_2 d\ln a_2 + n_3 d\ln a_3 = 0. \tag{2}$$

Here and henceforth the subscripts 1-3 pertain to the solvent, extraction reagent, and water, respectively.

Translated from Atomnaya Énergiya, Vol. 35, No. 2, pp. 109-116, August, 1973. Original article submitted November 22, 1972.

Considering that the differential of the logarithm of the activity is a complete differential of the composition, this equation is solved for constant n_1 and n_2 and variable n_3. Such an assumption is valid in the case when the concentration of the components is expressed in molarities m. Then

$$m_1\left(\frac{\partial \ln a_1}{\partial m_3}\right)_{m_1m_2} dm_3+m_2\left(\frac{\partial \ln a_2}{\partial m_3}\right)_{m_1m_2} dm_3+m_3\left(\frac{\partial \ln a_3}{\partial m_3}\right)_{m_1m_2}=0 \tag{3}$$

or

$$d\ln a_2+\frac{m_1}{m_2}d\ln a_1+\frac{m_3}{m_2a_3}\left(\frac{da_3}{dm_3}\right)dm_3=0. \tag{4}$$

Integrating Eq. (4) within the limits from 0 to m_3, we obtain

$$\ln a_2^*=\ln a_2-\frac{m_1}{m_2}\ln\frac{a_1^*}{a_1}-\frac{1}{m_2}\int_0^{m_3}\frac{m_3}{a_3}\left(\frac{da_3}{dm_3}\right)dm_3, \tag{5}$$

where a_i and a_i^* are the activities of the component in the binary and ternary solutions, respectively.

When, as is quite often the case for dilute solutions, the distribution of water in the solution satisfies Henry's law,

$$a_3=Hm_3, \tag{6}$$

where H is Henry's constant, we obtain

$$\ln a_2^*=\ln a_2-\frac{m_1}{m_2}\ln\frac{a_1^*}{a_1}-\frac{m_3}{m_2}. \tag{7}$$

Considering that the degree of hydration $h=(m_3-m_3^0)/m_2$, let us write Eq. (7) in the form

$$\ln\frac{a_2^*}{a_2}=-\frac{m_1}{m_2}\ln\frac{a_1^*}{a_1}-h-\frac{m_3^0}{m_2}, \tag{8}$$

where m_3^0 is the solubility of water in the pure solvent.

In the limit, for the solvent–extraction reagent system

$$a_1=N_1\approx 1-\frac{m_2}{m_1}, \tag{9}$$

while for the ternary solution

$$a_1^*=N_1\approx 1-\frac{m_2}{m_1}-\frac{m_3^0}{m_1}. \tag{10}$$

Consequently

$$\lim_{m_2\to 0}-\frac{m_1}{m_2}\ln\frac{a_1^*}{a_1}=\frac{m_3^0}{m_2}, \tag{11}$$

in this approximation, Eq. (5) takes the form

$$\ln\frac{a_2}{a_2^*}=h. \tag{12}$$

Thus, in the limiting case, the degree of hydration is a quantitative measure of the influence of water on the change in the activity of the extraction reagent in the transition from its binary solutions to solutions saturated with water. Since $a_2/a_2^*=\gamma^0$, where γ^0 is the zero activity coefficient, we can write

$$\ln\gamma^0=h. \tag{13}$$

With the aid of the value of the limiting degree of hydration of this extraction reagent, we can convert from activities determinable according to Eq. (5) for the standard state – an infinitely dilute solution in a dry solvent – to activities of the comparative standard state – an infinitely dilute solution of the extraction reagent in a ternary system.

According to Eq. (5), to calculate the activity of the extraction reagent in a ternary solution a_2^*, it is necessary to determine experimentally $a_2=f(m_2)$, $a_1^*=f(m_2, m_3)$, and $a_3=f(m_2, m_3)$. In this work the first two dependences were determined according to the data of cryoscopic measurements; $a_3=f(m_2, m_3)$ was found from the dependence of the solubility of water in an organic solution on its absolute activity a_W in the standard aqueous solution. Benzene was used as the solvent.

In these methods of investigation, the first factor of Eq. (5), i.e., $B_1 = \log a_2$, is found from the solution of the Gibbs–Duhem equation for a binary solution [20]. The dissociation of the amine salts in benzene was not considered.

For benzene solutions of various salts, the expression for the calculation of the second factor of Eq. (5) takes the form

$$B_2 = \frac{m_1}{m_2} \lg \frac{a_1^*}{a_1} = -0.0065\,(\theta^* - \theta)\,\frac{m_1}{m_2}\,, \tag{14}$$

where θ^* is the decrease in the freezing point of the ternary benzene solution; θ is the decrease in the freezing point of the salt solution, $m_3 = 0$.

The third factor B_3 of Eq. (5) was calculated on the basis of the dependence of the solubility of water m_3 in salt solutions on a_W:

$$B_3 = \frac{1}{2.303 m_2} \int\limits_0^{m_3} \frac{m_3}{a_3}\left(\frac{da_3}{dm_3}\right) dm_3 = \frac{1}{2.303 m_2} \int\limits_0^{a_3} \frac{m_3}{a_3}\, da_3\,. \tag{15}$$

It is easily calculated when the distribution of water obeys Henry's law (6), (7). It is known [21, 22] that nonlinear dependences of m_3 on a_3 are described with the requisite accuracy by the equation

$$\ln k a_3 / m_3 = \lambda m_3, \tag{16}$$

where k and λ are constants. In this case

$$B_3 = \frac{m_3\,(1 + \lambda/2 m_3)}{2.303 m_2}. \tag{17}$$

The values of B_3 are calculated either according to Eq. (17), using the values of λ preliminarily determined by calculation on a digital electronic computer, or by graphical integration of the dependence of m_3 / a_3 on a_3.

Thus, the selected combination of methods of investigation permits an easy determination of the activities of all the components of the ternary solution. Its shortcomings include the impossibility of determining the activities of the components at various temperatures without replacement of the solvent, as well as a certain difference in the temperature of cryoscopic and isopiestic measurements, usually equal to 1-2°C.

Experimental Section

Benzene, grade "for cryoscopy," was used in this work, having been purified by redistillation. TOA sulfate and TLA nitrate were prepared according to the method described in [15, 23]. The dependences of the solubility of water in salt solutions on its activity were determined isopiestically according to the method described earlier [24, 25]. The freezing point of salt solutions isopiestically saturated with water was determined according to a Beckman thermometer; the error of the determination was ±0.003°C.

Experiments on extraction were conducted in thermostatically controlled (at 6.0 ± 0.1°C) separatory funnels. The acid concentration in the amine phase was determined according to the difference of the initial and equilibrium concentrations of acid in the aqueous phase. In the case of sulfuric acid, the concentration was determined by titration with alkali in the presence of phenolphthalein. The nitric acid concentration was determined according to the data of the high-frequency electric conductivity of the aqueous phase. It is known that even at low equilibrium acidities of the aqueous phase, the extraction of nitric acid by amines is not limited by its formation of a salt, but is accompanied by extraction of the superstoichiometric acid. In this work, to eliminate this effect we studied the reextraction of nitric acid with double-distilled water from a solution of TLA nitrate in benzene, produced by dissolving the crystalline salt.

Discussion of Results

In studies conducted previously by the authors [24-28], it was established that, for sufficiently dilute solutions of extraction reagents, the dependence of the hydration on their concentration is described by the equation

$$C_w = C_w^0 a_w + h_1 a_w C_S, \tag{18}$$

where C_W^0 is the solubility of water in the pure solvent at $a_W = 1$; $h_1 = (C_{W,1} - C_W^0)/C_S$ is the degree of hydration of the extraction reagent when $a_W = 1$; $C_{W,1}$ is the solubility of water in solution when $a_W = 1$; C_S is the salt concentration. The results cited in Fig. 1 show that the deviations from Eq. (18) increase with increasing salt concentration. Moreover, the greater the degree of hydration of the salt, the more significant the deviations of the distribution of water from Henry's law. We should note that the dependences of the solubility of water in solutions of TOA sulfate on its activity are similar to those obtained by Roddy and Coleman at a temperature of 25°C [11].

It is extremely complicated to give an unambiguous interpretation of the causes of the deviation of the distribution of water from Henry's law. There should be no doubt that, in the case of solutions of TOA sulfate, the introduction of water leads to association of the salt [15]; this also follows from the dependence of the decrease in the freezing point of the solutions on the activity of water (Fig. 2b). This effect for solutions of TLA nitrate is less pronounced; the value of $\Delta\theta$ decreases from ~0.135 to ~0.10° in the transition to more concentrated salt solutions (Fig. 2a). Such an influence of water on the value of $\Delta\theta$ is most typical of the systems studied by the authors (see Fig. 6). The value of $\Delta\theta = 0.135°$ is close to the value corresponding to the appearance of "free" water in solution, the concentration of which is usually assumed to be equal to the solubility of water in pure benzene, $m_3^0 = 0.025$ mole/kg of benzene. Actually, $\Delta\theta = Km_3^0 = 5.1 \cdot 0.025 = 0.135°$, where K is the cryoscopic constant of benzene. However, the decrease in $\Delta\theta$ with the salt concentration at $a_W = 1$ may be a consequence both of a decrease in the concentration of "free" water and of an increase in the association of the salt.

From Fig. 3 it is evident that the water dissolved in the organic phase lowers the thermodynamic activity of the extraction reagents, and the influence exerted is greater, the higher its solubility in the organic phase.

Extraction of Acids by Amines. The effective extraction constant of acids by amines

$$K = \frac{[(R_3NH)_nX]}{[R_3N]^n a_{H_nX}} \cdot \frac{\gamma_{(R_3NH)_nX}}{\gamma_{R_3N}^n} = K_{\text{eff}} \frac{\gamma_{(R_3NH)_nX}}{\gamma_{R_3N}^n}, \tag{19}$$

as noted above, shows a substantial concentration dependence. Until recently, the components of the organic phase were not considered in calculations of the activity. Some authors believe that the slope of the curve in logarithmic coordinates, expressing the dependence of the acid concentration in the organic phase on the product $[R_3N]a_{H_nX}$, gives the average value of the degree of association of the salt at any point [8, 9, 16]. It has been established that in these coordinates, for the extraction of various monobasic acids by trilaurylamine, the dependences take an "anomalous" form [16]: the slope of the curve increases, reaches an infinite value, but then becomes negative. Such an "anomaly" is manifested to an even greater degree in the extraction of sulfuric acid by solutions of tri-n-octylamine (Fig. 4). In this interpretation, the presence of a vertical asymptote to the curves corresponds to complete aggregation of the salt into a macrocolloid or the formation of a new phase [9, 16]; however, this is not confirmed by the data of independent physicochemical measurements. In the cited studies, no satisfactory explanation for this phenomenon has been found.

With such an interpretation, on the basis of the data cited in Fig. 4, it might be concluded that the presence of vertical asymptotes to the curves correspond to an infinitely large value of the extraction constant. This also does not agree with the experimental data. The incorrect conclusion of a very great association of the salt arises because the slope of the curves does not have the physical meaning of degree of association of the salt or extraction constant ascribed to it (in the coordinates of Fig. 4). The latter are specific quantities and are equal to the products only in the case of linear dependences. The observed shape of the curves in a plot of $\log[(R_3NH)_nX]$ vs $\log\{[R_3N]a_{H_nX}\}$ is due to the concentration dependence of the effective extraction constant. Thus, the explanation of the "anomalous" patterns of extraction of acids by amines is reduced to the traditional problem of the extraction of acids by amines: the elucidation of the causes of the substantial increase in the values of K_{eff} with increasing concentration.

The activity coefficients γ_3, according to Eq. (5), are determined relative to the standard state of infinitely dilute solutions of the extraction reagents in dry benzene. For the transition to the standard state, infinitely dilute solutions in benzene, saturated with water at $a_W = 1$, i.e., corresponding to an extract of acids by amine solutions, we used function (13) and the values of the degree of hydration at $a_W = 1$,

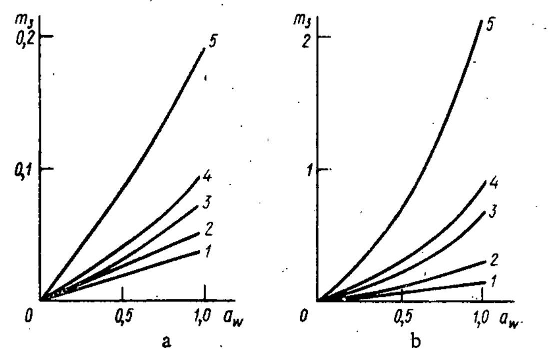

Fig. 1

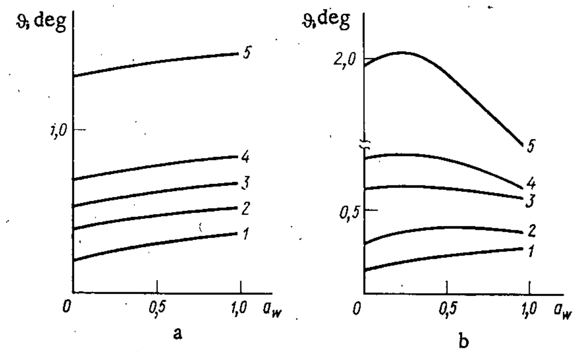

Fig. 2

Fig. 1. Dependence of the solubility of water in solutions of TLA nitrate (a) and TOA sulfate (b) in benzene on the activity of water at various salt concentrations m_2 (t = 6°C). a: 1) 0.057; 2) 0.120; 3) 0.190; 4) 0.260; 5) 0.565. b: 1) 0.029; 2) 0.059; 3) 0.124; 4) 0.161; 5) 0.364.

Fig. 2. Dependence of the change in the freezing point of solutions of TLA nitrate (a) and TOA sulfate (b) in benzene on the activity of water. Salt concentrations as in Fig. 1.

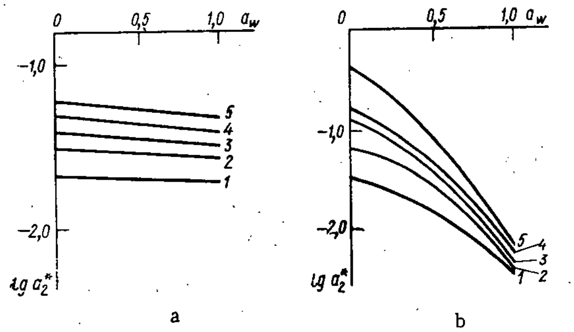

Fig. 3

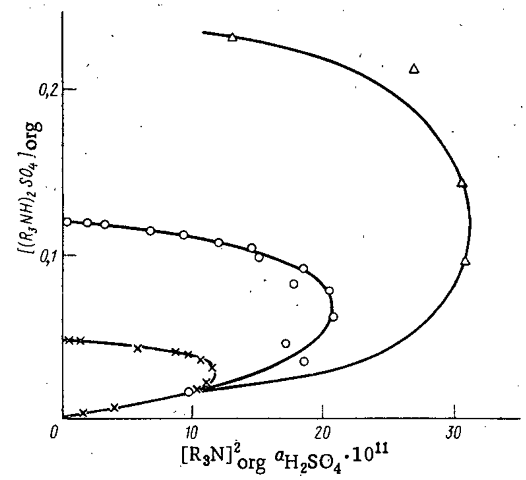

Fig. 4

Fig. 3. Influence of water on the thermodynamic activity of TLA nitrate (a) and TOA sulfate (b). Salt concentrations as in Fig. 1.

Fig. 4. Dependence of the total concentration $[(R_3NH)_2SO_4]_{org}$ on $[R_3N]^2_{org}a_{H_2SO_4}$ for the extraction of sulfuric acid by aqueous solutions of TOA, according to the data of [12], with an initial amine concentration: ×) 0.1 M; ○) 0.247 M; △) 0.5 M.

extrapolated to infinitely dilute salt solutions. The results of the calculation of the activity coefficients of salts in dry benzene solutions and solutions saturated with water are cited in Fig. 5.

From the Gibbs–Duhem equation, it follows that the transition to a real four-component organic phase amine salt–"free" amine–water–solvent should lead to changes in the activity coefficients of the components. However, at the present time a calculation of the activity coefficients of the components in such quaternary systems is difficult. Therefore, to calculate the extraction constants we used the values of γ_3 determined for the ternary system. The values of γ_{R_3N} were assumed equal to the values in their binary systems in benzene. The average ionic activity coefficients of the acids in aqueous solutions at 6.0 ± 0.1°C were obtained by interpolation according to the data cited in [29].

It is evident (Tables 1 and 2) that the values of the constants K obtained in this approximation, in contrast to K_{eff}, show a substantially smaller concentration dependence. The quite satisfactory equalization of the values of the constants shows that the change in the activity coefficients of the components in the transition to quaternary solutions is not too large. The result obtained permits us to conclude that the concentration dependences of the extraction constants noted are explained to a substantial degree by the influence of water on the activity of amine salts.

TABLE 1. Extraction of Nitric Acid by Benzene Solutions of TLA at t = 6°C

$m_{R_3NHNO_3}$	m_{R_3N}	$a_{HNO_3} \times 10^7$	γ_3	$K_{eff} \cdot 10^6$	$K \times 10^6$
0,011	0,105	0,514	0,711	2,04	1,76
0,022	0,090	0,977	0,600	2,50	1,81
0,034	0,078	1,245	0,495	3,50	2,09
0,046	0,067	1,530	0,401	4,48	2,17
0,057	0,056	1,770	0.333	5,72	2,30
0,068	0,045	2,290	0,292	6,60	2,33
0,081	0,033	3,413	0,264	7,20	2,29
0,105	0,011	9,310	0,230	10,25	2,83
0,117	0,0022	45,782	0.216	11,36	2,89
0,224	0,085	1,770	0,156	14,90	2,81
0,295	0,029	5,286	0,126	19,22	2,92
0,328	0,0022	45,78	0,116	31,84	4,32
0,190	0,0022	45,78	0,172	18,44	3,82
0,420	0,0023	47,80	0,101	38,20	4,65
0,770	0,0023	47,80	0,075	70,05	6,30
1,200	0,0023	47,80	—	102,44	—
1,600	0,0023	47,80	—	136,6	—

TABLE 2. Extraction of Sulfuric Acid by Benzene Solutions of TOA at t = 6°C

$m_{(R_3NH)_2SO_4}$	m_{R_3N}	$a_{H_2SO_4} \times 10^9$	γ_3	$K_{eff} \cdot 10^8$	$K \times 10^8$
0,00045	0,0580	0,488	0,992	2,75	2,73
0,0011	0,0565	2,05	0,984	1,68	1,65
0,0025	0,0545	4,83	0,977	1,75	1,71
0,0028	0,0535	5,35	0,976	1,83	1,78
0,0040	0,0507	7,22	0,962	2,16	2,07
0,0095	0,0400	13,81	0,911	4,31	3,91
0,0170	0,0255	33,90	0,814	7,73	6,30
0,0210	0,0180	70,70	0,777	9,19	7,13
0,0175	0,0830	7,21	0,800	3,53	2,82
0,0260	0,0640	9,71	0,726	6,54	4,75
0,0380	0,0400	24,50	0,628	9,69	6,10
0,0480	0,0220	73,50	0,555	13,53	7,50
0,0560	0,0101	334,0	0,497	16,49	8,18
0,0101	0,330	0,285	0,887	3,55	3,14
0,0340	0,270	0,623	0,666	7,51	5,01
0,0590	0,200	1,65	0,482	8,95	4,32
0,0890	0,130	3,38	0,355	15,62	5,53
0,110	0,0830	7,90	0,296	20,24	5,94
0,122	0,0650	11,00	0,281	26,20	7,35
0,157	0,0050	154,00	0,192	40,84	7,85
0,225	0,230	1,40	0,148	30,55	4,52
0,290	0,110	5,35	0,133	44,80	5,96

Let us note that in [30] the extraction of hydrochloric and hydrobromic acids by trilaurylamines was described considering the activity coefficients of the salts formed in their binary solutions. On the basis of the results of this work it was concluded that, "despite the high concentration of water in the organic phase, the activity coefficients of the salts are not subjected to its influence." This conclusion is not general, since it was based on data for a comparatively small interval of concentrations of TLA salts, in which their degrees of hydration evidently remain constant.

Interrelationship between the Degree of Hydration and Activity of the Extraction Reagents. The method of investigation outlined above was used for an experimental verification of Eq. (12) for the example of benzene solutions of salts of substituted ammonium bases with various anions, as well as for tri-n-butyl phosphate (TBP) and di-2-ethylhexylphosphoric acid (D2EHPA), widespread in extraction practice. The results obtained are cited in Fig. 6, from which it is evident that, for most of the systems studied, Eq. (12) corresponds with good accuracy to the experimental data. Solutions of TOA sulfate are an exception, since in this system the deviations of the distribution of water from Henry's law are most substantial.

Just as we should have expected, the decrease in the activity of water and the concentration of the extraction reagents leads to a decrease in the deviations of the experimentally determined values of $\ln (a_2 / a_2^*)$ from the values calculated according to Eq. (12). Thus, Eq. (12), although it was based on an extremely simplified model, is suitable for the evaluation of the influence of water on the activity of the extraction reagent in many systems.

The range of variation of the degree of hydration of the extraction reagents studied is rather large. The maximum decrease in the activity (by three orders of magnitude) in the systems studied by the authors is observed when water is introduced into solutions of tetra-n-octylammonium sulfate. The data cited in Fig. 6 confirm that, from the thermodynamic viewpoint, the degree of hydration is a quantitative measure of the influence of water on the change in the activity of the extraction reagent in the transition from binary solutions of the reagent to moist solutions. Considering this dependence, we can draw a conclusion of practical importance: the influence of water on the extraction equilibrium is most substantial in those cases when the degree of hydration of the extraction reagent depends on its concentration.

Influence of Water on the Extraction of Salts of Metals. In addition to a study of the causes of the substantial deviations from the law of mass action in the extraction of acids by amines, a no less interesting fact is the influence of the degree of substitution at the nitrogen atom of the bases on the extraction of salts of metals. It is known that, in the extraction from solutions of monobasic acids, the extraction of metal salts increases from salts of primary amines to salts of quaternary ammonium bases [3]. This sequence is due to the increase in basicity of the compounds in the indicated series and, as a result, is due to an intensification of the chemical affinity of the anions of amine salts for metal ions on account of the increasing ionic character of the intramolecular bond [31]. Together with this, in the case of extraction from solutions of sulfuric acid, an opposite tendency is observed: the best extraction reagents, for example, for uranyl sulfate, are salts of primary amines [3]. Until recently these patterns, noted by Flett in the survey report [32] as "curious," had not found a satisfactory explanation.

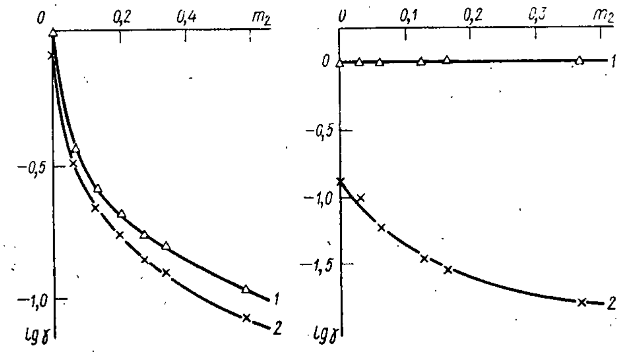

Fig. 5. Influence of water on the activity coefficients of TLA nitrate (a) and TOA sulfate (b) for dry (1) and moist (2) solutions.

The results of the calculation of the activity of sulfates and nitrates of substituted ammonium bases in the case of various activities of water are cited in Fig. 7. It is evident that in solutions saturated with water at $a_W = 1$, the same sequence of decreasing activity of the salts is preserved as for anhydrous systems. For sulfates the degree of reduction of their activity coefficients under the action of water is more pronounced.

Salts of ammonium bases and monobasic acids are weakly hydrated, as a result of which their reactivity series is unchanged in extraction systems. The degree of hydration of the sulfates and, evidently, salts of many monobasic acids exceeds the degree of hydration of the nitrates by an order of magnitude. Corresponding to the increase in electron-donor capacity of anions of the salts, their hydration on substituting a cation increases in the series: secondary, tertiary, quaternary alkylammonium; this leads to a progressive decrease in the thermodynamic activity of the salt. These changes are greater than the increase in the "absolute" reactivity in the same series. As a result, the series of extraction capacity is reversed, and the extraction of elements the complexes of which are hydrated substantially more weakly decreases from sulfates of primary amines to sulfates of quaternary ammonium bases.

On the basis of our investigations, it can also be concluded that water, like alcohols and certain protogenic solvents, increases the extraction of acids (see Tables 1 and 2), but has a depressing influence on the extraction of salts of metals by amine salts.

According to the published data on the hydration of amine salts, the influence of water on their activity should increase with increasing proton-donor capacity of their anions. In the same sequence we should expect an increase in the noncorrespondence of the degree of association of the salts determined from the extraction data, for example, by the method in [33], and from the results of independent physicochemical measurements. A characteristic example is the extraction of uranyl sulfate by solutions of TOA sulfate. The first-degree dependence of the distribution coefficients of salts of metals on the TOA sulfate concentration in logarithmic coordinates served as a basis for assuming the formation of a colloidal solution in the organic phase [1]. The latter conclusion was not confirmed by an experimental verification, and up to the present time the causes of such behavior of this extraction system have not been revealed.

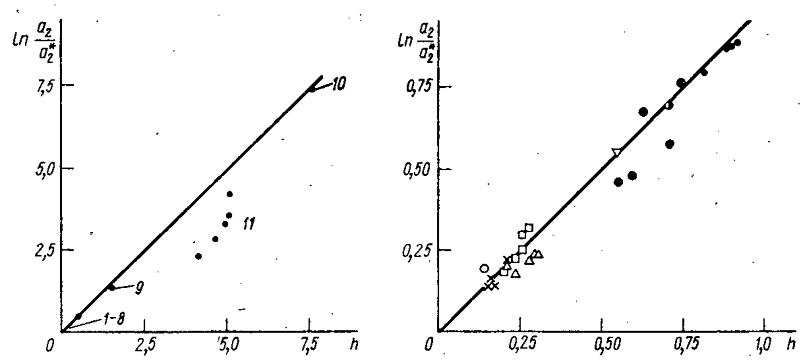

Fig. 6. Interrelationship between the values of $\ln(a_2/a_2^*)$ and h of various extraction reagents in benzene: 1) (▽) dioctylamine chloride, $m_2 = 0.058$; 2) (□) TBP, $m_2 = 0.114$–0.810; 3) (△) TLA nitrate, $m_2 = 0.057$–0.810; 4) (·) TOA chloride, $m_2 = 0.059$–0.250; 5) (×) D2EHPA, $m_2 = 0.119$–0.692; 6) (●) TLA bisulfate, $m_2 = 0.059$–0.865; 7) (○) di-n-nonylamine nitrate, $m_2 = 0.118$; 8) (◑) tetraoctylammonium nitrate, $m_2 = 0.121$; 9) di-n-nonylamine sulfate, $m_2 = 0.121$; 10) tetraoctylammonium sulfate, $m_2 = 0.119$; 11) TOA sulfate, $m_2 = 0.029$–0.364.

Declassified and Approved For Release 2013/01/22 : CIA-RDP10-02196R000400020002-7

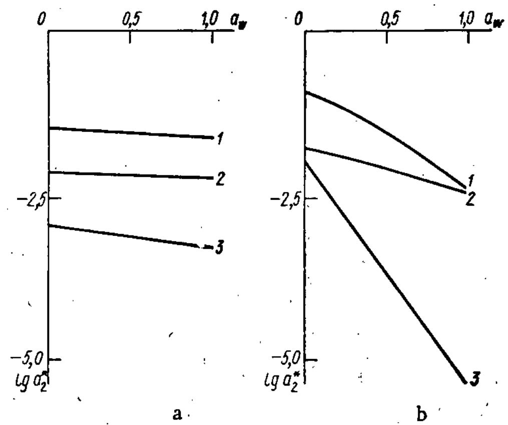

Fig. 7. Influence of water on the thermodynamic activity of nitrates (a) and sulfates (b) of substituted ammonium bases in benzene: 1) tri-n-octylamine; 2) di-n-nonylamine; 3) tetra-n-octylammonium.

From Fig. 3b it follows that with increasing activity of water, the difference between the activities of TOA sulfate in solutions of different concentrations is equalized. Consequently, the small dependence of the extraction of salts of metals by solutions of TOA sulfate on its concentration is also due to the influence of water, which decreases the activity coefficients of the salt to a greater degree, the higher its concentration. These dependences should be observed in systems in which the distribution of water deviates substantially from Henry's law. The deviations from Henry's law may be associated with an increase in the association of the salt and are considered as an approximation of the thermodynamic instability of the organic phase with respect to stratification.

It has been established, for example, that for 0.1 M solutions of TOA chloride, deviations from Henry's law are observed only for solutions in the least polar solvent – cyclohexane [24]. In the transition to methyldi-n-octylamine and dimethyldecylamine chlorides, they already appear in more polar solvents (toluene and nitrobenzene). The influence of methyl substituents on hydration is also analogous for solutions of salts of quaternary ammonium bases [25]. Such patterns are characteristic of the formation of a second organic phase in the extraction systems. For example, in the extraction of hydrochloric acid by solutions of TOA, the formation of the second phase is observed in cyclohexane and saturated hydrocarbons [34]. Consequently, a correlation of the patterns of formation of three-phase extraction systems to the principles of the deviation of the distribution of water from Henry's law is observed. In view of this, the suggestion of the authors of [1] that TOA sulfate forms a colloidal solution had a definite meaning, since, judging by the substantial deviations of the distribution of water from Henry's law (see Fig. 1b), this system is close to stratification.

Thus, the data of this work show the great, sometimes decisive significance of hydration for an understanding of certain extraction principles.

LITERATURE CITED

1. C. Coleman et al., Industr. and Engng. Chem., 50, 1756 (1958).
2. C. Coleman, Nucl. Sci. Engng., 17, 274 (1963); Atom. Energy Rev., Vol. 2, IAEA, Vienna (1964), p. 3.
3. M. Zifferero, Proceedings of the Symposium on Aqueous Reprocessing for Irradiated Fuels, Bruxelles, April 23-24 (1963).
4. W. Müller, Actinides Rev., 1, 71 (1967).
5. Yu. G. Frolov, A. V. Ochkin, and V. V. Sergievskii, Atom. Energy Rev., Vol. 7, IAEA, Vienna (1969), p. 71.
6. C. Coleman, Process Chemistry, Vol. 4, Oxford (1970), p. 233.
7. V. S. Shmidt, Extraction by Amines [in Russian], Atomizdat, Moscow (1970).
8. W. Müller, Chemiker-Zeitung, 95, 499 (1971).
9. R. Diamond, in: The Chemistry of Extraction [Russian translation], A. A. Pushkov (editor), Atomizdat, Moscow (1971), p. 180.
10. C. Coleman and J. Roddy, in: The Chemistry of Extraction [Russian translation], A. A. Pushkov (editor), Atomizdat, Moscow (1971), p. 196.
11. J. Roddy and C. Coleman, J. Inorg. Nucl. Chem., 31, 3599 (1969).
12. K. Allen, J. Phys. Chem., 60, 239 (1956).
13. K. Allen, Phys. Chem., 62, 1119 (1958).

14. V. V. Fomin, P. A. Zagorets, and A. F. Morgunov, Zh. Neorganich. Khim., 4, 700 (1959).
15. Yu. G. Frolov and V. V. Sergievskii, Transactions of the D. I. Mendeleev Moscow Chemicotechnical Institute [in Russian], No. 49 (1965), p. 190.
16. W. Müller and R. Diamond, J. Phys. Chem., 70, 3469 (1966).
17. W. Müller and G. Duyckaerts, Euratom Rep., 2246e (1965).
18. E. Lassettre, Chem. Rev., 20, 259 (1937).
19. R. Van Duyne et al., J. Phys. Chem., 70, 269 (1967).
20. N. A. Izmailov, The Electrochemistry of Solutions [in Russian], Khimiya, Moscow (1966).
21. G. Hardy et al., Trans. Faraday Soc., 60, 1626 (1964).
22. A. Apelblat, J. Chem. Soc., Ser. B, 175 (1969).
23. A. Curtis, in: The Chemistry of Extraction [Russian translation], A. A. Pushkov (editor), Atomizdat, Moscow (1971), p. 223.
24. Yu. G. Frolov et al., Radiokhimiya, 14, 578 (1972).
25. Yu. G. Frolov et al., Radiokhimiya, 14, 643 (1972).
26. Yu. Frolov et al., Proceedings of the International Conference on Solvent Extraction, Society of the Chemical Industry, London (1971), p. 1229.
27. Yu. G. Frolov, A. P. Zuev, and V. V. Sergievskii, Transactions of the D. I. Mendeleev Moscow Chemicotechnological Institute [in Russian], No. 71 (1972), p. 109.
28. Yu. G. Frolov, V. V. Sergievskii, and A. P. Zuev, Izv. VUZ, Khim. i Khim. Tekhnol., 15, 59 (1972).
29. G. Harned and B. Owen, The Physical Chemistry of Solutions of Electrolytes [Russian translation], IL, Moscow (1952).
30. O. Levy et al., J. Inorg. Nucl. Chem., 33, 551 (1971).
31. V. V. Sergievskii and Yu. G. Frolov, Zh. Strukt. Khim., 8, 891 (1967).
32. D. Flett, Solvent Extraction in Metallurgical Processes, Antwerpen, May 4-5 (1972).
33. E. Hegfeldt, Ion Exchange [Russian translation], Ya. M. Marinskii (editor), Mir (1968).
34. M. Robaglia and T. Kikindau, Compt. Rend. Acad. Sci., Ser. C, 271, 1036 (1970).

PECULIARITIES OF THE MASS TRANSPORT OF PLUTONIUM NITRATE IN POLYVINYL CHLORIDE PLASTIC

A. L. Kononovich, V. N. Klochkov, and D. S. Gol'dshtein

UDC 621.039.341

In the context of the problem of the decontamination of polymer protective coatings from plutonium isotopes, the question of the diffusion of the contaminant into the material is of central importance. In certain cases the adsorbed phase hinders the removal of the radioactive substance. In this work we study the diffusion of Pu^{239} from a solution of its nitrate into polyvinyl chloride plastic (formula 57–40), which is widely used in atomic technology.

The process of mass transport in polymers can be described by complex laws [1-3], which are frequently irreducible to Fick's law.

The purpose of the work was to follow experimentally the development of the adsorbed phase with the passage of time and to construct, insofar as possible, a simplified phenomenological model for the description of this process.

The method that we used in the work was to measure the distribution function of the α-active substance through the depth of the material, on the basis of the observation of the energy spectrum of α-particles [4]. Passing through a layer of material, α-particles lose part of their energy. The deeper that the α-active substance is found, the lower is the average energy of the particles when they emerge at the surface. The distribution of the substance through the depth of the material can be calculated according to the energy spectrum of α-radiation close to the surface. This method allows the distribution function to be determined with a resolution of 1-2 μ close to the surface and of 5 μ at a depth close to the length of the range of the α-particle in the given material.

Radioactive contamination caused by solutions of plutonium nitrate was considered. For their preparation we used a solution of plutonium nitrate in 2 N nitric acid, containing no less than 85% plutonium in the tetravalent state.

Before the beginning of the experiments the surface of the samples was thoroughly washed with distilled water and alcohol to remove possible extraneous contaminants, and then the samples were immersed in the active solution. Before the measurement, the samples, removed from the active solution, were rinsed with cold (no more than 12°C) distilled water and dried. After the end of the measurement, the samples were again placed in the solution. The time during which the samples were outside the radioactive solution did not exceed 30 min, i.e., was small in comparison with the total time of contamination. At the same time, we monitored the constancy of the specific activity of the solutions.

The results of the investigations showed that samples of plastic exposed for 690 h at a temperature of 42°C to solutions containing only the plutonium salt at a concentration of 0.3 μCi/ml and nitric acid (pH = 0.1 and 2.2) were contaminated only on the surface. No diffusion was detected. The explanation for this is that a well-dissociating salt is not extracted into nonpolar organic compounds from weak solutions of electrolytes [5, 6]. To create conditions promoting extraction, usually salts, so-called salting-out agents, are added to the solution.

In this work, sodium nitrate (7 eq/liter), recommended by Walker [7] and used by him for the study of the limits of deactivation of epoxide coatings, was used as the salting-out agent. The nitric acid concentration in the contaminating solution was 0.5 N.

Translated from Atomnaya Énergiya, Vol. 35, No. 2, pp. 117-119, August, 1973. Original article submitted September 11, 1972.

TABLE 1. Diffusion Coefficients and Rates of Displacement of the Beginning of the Count in the Sorption of Plutonium from Nitric Acid Solution*

Temperature, °C	Time, h	Diffusion coefficient, cm^2/sec	Rate of displacement of beginning of count, $g/cm^2 \cdot sec$
42	120 216 289 360	$8{,}3\cdot10^{-14}$ $8{,}3\cdot10^{-14}$ $8{,}3\cdot10^{-14}$ $8{,}3\cdot10^{-14}$	
Average value		$8{,}3\cdot10^{-14}$	$8{,}4\cdot10^{-11}$
52	48 96	$3{,}1\cdot10^{-13}$ $3{,}5\cdot10^{-13}$	
Average value		$3{,}3\cdot10^{-13}$	$8{,}4\cdot10^{-10}$
63	26 70	$1{,}3\cdot10^{-12}$ $1{,}4\cdot10^{-12}$	
Average value		$1{,}3\cdot10^{-12}$	$2{,}5\cdot10^{-9}$

*The values of the parameters were selected graphically.

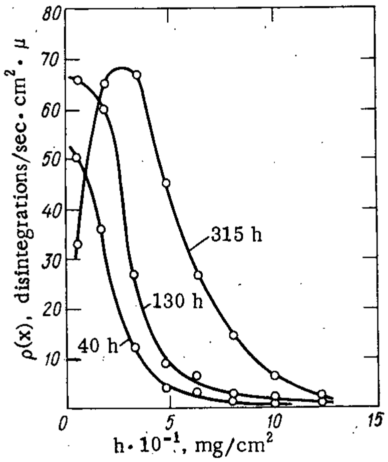

Fig. 1. Formation of an adsorbed phase of plutonium at the temperature 42°C.

In the contamination of samples from a solution of plutonium nitrate with sodium nitrate, we observed the formation of an adsorbed phase. The experiments were conducted at temperatures of 42, 52, and 63°C. The results of measurements obtained for various durations of the process are shown in Fig. 1.

Beginning at some value of the thickness, the specific activity of the layers close to the surface drops. This is probably due to a change in the properties of the plastic on account of swelling or chemical reaction with inactive components of the solution, or to a redistribution of the plasticizing additives. Thus, the process of mass transport is not Fick diffusion with a constant concentration on the surface. Nonetheless, the process was described using a model which assumes that the transport of activity in the volume of the plastic occurs according to Fick's law.

This model was brought into agreement with the experimental data by the subsequent introduction of a correction at the beginning of the depth reading.

In the case of the Fick's-law diffusion of a chemically unchanged substance, the distribution function of the sorbate through the depth of the plastic is determined by the expression [8]

$$\rho(x) = \rho_0 \operatorname{erfc} \frac{x}{2\sqrt{Dt}}, \tag{1}$$

where ρ_0 is the concentration of the substance close to the surface; x is the distance, counted perpendicular to the free surface into the depth of the sample; D is the diffusion coefficient; t is the time;

$$\operatorname{erfc} x = 1 - \frac{2}{\sqrt{\pi}} \int_0^x e^{-\alpha^2} d\alpha.$$

For a preliminary evaluation of the applicability of the model, we considered the experimental dependence of the amount of the sorbed substance on the time, determined by a measurement of the total amount of the substance according to the x-radiation of Pu^{239} [9]. It was shown that the amount of the radioactive substance is a linear function of $t^{0.5}$, just as in the case of Fick diffusion in a semiinfinite layer of the substance.

The distribution functions of plutonium in polyvinyl chloride plastic (see Fig. 1) are well described by Eq. (1), if we consider that the origin is not the surface of the material, but some point $x_0(t)$.

Table 1 presents the values of the diffusion coefficients and the rate of displacement of the beginning of the count for various moments of time at various temperatures. The origin of the displacement of the beginning of the count can be explained either by sweating out of a component of the plasticizer in which plutonium has low solubility or by a slow chemical reaction.

We should mention that the technology of the preparation of polyvinyl chloride plastics (formula 57-40) provides for the addition of stearin and barium stearate to it, which, being subsequently deposited on the surface, improve the deactivation properties of the material [10]. It can be considered proven that in such a plastic, when it is contaminated by a solution of plutonium nitrate with a salting-out agent, there is a penetration of Pu^{239} into the deep layers of the material, and the process of transfer is described approximately by Fick's law with some effective diffusion coefficient. The dependence of the diffusion coefficient on the temperature, within the limits of error, obeys the Arrhenius equation:

$$D = D_0 e^{-\frac{E_0}{RT}},$$

where T is the temperature, °K; R is the universal gas constant.

The corresponding activation energy $E_0 = 28 \pm 5$ kcal/mole. Such a high value of the activation energy shows that in the process of migration chemical reactions occur, the nature of which is not yet clear.

It is well known that the rate of displacement of the beginning of the count in the indicated temperature interval is approximately described by an exponential law. It is possible to estimate the activation energy of the process that is responsible for this phenomenon. Its value is 12-35 kcal/mole. This circumstance also is an indication of the chemical nature of the process.

LITERATURE CITED

1. J. Crank and G. Park, Trans. Faraday Soc., 47, 1072 (1951).
2. W. Barkas, Swelling Stresses in Gels, Forest Products Research Special Report No. 6, HMSO (1945).
3. F. Long and I. Watt, J. Polymer Sci., 21, 554 (1956).
4. A. L. Kononovich, N. V. Bogolapov, V. N. Klochkov, and I. E. Konstantinov, At. Énerg., 33, No. 5, 919 (1972).
5. A. S. Solovkin, Salting Out and the Quantitative Description of Extraction Equilibria [in Russian], Atomizdat, Moscow (1969).
6. G. Morrison and H. Freiser, Solvent Extraction in Analytical Chemistry, Wiley, New York (1957).
7. P. Walker, J. Oil and Colour Chemists' Assoc., 49, 117-136 (1966).
8. W. Jost, Diffusion in Solids, Liquids, and Gases. Rev., Academic Press, New York (1960).
9. A. L. Kononovich and I. E. Konstantinov, in: Medicotechnical Problems of Individual Protection of Man [in Russian], No. 10, Meditsina, Moscow (1972), p. 103.
10. S. M. Gorodinskii, V. L. Karpov, L. M. Nosova, et al., in: Protective Coatings in Atomic Technology [in Russian], S. M. Gorodinskii (editor), Gosatomizdat, Moscow (1963), p. 25.

SELECTION OF AN OPTIMUM ANALYTIC PROCEDURE DURING INSTRUMENT ACTIVATION ANALYSIS

A. N. Petrenko and B. Ya. Narkevich

UDC 543.53

The problem of the selection of an optimum analytic procedure during the instrument activation analysis of multicomponent samples is considered. The heart of the problem is the determination of optimum time parameters (exposure time t_1, delay after exposure t_2, and measurement time t_3), and the energy at which the identification of the radioactive isotope of interest is conducted, as well as the flux density of the activating particles guaranteeing the required accuracy of the analysis.

Criteria for the optimization of the analytic procedures utilized in the practice of activation analysis are considered; an expression for the criterion allowing one to analyze thoroughly the possibility of selecting optimum conditions is presented. The conditions under which limitations put on the counting statistics are fulfilled, with a slight deformation of the amplitude distribution for the pulses in the photopeak of the γ-line being analyzed caused by the superposition of the amplitude distributions of pulses in the photopeaks of background γ-lines, are described by the ratio of the analyzed and the background activities:

$$R=\frac{\sqrt{N_c+2N_{b_1}}}{N_c}+\frac{N_{b_2}}{N_c},$$

where N_c is the number of recorded pulses for an analyzed γ-line in its energy range; N_{b1} and N_{b2} are the numbers of recorded pulses in the energy range of the analyzed γ-line from the background γ-lines satisfying the conditions $|E - E_i| \geq 2\sigma(E)$ and $|E - E_j| < 2\sigma(E)$, respectively; E, E_i, and E_j are the energies of the analyzed and the corresponding background γ-lines; $\sigma(E)$ is the parameter of the Gaussian distribution characterizing the width of the photopeak.

It is shown that the criteria for the optimization recommended in [1-3] are particular cases of the criterion obtained. Great emphasis is laid on the generality of the criterion which ensures that it may be applied effectively for any values of N_c, N_{b1}, N_{b2}.

It is necessary to establish the extent to which the parameters obtained by calculational methods are optimum for the actual experimental conditions and the actual initial data, since the calculation is conducted for fully determined values of the nuclear-physical characteristics and the constants for the matrix elements of a sample, which are known with definite precision or can be varied under the experimental conditions. To solve this problem, a matrix was constructed such that the characteristics of its elements would ensure a minimum for the available N_c and maxima for N_{b1} and N_{b2}. The problem was reduced to the search

$$(R)_{\text{opt}}=\min_{t_1,\,t_2,\,t_3}\,(\max_{\mathscr{L}} R),$$

where $\mathscr{L}$ is a set of nuclear-physical characteristics and constants for the matrix elements of the sample.

The time parameters found in this way, guaranteeing $R \leq (R)_{\text{opt}}$ under the conditions of the experiment, should be regarded as the solution to the problem of the selection of an optimum analytic procedure.

The search for $(R)_{\text{opt}}$ was accomplished by the method of steepest descent. The algorithm constructed for the solution of the problem was realized by a program composed for a BÉSM-4 electronic computer. As an example, a calculation for the selection of an analytic procedure for the instrument

Translated from Atomnaya Énergiya, Vol. 35, No. 2, pp. 121-125, August, 1973. Original article submitted February 21, 1972.

activation analysis of several elements contained in 1 g of dry mammalian blood using a 14 MeV neutron generator is presented.

LITERATURE CITED

1. B. G. Egiazarov, V. A. Zyubko, and A. I. Novikov, At. Énerg., 24, 435 (1968).
2. B. G. Egiazarov, V. A. Zyubko, and R. P. Selyutin, At. Énerg., 27, 460 (1969).
3. S. Reynolds, Nucleonics, 22, No. 8, 104 (1964).

EFFECTIVE RESONANCE INTEGRAL FOR A WIDELY SPACED LATTICE AND FAST-NEUTRON MULTIPLICATION

A. Ya. Burmistrov and B. P. Kochurov

UDC 539.125.5.173.162.3:539.125.5.162.3

Fast neutrons are not uniformly distributed over a cell; the flux is higher in a slug than in the moderator. This is particularly important for a widely spaced lattice with a spectrum different from the Fermi spectrum and necessitates corrections to the resonance integral [1] by means of semiempirical formulas

TABLE 1. The Dependence of $\varepsilon - 1$ on a, ρ, and β for Graphite and Heavy Water Moderators

Moderator	ρ, cm	β	a, cm* 20	28,3	34,6	40
C	1,25	1,0	0,0444	0,0422	0,0417	0,0415
	1,75		0,0613	0,0575	0,0566	0,0562
	2,5		0,0847	0,0781	0,0765	0,0758
D_2O	1,25	1,0	0,0385	0,381	0,0380	0,0379
	1,75		0,0520	0,0511	0,0509	0,0509
	2,5		0,0702	0,685	0,0682	0,0681
	3,0	1,0	0,0812	0,0788	0,0783	0,0782
		0,5	0,0474	0,0457	0,0454	0,0453
		0,25	0,0258	0,0248	0,0246	0,0246
		0,1	0,0109	0,0105	0,0104	0,0104
	4,0	1,0	0,1007	0,0963	0,956	0,0953
		0,5	0,0620	0,0586	0,0580	0,0578
		0,25	0,0347	0,0326	0,0322	0,0321
		0,1	0,0150	0,0140	0,0138	0,0138
	5,0	1,0	0,1176	0,1106	0,1093	0,1089
		0,5	0,0765	0,0705	0,0695	0,0691
		0,25	0,0442	0,0401	0,0395	0,0392
		0,1	0,0195	0,0175	0,0172	0,0171
	6,0	1,0	0,1328	0,1221	0,1202	0,1197
		0,5	0,0915	0,0815	0,0799	0,0794
		0,25	0,0548	0,0476	0,0465	0,0461
		0,1	0,0248	0,0211	0,0206	0,0204

*a, lattice pitch, cm.

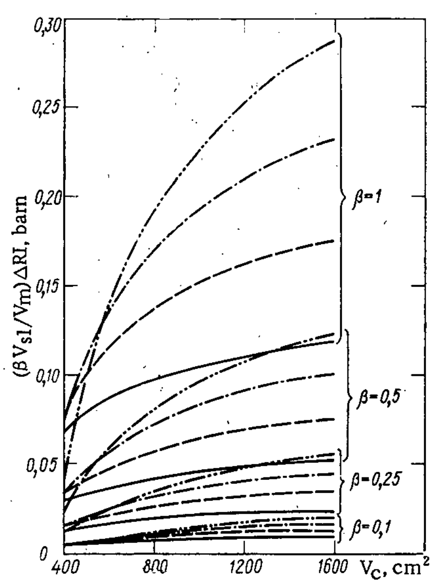

Fig. 1. $(\beta V_{sl}/V_m)\Delta RI$ as a function of the volume of a heavy water cell V_c, the uranium fraction of a slug β, and the slug radius ρ: – ·· –) 6 cm; – · –) 5 cm; – – –) 4 cm; ——) 3 cm.

Original article submitted June 28, 1972; abstract submitted April 3, 1973.

[2]. The fast fission factor ε for a 0.8 MeV fission threshold (Table 1) and the correction to the resonance integral ΔRI in the 10 keV to 0.8 MeV range (Fig. 1) were calculated by a program based on the solution of a multigroup system of Peierls integral equations in a multizone cylindrical cell. Assuming identical spatial and energy distributions of sources due to fast and thermal neutron fissions, the solution is obtained by a single calculation with subsequent source renormalization. The error introduced by this assumption can be removed by an iterated calculation. The fast fission factor ε and the resonance escape probability φ in the 10 keV to 0.8 MeV energy range are written as bilinear functionals of the neutron flux.

The effect of the reflection of neutrons from the moderator into a slug is more important for graphite than for heavy water (Table 1) because there is a smaller energy loss in scattering in graphite. As the lattice pitch is decreased there are more straight paths of neutrons from slug to slug and ε is increased. The increase in ΔRI with cell volume V_c is caused by the increase in the nonuniformity of the neutron distribution over the cell. The value of ΔRI is approximately one third as large for a graphite moderator as for heavy water. Replacing the fission spectrum by the delayed neutron spectrum increases the correction ΔRI by a factor of about 2.5.

LITERATURE CITED

1. V. I. Naumov and L. N. Yurova, in: Physics of Nuclear Reactors [in Russian], L. N. Yurova (editor), No. 1, Atomizdat, Moscow (1968), p. 133.
2. E. Hellstrand, in: Reactor Physics in Resonance and Thermal Regions, Vol. 2, MIT Press, Cambridge (1966), p. 151.

AN APPROXIMATE METHOD FOR PREDICTING THE VERTICAL MIGRATION OF RADIOACTIVE CONTAMINATIONS IN SOILS

V. M. Prokhorov and M. V. Ryzhinskii

UDC 631.43

A simple approximate method for predicting the migration of radioactive isotopes along the profiles of soils is proposed, assuming that the migration is of a diffusive (or quasidiffusive) character, and that the equations of a homogeneous medium are applicable to inhomogeneous media. The unique characteristic of the migration is the apparent diffusion coefficient, which takes on several values (according to the number of layers of soil with different properties), and which is determined by only one piece of data: the vertical distribution of the radioisotope. The method is insensitive to the boundary conditions, which allows the actual conditions at the surface of the soil to be reduced to three cases: a single contamination, a constant concentration of radioisotopes, and a linearly increasing concentration of radioisotopes. Formulas for performing the calculations in these cases are presented, along with graphs for practical calculation of the migration.

An analysis is conducted of previously published data for the migration of once-introduced Sr^{90} in eight homogeneous soils and also for migration in 12 inhomogeneous soils of Sr^{90} which reached the Earth as a result of global fallout. In the case of homogeneous soils, the relative differences between the calculated and actual values of Sr^{90} content, averaged over the layers and sampling periods, varied between 25 and 43% for the various soils. The mean absolute deviations were at most 0.05–0.08 (taking the total Sr^{90} content in the soil profile to be equal to one). In the case of inhomogeneous soils, the average over sampling periods of the relative deviations ranged between 3.6 and 37%, with a spread of between 15 and 22% in the deviations when averaged over the layers and sampling periods; in this case the mean absolute deviations were between 0.02 and 0.07. The method is useful for making approximate estimates of the temporal redistribution of radioisotopes both in homogeneous soils and in soils the composition of which varies with depth.

Original article submitted July 17, 1972; abstract submitted February 8, 1973.

DYNAMICS OF FUEL IN A PULSED REACTOR

OSCILLATIONS OF A ROD WITH A SHELL

V. L. Lomidze

UDC 621.039.553.3

In the fast (~100 μsec) extraction of heat in the fuel of a pulsed reactor, the temperature expansion of the material is counteracted by inertial forces, which are the cause of the oscillations and stresses in the fuel rods and the support structures [1].

In the paper we investigate the dynamics of a fuel element under conditions characteristic of a pulsed reactor. The element is a thin fuel rod of length L, suspended in a thin shell of length $L_s > L$ for a fixed upper end (at $x = L_s$). The lower end of the rod ($x = 0$) rests on the bottom of the shell. The heating of the core follows the law $T(x, t)$, and up to the moment t_j of its subjump the motion of the fuel element is described by a system of two wave equations, the solution of which has a comparatively simple form, if the function $T(x, t)$ is used in the form

$$T(x, t)=\left(\delta_a+\delta_0 \sin \frac{\pi x}{L}\right) T(t). \tag{1}$$

Here δ_0 and δ_a are the components of the coefficient of variation of the heat release, when $\delta_a + (2/\pi)\delta_0 = 1$; and $T(t)$ is the heating averaged over the length of the rod at the moment t. The stresses in the shell are expressed by the equation

$$\sigma_s(z)=\frac{E_s}{1+\gamma}\begin{cases} \dfrac{\alpha\delta_a}{\lambda} T\left(\dfrac{z}{c_s}\right)-\xi_z'\left(\dfrac{z}{c_s}\right), & (0<z<\lambda L); \\ \dfrac{\alpha\delta_a}{\lambda} T\left(\dfrac{z}{c_s}\right)-\xi_z'\left(\dfrac{z}{c_s}\right)-\dfrac{2\alpha\delta_a}{\lambda} T\left(\dfrac{z-\lambda L}{c_s}\right), & (\lambda L<z<2\lambda L); \\ \dfrac{\alpha\delta_a}{\lambda} T\left(\dfrac{z}{c_s}\right)-\xi_z'\left(\dfrac{z}{c_s}\right)-\dfrac{2\alpha\delta_a}{\lambda} T\left(\dfrac{z-\lambda L}{c_s}\right)+\dfrac{2\alpha\delta_a}{\lambda(1+\gamma)} & \\ \quad\times T\left(\dfrac{z-2\lambda L}{c_s}\right)+\dfrac{2\gamma}{1+\gamma}\xi_z'\left(\dfrac{z-2\lambda L}{c_s}\right), & (2\lambda L<z<2L_s), \end{cases} \tag{2}$$

where E_s and $\gamma = \rho_s c_s/\rho_c$ are the modulus of elasticity and the rigidity of the shell; $\rho(\rho_s)$ and $c(c_s)$ are the linear density and the velocity of sound in the rod (shell); $L_s/c_s > L/c$, $\lambda = c_s/c$; α is the coefficient of linear expansion of the fuel; $z = c_s t - x$;

$$\xi(t)=-\alpha\delta_0 c\int_0^t \sin\frac{\pi c}{L}t' T(t-t')\,dt'. \tag{3}$$

In particular, if $T(t) = T_0(t/\tau)$ on the segment $[0, \tau]$ and is constant for $t \geq \tau$, the maximal stresses depend on the variation in the heat release and the heating time τ as follows:

$$\sigma_{sm}=\frac{\alpha T_0 E}{\lambda(1+\gamma)}\begin{cases} \delta_a=\delta_0\dfrac{\sin\frac{\pi}{2}\theta}{\frac{\pi}{2}\theta}, & \left(0\leqslant\theta\equiv\dfrac{\tau c}{L}\leqslant 1\right); \\ \dfrac{1}{\theta}, & \theta\geqslant 1. \end{cases} \tag{4}$$

TABLE 1. Dependence of Stresses σ_{sm} in the Shell, the Impulse J, and the Velocity v_j of the Subjump of the Rod on the Heating Time θ

θ	σ_{sm}, kgf/m^2·°C	J, kgf·sec/m^2·°C	v_j, cm/sec·°C	$\gamma=\infty$ J	$\gamma=\infty$ v_j
0	1,6·10^5	4,28	1,02	17,64	4,20
1,2	1,3·10^5	3,49	0,83	14,38	3,41
2,29	0,7·10^5	0,43	0,29	5,08	1,21

The impulse (kgf·sec/m²) obtained by the rod for the subjump is

$$J=\frac{\gamma}{1+\gamma}\alpha T_0 E\frac{L}{c}\begin{cases} 1-\left[\frac{1}{4}\delta_a\theta+\frac{\delta_0}{\pi}\left(1-\frac{\sin\pi\theta/2}{\pi\theta/2}\right)\right] & (0\leqslant\theta\leqslant 2); \\ \frac{1}{\theta} & \theta\geqslant 2. \end{cases} \tag{5}$$

Original article submitted August 28, 1972; abstract submitted March 9, 1973.

Equations (4) and (5) show that the spatial dependence of the temperature only appears for heating times $\tau < L/c$ and $\tau < 2L/c$, respectively. It turns out that σ_{sm} depends considerably on the variation in heat release for very fast heating ($\tau \ll L/c$), whilst the impulse J is sensitive to the quantity k_x only for $\tau \sim L/c$.

Table 1 gives data on the calculation of J and σ_{sm}, and also the speed of the subjump of the rod v_j for a steel shell ($L_s = 80$ cm; $c_s = 5 \cdot 10^5$ cm/sec; $E_s = 2 \cdot 10^{10}$ kgf/m^2) and the core from UO_2 ($L = 40$ cm; $c = 3 \cdot 10^5$ cm/sec; $E = 0.95 \cdot 10^{10}$ kgf/m^2; $\alpha = 1.4 \cdot 10^{-5}$ deg^{-1}). The function T(t) was used in the form $(T_0/2)(1 - \cos(\pi t/\tau))$ $(0 \le t \le \tau)$, which is closer to the actual situation. The variation in the heat release was taken into account by the coefficient $k_x = \delta_\alpha + \delta_0 = 0.519 + 0.754 = 1.273$.

LITERATURE CITED

1. J. Randles and R. Jaarsma, Some Problems of Stress Wave Production Encountered in the Study of Pulsed Fast Reactor Dynamics, EVR-3654e (1967).

DYNAMICS OF FUEL IN A PULSED REACTOR

TEMPERATURE SHOCKS IN RODS MADE FROM PELLETS

V. L. Lomidze

UDC 621.039.553.3

We consider the problem of the rapid heating of a thin fuel core of length L, consisting of a large number of elastic pellets. We investigate the effect of the dynamics of pellets that disintegrate as a result of the temperature shock on the kinetics of the pulsed reactor.

A rapidly heated column of pellets, up to the beginning of its disintegration into its components, can be assumed to be an entirely elastic rod, since during this time it undergoes only compressive stresses (owing to the inertia of the material to temperature expansion). A pellet with coordinate x breaks off, with velocity $v_j(x)$, from the part of the rod that has not yet disintegrated at the moment $t_j(x)$, when the compressive stresses at this point vanish. We can show that if, in the region of continuity of $t_j(x)$, the following condition is satisfied:

$$c\left|\frac{dt_j(x)}{dx}\right| \leqslant 1; \quad 0 \leqslant x \leqslant L, \tag{1}$$

i.e., the velocity of sound c in the material of the core nowhere exceeds the velocity of its disintegration, then in order to find the distributions $t_j(x)$ and $v_j(x)$ it is sufficient to use the solution of the problem on the stresses $\sigma(x, t)$ over the entire rod. If the column of pellets, initially at rest on the rigid base, is heated according to a stepwise linear law (i.e., $T(x, t) = T_0(t/\tau)$ for $0 < t < \tau$ and $T(x, t) = T_0 = \text{const}$ for $t > \tau$), condition (1) is satisfied everywhere in the indicated region and the distribution of the velocities of the pellets along the length of the rod takes the form

$$v_j(x) \equiv \frac{1}{\rho}\int\limits_0^{t_j(x)} \frac{\partial\sigma(x,t)}{\partial x}\,dt = \begin{cases} \left.\begin{aligned} &2\alpha T_0\frac{x}{\tau}, \quad 0 \leqslant x \leqslant \frac{\tau c}{2} \\ &\alpha c T_0, \quad \frac{\tau c}{2} \leqslant x \leqslant L \end{aligned}\right\} \tau \leqslant \frac{2L}{c}; \\ 2\alpha T_0\frac{x}{\tau}, \quad 0 \leqslant x \leqslant L; \qquad \tau \geqslant \frac{2L}{c}, \end{cases} \tag{2}$$

where ρ is the density of the fuel; α is the coefficient of linear expansion; and T_0 is the heating for time τ.

Taking account of the spatial dependence of the temperature characteristic for reactors, the form of $v_j(x)$ proves to be more complicated. Furthermore, in some region smaller than [0, L], the function

Original article submitted August 28, 1972; abstract submitted March 9, 1973.

$v_j(x)$ is found approximately, since, for nonuniform heat release, condition (1) is satisfied not everywhere in the region of continuity of $t_j(x)$.

The information on the distributions $t_j(x)$ and $v_j(x)$ allows us to estimate the reactivity $\varepsilon(t)$ introduced by the disintegrating pellets. For example, for the simultaneous subjump of all the pellets upward with initial velocity distribution $v_j(x) = \alpha c T_0(x/L)$, the indicated reactivity can be represented in the form

$$\varepsilon(y) = \varepsilon_{\exp} \frac{(\alpha c T_0)^2}{g} \begin{cases} y - \frac{1}{2} y^3, & 0 \leqslant y \leqslant 1; \\ 2y(1-y) + \frac{1}{2} y^3, & 1 \leqslant y \leqslant 2. \end{cases} \tag{3}$$

Here $g = 9.81$ m/sec^2; $y = gt/\alpha c T_0$ and $\varepsilon_{\exp}$ is the coefficient of reactivity based on the thermal expansion of the fuel. In order to derive this equation we assume that the reactivity introduced for a departure of unit length from the fuel rod depends linearly on x [1]. If $\alpha = 1.4 \cdot 10^{-5}$ deg^{-1}; $c = 3 \cdot 10^3$ m/sec; $T_0 = 10°C$; and $\varepsilon_{\exp} = -0.015$ cm^{-1}, the extremal value (3) will equal -0.0147. The moment $y = 2$, when the reactivity (3) vanishes, corresponds to 0.0857 sec. For a frequency of 50 sec^{-1} the distance between the power pulses is 0.02 sec. Hence it follows that the four following pulses will not be realized, since the instantaneous supercriticality, which should be produced by then, is approximately 10^{-3}. We see that under such conditions it is not possible for the reactor to operate stably. Furthermore, such a mode is also inadmissible according to the conditions of nuclear safety (especially at low frequencies, when the temperature coefficient of reactivity has a considerable effect).

LITERATURE CITED

1. J. Randles, J. Nucl. Energy, P. A/B, 20, No. 1, 1-16 (1966).

CHOICE OF THE OPTIMUM VALUE FOR THE CONCENTRATION OF THE KEY ISOTOPE IN THE WASTE SECTION OF A CASCADE USED IN SEPARATING MULTICOMPONENT ISOTOPE MIXTURES

N. A. Kolokol'tsov,* N. I. Laguntsov, and G. A. Sulaberidze

UDC 621.039.31

In [1] we discussed so-called Q-cascades, which can be used for separating a multicomponent isotope mixture into two groups of isotopes: a lighter group and a heavier group. The separation in the cascade takes place in such a way that the isotope concentrations in one group (including the intermediate key isotope or the generated isotope) in the outlet of the cascade will increase, while the concentrations of the other group will sharply decrease. Since enrichment takes place in the entire group, the concentration of the key isotope in the outlet of the Q-cascade will be bounded. This follows directly from the formula for the ratio of the concentrations of any i-th and n-th isotopes in the outlet of a Q-cascade with s_P stages in the product section and s_W stages in the waste section:

$$\frac{c_{iP}}{c_{nP}}=\frac{\exp(Q_i s_W)-1}{\exp(Q_n s_W)-1}\cdot\frac{\exp(Q_n s_W)-\exp(-Q_n s_P)}{\exp(Q_i s_W)-\exp(Q_i s_P)}\,\frac{c_{iF}}{c_{nF}},\tag{1}$$

where c_{iF} and c_{nF} are, respectively, the concentrations of the i-th and n-th isotopes in the feed; Q_i are constants related by the following equation:

$$Q_i-Q_n=\varepsilon_{in}\tag{2}$$

(here ε_{in} is the enrichment factor for the isotope vapors numbered i and n).

If n is the number of the key isotope and the isotopes are numbered in order of increasing mass, then the Q_i are chosen in such a way that all the values for $i \leq n$ will be positive and all those for $i > n$ will be negative. Then for cascades with a sufficiently long product section, i.e., for any i such that $\exp(|Q|\,s_P) \gg 1$ [see Eq. (1)], we obtain a limiting value for the concentration of the key isotope, $c_{nP}^{\max}$, for a selected number of stages in the section, s_W:

$$c_{nP}^{\max}\approx\frac{c_{nF}}{\sum\limits_{i=1}^{n}\beta_i c_{iF}},\tag{3}$$

where

$$\beta_i=\frac{1-\exp(-Q_i s_W)}{1-\exp(-Q_n s_W)}.\tag{4}$$

The number of stages s_W and the concentration c_{nW} of the key isotope in the waste section are related by the formula

$$c_{nW}\approx\frac{c_{nF}\exp(-Q_n s_W)}{\sum\limits_{i=1}^{n}c_{iF}\exp(-Q_i s_W)+\sum\limits_{i=n+1}^{m}c_{iF}}\tag{5}$$

(m is the number of components in the mixture).

*Deceased.

Translated from Atomnaya Énergiya, Vol. 35, No. 2, pp. 127-128, August, 1973. Original letter submitted April 25, 1973.

In the limiting case, as $s_W \to \infty$, Eq. (3) takes on the form [2]:

$$c_{nP}^{\max} \approx \frac{c_{nF}}{\sum_{i=1}^{n} c_{iF}}, \tag{6}$$

and as $s_W \to 0$, we have

$$c_{nW}^{\max} \approx \frac{c_{nF}}{\sum_{i=1}^{n} \frac{Q_i}{Q_n} c_{iF}}, \tag{7}$$

where $Q_i/Q_n \geq 1$ $(i = 1, \ldots, n)$. Thus, the maximum admissible value $c_{nW}^{\max}$ of the concentration when there is a waste section is given by the relation

$$\frac{c_{nF}}{\sum_{i=1}^{n} \frac{Q_i}{Q_n} c_{iF}} < c_{nP}^{\max} < \frac{c_{nF}}{\sum_{i=1}^{n} c_{iF}}. \tag{8}$$

If the concentration c_{nP} of the key isotope is given, we can find from (3), (4), and (5) the value of $c_{nW}^{\max}$ corresponding to the minimum length $(s_W)_{\min}$ of the waste section. Since we have assumed that $\exp(|Q_i| s_P) \gg 1$, then, as $c_{nW} \to c_{nW}^{\max}$, the total flow through the cascade increases beyond all bounds.

The required c_{nP} value can be obtained for any values $s_W > (s_W)_{\min}$; as s_W increases, s_P will naturally decrease. As $s_W \to \infty$ (i.e., as $c_{nW} \to 0$), the total flow will also increase beyond all bounds, and consequently the optimum value s_W (or c_{nW}) corresponding to the minimum ΣL will lie in the interval between $(s_W)_{\min}$ and $s_W \to \infty$.

Because of the presence of an optimal waste section in multicomponent separating cascades they are substantially different from two-component cascades, in which the minimum ΣL always corresponds to the case $s_W \to 0$, and in which, furthermore, there is no restriction on the choice of the limiting value of the enriched-isotope concentration.

LITERATURE CITED

1. N. A. Kolokol'tsov et al., At. Énerg., 29, No. 6, 425 (1970).
2. V. P. Minenko, At. Énerg., 33, No. 2, 703 (1972).

X-RAY DIFFRACTION STUDIES OF THE THERMAL EXPANSION OF NEPTUNIUM DIOXIDE

L. V. Sudakov, I. I. Kapshukov, and V. M. Solntsev

UDC 541.45:546.799.3

Np^{237} dioxide has been gaining increasing favor in practical applications, but data on the thermal expansion of NpO_2 is not yet to be found in the literature.

We measured the thermal-expansion coefficient of the crystal lattice of $NpO_{2.00 \pm 0.01}$ over the temperature range from room temperature to 1000°C, using the high-temperature x-ray diffraction method. The stoichiometry of the specimens was determined by a procedure described elsewhere [1]. We used a thin-walled hermetically sealed quartz capillary tube containing ~1 mg NpO_2 in the x-ray investigation; platinum served as standard. The platinum lines were consulted in determining the temperature (±10°C), and data on the thermal-expansion coefficient of platinum were taken from [2].

The diagram (Fig. 1) shows how the lattice constant of NpO_2 varies as a function of the temperature (mean error $\Delta a = \pm 0.001$ Å). Over the temperature range from room temperature to 700°C, the thermal-expansion coefficient of neptunium dioxide remains constant at $9.5 \pm 0.15 \cdot 10^{-6}$ deg^{-1}; as the temperature rises, the linear expansion coefficient follows suit, to attain a value of $11.0 \pm 1.0 \cdot 10^{-6}$ deg^{-1} at 1000°C.

The data obtained are in close agreement with values of the thermal-expansion coefficient reported for dioxides of other actinoid elements [3, 4].

The authors are indebted to V. P. Sheshunov for his kind assistance in conducting the experiment.

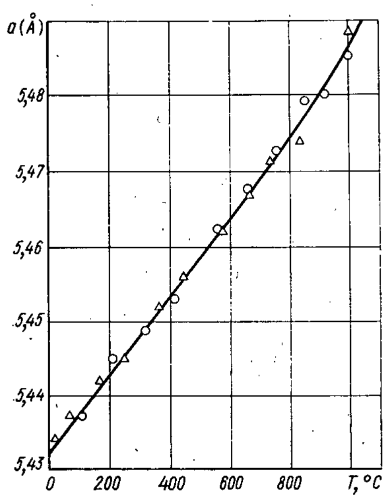

Fig. 1. Variation of the crystal lattice parameter of NpO_2: △) on heating; ○) on cooling.

LITERATURE CITED

1. L. V. Sudakov, V. M. Solntsev, I. I. Kapshukov, Yu. I. Belyaev, and V. M. Chistyakov, NIIAR Preprint P-138 [in Russian], Dimitrovgrad (1972).
2. V. A. Finkel', High-Temperature X-Ray Diffraction Studies of Metals [in Russian], Metallurgizdat, Moscow (1968).

Translated from Atomnaya Énergiya, Vol. 35, No. 2, p. 128, August, 1973. Original letter submitted May 4, 1972.

3. C. Kempter and R. Elliott, J. Chem. Phys., 6, 1524 (1959).
4. P. Baldock et al., J. Nucl. Materials, 18, No. 3, 305 (1966).

DETECTION OF IONIZING RADIATION BY MEANS OF A DIELECTRIC LIQUID IN AN ELECTRIC FIELD

A. P. Suslov, V. S. Zavgorodnii, and G. N. Patrushev

UDC 539.1.074

In the present study an attempt is made to make use of the pondermotive forces generated in a liquid dielectric in order to detect the energy absorbed from ionizing radiation.

If the plates of a parallel-plate capacitor are partially immersed in a liquid dielectric (with the other part remaining in air) and a voltage is supplied to them, there occurs a displacement of the liquid dielectric in the space between the electrodes, given approximately by the expression [1]

$$h_0 = \frac{\varepsilon_0 (\varepsilon_l - \varepsilon_g) u_0^2}{2\rho g d^2 \cos\varphi}, \tag{1}$$

where h_0 is the displacement of the liquid dielectric caused by the electric field; u_0 is the voltage applied to the electrodes; ε_g and ε_l are the relative permittivities of the gas and liquid dielectrics, respectively; ρ is the density of the liquid dielectric; ε_0 is the electric constant; g is the gravitational acceleration; d is the interelectrode spacing; and φ is the angle between the longitudinal axis of the electrodes and the direction of the force of gravity.

A change in the conductivity of the elevated liquid dielectric occurs as a result of radiation, which in turn leads to an increase in the rate of displacement (settling) in the interelectrode space. A study of this phenomenon which takes into account the transients occurring in the nonlinear circuit consisting of a capacitance discharging through a resistance (the liquid and gaseous dielectrics) shows that the change of the height of the liquid dielectric in the interelectrode space is given by the equation

$$h_t = \frac{\varepsilon_0 (\varepsilon_l - \varepsilon_g) g_0^2 e^{-2\frac{t}{\tau(p)}}}{2\rho g d^2 \cos\varphi \left(C_0 + \Delta C e^{-2\frac{t}{\tau(p)}}\right)^2}, \tag{2}$$

where ΔC is the change in the capacitance of the capacitor (the system consisting of the liquid and gas) due to the rise of the liquid dielectric to a height h corresponding to an initial charge q_0; $\tau(p)$ is the time constant of the capacitor (the system of liquid and gas); C_0 is the capacitance of the capacitor for $q_0 = 0$.

A UÉDÉ-60-250 calibration apparatus was used to make the measurements. An RUM-13 x-ray apparatus was used as a radiation source. The operating ranges of tube voltage and current were 100-250 kV and 5-13 mA, respectively. The current stabilization was between 2 and 0.02%. The maximum error in the radiation dose rate was ±3%.

The radiation was detected by a specially prepared detector filled with kerosene which had been purified by double distillation under vacuum. The level of the liquid dielectric in the interelectrode space was read on a millimeter scale at certain values of the time interval τ which were measured with a timer, taking $\tau = 0$ at the beginning of the exposure to radiation. The maximum errors in the measurements were ±0.5 mm and ±0.1 sec, respectively.

The detector was charged to 4000 V. It was disconnected from the power supply and the timer was switched on at the instant that the irradiation began.

Translated from Atomnaya Énergiya, Vol. 35, No. 2, pp. 129-130, August, 1973. Original letter submitted July 4, 1972; revision submitted February 13, 1973.

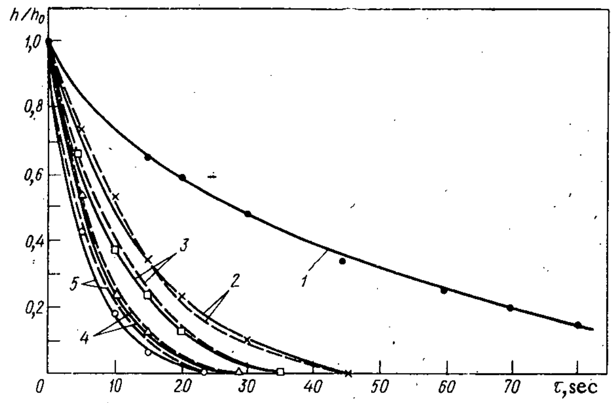

Fig. 1

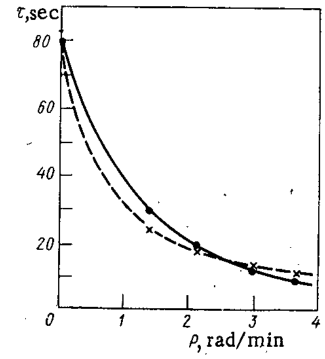

Fig. 2

Fig. 1. Level of the liquid dielectric as a function of time, for various dosage absorption rates (rad/min): 1) P = 0; 2) 1.42; 3) 2.142; 4) 3.04; 5) 3.642.

Fig. 2. Dependence of the time constant of the capacitor on the dosage absorption rate: ——) experimental; – – –) calculated.

The experimentally determined time dependence of the elevation of the liquid dielectric for various dosage absorption rates is shown in Fig. 1. The dependence of the time constant of the capacitor on the dosage absorption rate is shown in Fig. 2.

Figure 2 shows that the variation of the time constant of the capacitor with the dosage absorption rate can be fitted with a maximum error of ±15% by the following empirical formula:

$$\tau = \frac{\tau_0}{1+1.6P}, \qquad (3)$$

where P is the dosage absorption rate, rad/min; τ_0 is the time constant of the capacitor (for P = 0), sec.

The curves which were calculated by using Eqs. (2) and (3) are shown in Fig. 1 by dashed lines. It is clear from Fig. 1 that the difference between the absolute values of the theoretical and experimental curves is at most of the order of tenths of a millimeter (Δh_{max} = 0.83 mm). The relative error is ±40%. Such a large error is explained by the small absolute values of the height of the column of liquid in the lower part of the curve.

It can be concluded from the present study that it is possible in principle to utilize the pondermotive forces which arise in a liquid dielectric for the purpose of detecting an absorbed dose of ionizing radiation.

LITERATURE CITED

1. Yu. V. Tarasov, Trudy Leningradskogo Instituta, Aviats. Priborostroeniya, No. 58, 149 (1968).

INVESTIGATION OF THE RADIOACTIVITY OF DINOSAUR BONES WITH A HIGH-RESOLUTION GAMMA SPECTROMETER

T. Gun-Aazhav, Sh. Gérbish, O. Otgonsurén, Zh. Séréétér, and D. Chultém

UDC 539.106

Spectrum of γ-Quanta. In recent years several studies have appeared on the investigation of deposits of uranium in fossil bones of ancient animals [1-5]. In [2-3] the uranium concentration in ancient bones was determined by means of dielectric detectors directly according to the fission of U^{235} by thermal neutrons, and it was shown that dinosaur bones contain up to 10^{-3} g/g of U, i.e., 1 kg/ton of U, if we assume a ratio U^{238}/U^{235} equal to ~140. In [4, 5] the uranium content in the same bones was determined by the method of scintillation spectrometry according to the radiation of the decay products of U^{238}. A comparison of the spectra of the investigated sample and a mineral with a known uranium concentration showed that the uranium concentration in the bones of fossil dinosaurs also is tenths of a percent.

In this work we studied the γ-radiation spectrum of ancient bones with the aid of a Ge(Li) spectrometer with a high energy resolution (about 6 keV for the line 662 keV of Cs^{137}).

One of the measured spectra of a powdered sample of dinosaur bone is shown in Fig. 1a; Table 1 presents an identification of the lines of the sample.

The measured values of the γ-quantum energy coincide with high accuracy with the data of [6, 7], in which the γ-radiation of Ra^{226} and its decay products was investigated with a Ge(Li) spectrometer.

The observable γ-spectrum of the bones of ancient animals is a spectrum of natural radioactive series. Most of the observed lines belong to the uranium–radium series (chiefly RaB and RaC). Among the lines of the spectrum there are four lines of the thorium series (239, 910, 1595, 2615 keV) and one line of actinouranium (185 keV). Although such a ratio among the γ-radiations somewhat resembles the spectrum of equilibrium minerals of uranium and thorium [8], strict quantitative information on the content of these elements in the investigated samples cannot be obtained from these data. They permit only a qualitative conclusion that the ancient bone contains a rather large amount both of uranium [1-5] and of thorium.

Disturbance of Radioactive Equilibrium. The difficulty of the quantitative determination of uranium and thorium in bones according to their γ-activity is associated with the possible deviation from radioactive equilibrium. Since the age of the investigated bones, according to the data of the paleontological method, is about 70 million years, it can be considered with great probability that the time elapsed is sufficient for radioactive equilibrium to have been established between uranium and its products, regardless of whether all the uranium was in the bones from the very beginning (biochemical origin) or whether it accumulated over a long geological period (geochemical origin). However, other causes of deviation from radioactive equilibrium are also possible, for example, a disturbance of this equilibrium as a result of the removal of uranium from bones or the migration of its decay products (thorium, radium, radon, etc.). But on the other hand, if the process of accumulation of uranium in bones is due to its absorption from aqueous solutions by the isomorphous replacement of calcium ions by UO_2 ions [2, 3], then the absorbed uranium should be preserved in the bone as a result of the very poor solubility of calcium phosphate (hydroxyapatite) in water.

Mongolian State University, Ulan-Bator. Translated from Atomnaya Énergiya, Vol. 35, No. 2, pp. 130-132, August, 1973. Original letter submitted August 22, 1972; revision submitted January 19, 1973.

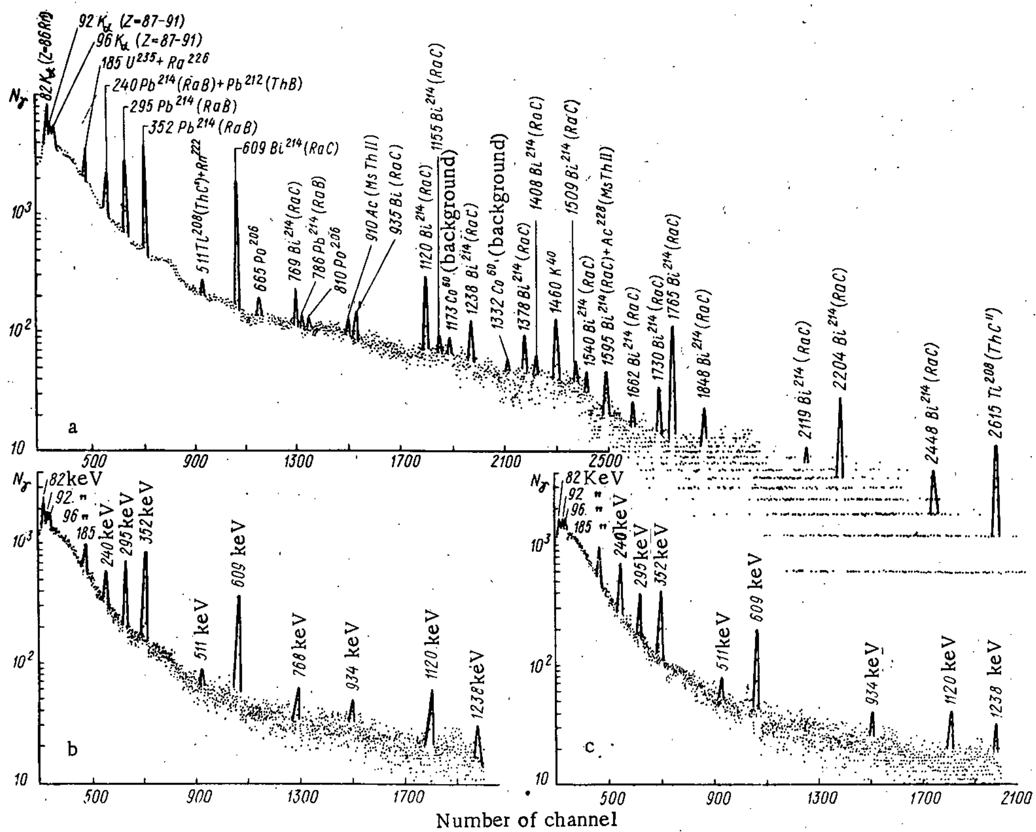

Fig. 1. Gamma spectrum of bones of ancient animals: a) exposure 10 h, weight of sample 300 g; b) exposure 1 h, weight of sample 50 g; c) the same exposure and geometry as in case b, but after heating of the sample at 700°C for 7 h.

TABLE 1. Identification of the Lines of the γ-Spectrum of Dinosaur Bone

Isotope	Energy of ν quantum, keV
K_α (Rn)	82
K_α (U)	96
Th^{234} (UX_1)	92
$Ra^{226}+U^{235}$	185
Pb^{214} (RaB)	240*, 295, 352, 786
Bi^{214} (RaC)	609, 769, 935, 1120, 1155, 1238, 1378, 1408, 1509, 1540, 1595†, 1662, 1730, 1765, 1848, 2119, 2204, 2448
Ac^{228} (MsTh II)	910
Tl^{208} (ThC")	2615
Tl^{208} (ThC")$+Rn^{222}$	511
K^{40}	1460
Co^{60} (background)	1173, 1332

*239 keV (ThB) + 242 keV (RaB).
†1595 keV (RaC) + 1593 keV (MsTh II).

Thus, in the opinion of the authors of this work, the basic role in the disturbance of radioactive equilibrium in ancient bones should be played not by processes of removal of the parent elements, but by the migration of the daughter elements in geochemical processes and the evolution of gaseous decay products (isotopes of radon).

For an illustration of the effect of emanation of radon, we investigated the dependence of the spectral composition of the γ-quanta of the bone on the conditions of diffusion. Bone powder weighing 50 g was heated at a temperature of 700°C for 7 h in a stream of nitrogen.

The γ-spectra of this sample taken before and after heating under entirely uniform conditions (geometry, duration of measurement, and system of operation of the spectrometer) are shown in Fig. 1b, c. The time interval between the end of heating and the beginning of measurement of the spectrum was 1 h, and the duration of measurement was 5 h.

In fact, as we had assumed, the intensity of the lines belonging to radon and its short-lived decay products proved substantially lower after heating than before heating. For example, the x-ray line 82 keV ($Z \approx 86$) and the lines 295 and 352 keV (RaB), 609, 768, 934, 1238 keV (RaC) were approximately halved. Just as we expected, the x-ray line 96 keV ($Z \approx 92$) and the compound line 185 keV ($U^{235} + Ra^{226}$) were unchanged. The intensity of the line 511 keV (ThC" + Rn) decreased by only 10%, while the intensity of the line 240 keV (RaB + ThB), on the contrary, increased by approximately 10%. The last two results are explained by the relatively long half-life (10.6 h) of ThB (Pb^{212}).

According to the general theory of diffusion, the release of radon from a uranium-containing substance will be determined by the structure of the material (particle size, porosity, etc.), the diffusion coefficients (which in turn are a function of the temperature and activation energy), and the time.

Our experiment showed that for bones of ancient animals the coefficient of evolution of radon is large, which is explained by its porous structure.

Therefore, the difference of the γ-activities of bone samples [5] taken from different localities and at different times of year (the temperature of the sand in the Gobi desert fluctuates greatly during the year) is more likely associated with the difference in the conditions of diffusion of radon than with the difference in the content of uranium in these bones and, consequently, it cannot characterize the uranium content of the corresponding regions. The same conclusion is confirmed by data obtained by the method of dielectric detectors.

From all the aforementioned it follows that the determination of the uranium content in different bone samples according to their γ-activities is possible only under definite conditions which ensure equilibrium in the radioactive series (for example, after their storage in an ampule for no less than one month).

Nuclear Paleontology. In connection with the detection of an increased content of natural radioactive elements in the bones of ancient animals, there arise questions of which the solution is of great significance for paleontology: the evaluation of the geological age of fossilized animals, the search for skeletons of these animals by a radiometric method, radiation safety of service personnel in paleontological museums and co-workers of laboratories, etc.

It should be noted that for a correct evaluation of the age of bones according to uranium and thorium it is necessary to know the rate of accumulation of these elements and the amount of radiogenic isotopes of lead. This question should become the subject of special investigations, while the well-known nuclear-physical methods of geochronology should be somewhat modified for the case of slow accumulation of the parent nuclei.

A study of the process of accumulation and migration of radioactive elements and their decay products in the bones of ancient animals may be of indirect interest for geology as well (in particular, for the geochemistry of uranium and thorium, phosphate minerals of the type of apatite, including phosphorite).

A study of the content in bones of other elements, primarily rare-earth elements, which are usually geochemically correlated with uranium and thorium, is also of great interest.

We should mention that in the investigations of the radioactivity and material composition of the bones of ancient animals (both elemental and isotopic) the methods of nuclear physics can be widely applied: nuclear spectroscopy, radiochemistry, mass spectrometry, and various forms of activation analysis. For the investigation of the chemical form of the uranium found in bones the method of nuclear γ-resonance spectrometry can be used.

The authors would like to thank co-workers of the Paleontological Laboratory of the Scientific-Research Institute of Geology in Ulan-Bator, R. Barsbold and D. Dashzévég, for kindly providing the valuable material – dinosaur bones – for the investigation.

LITERATURE CITED

1. K. Oakley, Analytic Methods of Dating Bones, Oxford (1954).
2. O. Otgonsurén, V. P. Perelygin, and D. Chultém, Nauch. Soobshch. Mongol'skogo Gos. Univ. (Ulan-Bator), No. 18 (1969).
3. O. Otgonsurén, V. P. Perelygin, and D. Chultém, At. Énerg., 29, 301 (1970).
4. I. Chadraabal et al., Proceedings of Mongolian State University [in Russian], Ulan-Bator (1970).
5. Z. Jaworowski and J. Pensko, Nature, 214, 161 (1967).
6. H. Maria and M. Ardisson, Compt. Rend. Acad. Sci. France, 265B, 787 (1967).
7. K. Ya. Gromov, B. M. Sabirov, and Ya. Ya. Urbanets, Izv. Akad. Nauk SSSR, Ser. Fiz., 33, 1646 (1969).
8. N. G. Gusev et al., Radioactive Isotopes as γ-Emitters [in Russian], Atomizdat, Moscow (1964).

THE PHOTOCHEMICAL SEPARATION OF HYDROGEN ISOTOPES USING DEUTERIUM-VAPOR TUBES

Yu. G. Basov, V. S. Greben'kov, and E. A. Oginskaya

UDC 621.039.335

It was emphasized in [1-3] that, in the presence of light radiation selectively exciting the molecules of the isotopes, effective separation can be obtained in the process of photochemical reaction. In this way, mercury isotopes were separated [1] using a mercury light source with monoisotopic filling.

The present paper presents a description of experiments on the separation of the protium and deuterium isotopes of hydrogen during the illumination of an oxygen–hydrogen gas mixture by deuterium-vapor tubes.

The choice of hydrogen for the conduct of the reaction was determined by the knowledge that the interaction of H_2 with O_2 occurs in the following stages [4]:

$$H_2(^1\Sigma_g) + h\nu \longrightarrow H(^2S) + H(^2S), \tag{1}$$

$$H(^2S) + O_2(^3\Sigma_g^-) \longrightarrow HO_2 \text{ (doublet)}, \tag{2}$$

$$HO_2 \text{ (doublet)} + H(^2S) \longrightarrow H_2O(^1A_1) + O(^3P), \tag{3}$$

$$O_2(^3\Sigma_g^-) + O(^3P) \longrightarrow O_3(S_0). \tag{4}$$

As is seen from this scheme, in this case the reaction occurs when the radiation acts only on hydrogen molecules. The oxygen atoms, formed in stage (3) or during the photodissociation of O_2, participate only in the formation of ozone. If, however, the temperature of the gas in the reaction vessel is maintained above 90°C, then ozone will not be produced in the reaction products. For the reaction, for example, of hydrogen with nitrogen, when ammonia is formed both in the reaction of H atoms with N_2 and in the reaction of N atoms with H_2 [5], the selective separation of hydrogen isotopes cannot occur due to the large contribution to the isotope effect of the stage with the participation of N and H_2.

In contrast to a low pressure mercury-vapor tube having a line spectrum of radiation in the ultraviolet region, hydrogen- and deuterium-vapor tubes are characterized by continuous radiation in this spectral region; therefore, we did not expect to obtain selective excitation of deuterium in the experiments conducted. However, since the intensity of the ultraviolet radiation of a deuterium-vapor tube is significantly higher than in a low-pressure hydrogen or mercury-vapor tube in the range of wavelengths corresponding to the dissociation energies for H_2 and D_2, it was possible to expect an increase in the separation factor for the isotopic molecules mentioned as compared with the data obtained for a mercury-vapor tube [3]. Therefore, a deuterium-vapor tube was selected for the conduct of a photochemical reaction with the participation of hydrogen, deuterium, and oxygen.

TABLE 1. Transmission Coefficients for Quartz Windows of Deuterium-Vapor Tubes

Window	λ, nm			
	160	186	220	270
First	0,79	0,85	0,90	0,92
Second	0,78	0,83	0,88	0,92

A diagram of the experimental apparatus is presented in Fig. 1. Two deuterium-vapor tubes, uniform in construction [6], 1 and 4, with an initial pressure for the D_2 equal to 8 mm Hg, were welded onto a cylindrical reaction tube 3; attached to the reaction tube were three tubes for connection with a gas cylinder 2, a circulation pump 5, and a collector 8. The pressure was measured by a manometer 6, and samples for gas and

Translated from Atomnaya Énergiya, Vol. 35, No. 2, pp. 132-134, August, 1973. Original letter submitted October 17, 1972.

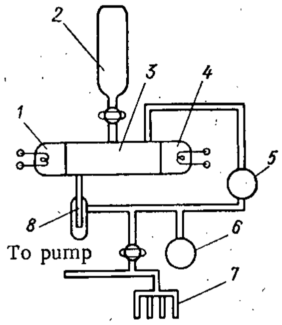

Fig. 1. Diagram of experimental apparatus.

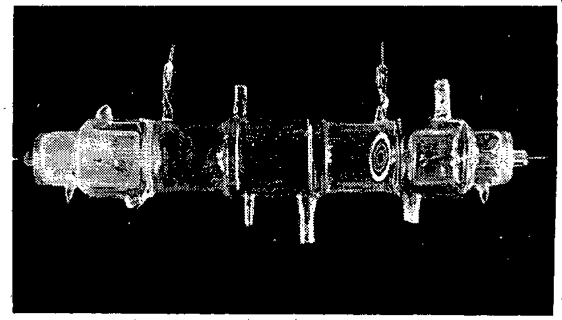

Fig. 2. Common form of photochemical reactor.

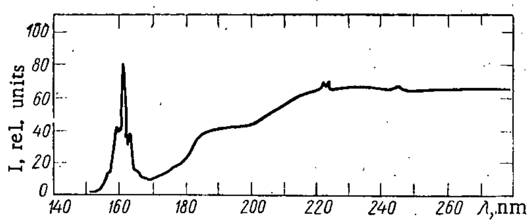

Fig. 3

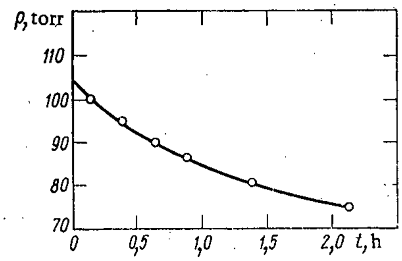

Fig. 4

Fig. 3. Radiation spectrum distribution for the quartz capillary tubes used in the experiments.

Fig. 4. Pressure variation during operation of apparatus.

isotope analysis by an MKh-1302 mass-spectrometer were collected in the ampules 7. Water vapor, formed in the photochemical reaction of hydrogen with oxygen under the influence of light radiation, was frozen out in the collector 8.

The experimental reactor utilized in the experiments is shown in Fig. 2. The photochemical reactor was welded to the glass components of the apparatus through glass connections.

The transmission coefficients for the quartz windows of deuterium-vapor tubes are cited in Table 1, from which it is seen that in the spectral region that we investigated ($\lambda \approx 270$ nm), corresponding to the dissociation energies of H_2 and D_2, the windows used transmitted ultraviolet radiation practically completely.

The spectral distribution for the quartz capillary tubes utilized in the experiment is presented in Fig. 3. From Fig. 3, it is seen that the spectrum of deuterium-vapor tubes is characterized by high-power emission bands at $\lambda \approx 160$ nm with a decrease in the intensity of the radiation for $\lambda = 165$-180 nm and a subsequent increase in continuous radiation with an increase in wavelength. It should be noted that tubes filled with H_2 have a similar form of spectral distribution, but with decreased intensity in the radiation at all wavelengths.

The $D_2 : H_2 : O_2$ reaction mixture was composed in the ratio 4 : 1 : 48. Deuterium in conformity with TU-6-02-628-71 was utilized. The oxygen and H_2 were purified and dried in a special apparatus before preparing the mixture.

The characteristic time-dependence for the pressure variation during the operation of the experimental apparatus is presented in Fig. 4. The initial pressure in the circulation system was 110 mm Hg. The total electrical power input to the tubes was 340 W.

As a result of the experiments it was learned that, during the photochemical reaction of hydrogen with oxygen with the formation of water, deuterium accumulates in the residue of an incompletely reacting gas with a separation factor of 2.3 ± 0.4. When conducting experiments in the course of 2-3 h, the enrichment factor was increased from 1.965 up to 2.36.

Thus, in the case being considered, the enrichment factor has substantially larger values than during the photochemical separation of hydrogen isotopes by means of a low-pressure mercury-vapor tube. In this connection, the method described for the separation of hydrogen isotopes can be utilized for the concentration of deuterium.

In conclusion, the authors express their appreciation to T. V. Nikol'skaya, V. N. Chibis, and V. V. Baraev for aid in the preparation of the experimental apparatus and the conduct of the experiments.

LITERATURE CITED

1. R. Pertel and H. Gunning, Canad. J. Chem., 26, 219 (1947).
2. Yu. G. Basov, At. Énerg., 32, 842 (1972).
3. B. U. Utirov et al., At. Énerg., 32, 169 (1972).
4. Yu. G. Basov, Candidate's Dissertation [in Russian], MGU (1968).
5. K. M. Salimov, Candidate's Dissertation [in Russian], MGU (1969).
6. A. M. Shupeneva et al., "A gas-discharge spectrum tube," Byul. Izobret., No. 36, 82 (1970).

COMPARISON OF TWO ALGORITHMS FOR THE EMERGENCY SHIELDING OF A REACTOR DURING REACTIVITY DISTURBANCES

A. A. Sarkisov and V. N. Puchkov

UDC 621.039.566.8

The difference between the emergency-shielding (ES) algorithms being compared is that, in one, the instantaneous value of the relative reactor power is bounded, $N/N_0 \leq (N/N_0)^*$, while, in the other, it is the relative rate of increase in neutron density n(t) that is bounded, i.e., the reactor-excursion period

$$T=\left[\frac{1}{n(t)}\cdot\frac{dn(t)}{dt}\right]^{-1}\geqslant T^*.$$

A similar problem was posed in [1], but the authors considered only cases of discontinuous introduction of reactivity, which allowed them to use the elementary kinetic equation to describe the process.

In the present work we studied the emergency modes of a water-cooled nuclear reactor using U^{235} fuel. Disturbances were introduced by changing the reactivity at certain constant rates.

In the mathematical description of the process, we used kinetic equations with six groups of delayed neutrons. The parameters β and l were chosen according to the recommendations of [2] for reactors of the given type ($\beta = 0.0064$; $l = 5 \cdot 10^{-5}$ sec). To simplify the description, we did not take the neutron space distribution into account and we assumed the one-group representation of the neutron spectrum to be valid. Moreover, we did not take into account the inverse temperature relationship, since our problem was to compare shielding algorithms for transient processes with the highest possible rate of reactivity introduction. The model would approximate more closely the experimental conditions if a negative inverse temperature relationship were included in it.

The study was made on an electronic model of the reactor neutron kinetics, which was realized on a MN-14 analog computer. We considered only operating (not start-up) reactor modes, in which the initial conditions are $N/N_{\text{given}} = 1$ and $\rho_0 = 0$. Disturbances were introduced by varying the reactivity ρ linearly at various rates ($\dot{\rho} = 8 \cdot 10^{-5}$-$120 \cdot 10^{-5}$ sec^{-1}).

The initial curves obtained with the model are the dependences $N/N_0 = f(\dot{\rho}, t)$ and $T = \varphi(\dot{\rho}, t)$. They are shown in Fig. 1 in generalized form.

Using the data obtained, the response rates of the emergency-shielding channels can be compared. Initially, we will assume that the shielding channel for the relative rate of neutron-density increase is inertialess ($\tau = 0$). Then for any given T^*, based on the data obtained from the model, we can construct a curve dividing the graph into two regions: a region of shielding actuation over N/N_0 and a region of actuation over T. In Fig. 2 such curves are shown for $T^* = 15$ sec. If the points are below the curve, the shielding is actuated only upon a signal that the given power level has been exceeded; if they are above the curve, shielding is actuated on a signal that the relative neutron-density rate of increase is inadmissible. Thus, when $\dot{\rho} = 20 \cdot 10^{-5}$ sec^{-1}, and setting $T^* = 15$ sec and $(N/N_0)^* = 1.2$, in all cases the shielding will be actuated by a signal that the given power has been exceeded.

Actually, the channels for measuring the period cannot be inertialess, since the differential amplifier used in them cannot, in principle, have a time constant equal to zero. Thus, the necessity arises for comparing the shielding-channel response times with various time constants τ of the differentiating

Translated from Atomnaya Énergiya, Vol. 35, No. 2, pp. 134-135, August, 1973. Original letter submitted October 18, 1972.

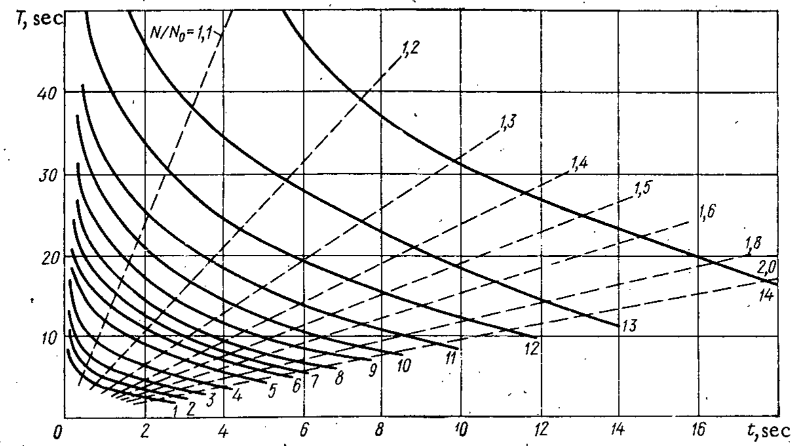

Fig. 1. Dependence of T and N/N_0 on the time t for various rates of introducing reactivity ρ: 1) $120 \cdot 10^{-5}$; 2) $100 \cdot 10^{-5}$; 3) $80 \cdot 10^{-5}$; 4) $60 \cdot 10^{-5}$; 5) $50 \cdot 10^{-5}$; 6) $40 \cdot 10^{-5}$; 7) $36 \cdot 10^{-5}$; 8) $32 \cdot 10^{-5}$; 9) $28 \cdot 10^{-5}$; 10) $24 \cdot 10^{-5}$; 11) $20 \cdot 10^{-5}$; 12) $16 \cdot 10^{-5}$; 13) $12 \cdot 10^{-5}$; 14) $8 \cdot 10^{-5}$ $\sec^{-1}$.

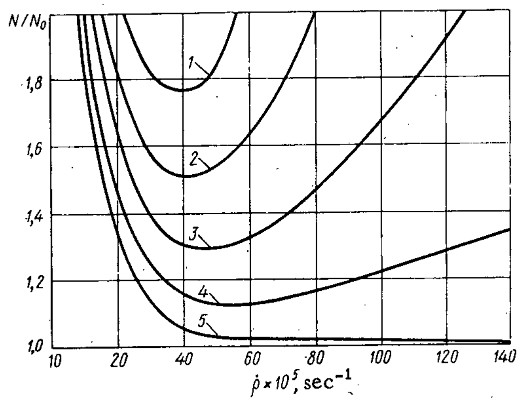

Fig. 2

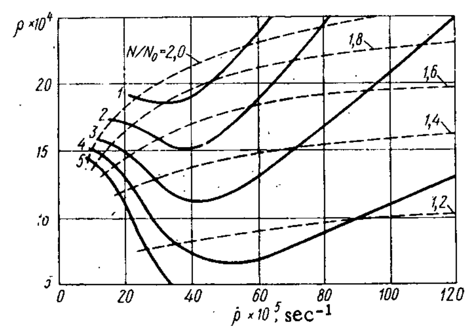

Fig. 3

Fig. 2. Limiting curves for various time constants τ: 1) 4; 2) 3; 3) 2; 4) 1; 5) 0 sec.

Fig. 3. Dependence of the reactivity introduced up to the instant of ES actuation by a signal $T^* = 15$ sec on the rate of introduction of reactivity and the time constant τ: 1) 4; 2) 3; 3) 2; 4) 1; 5) 0 sec.

network. For the variant being studied ($T^* = 15$ sec), such curves are shown in Fig. 2 for $\tau = 1$, 2, 3, and 4 sec.

In power reactors, it is uncommon to use power settings $(N/N_0) > 1.7$. It follows from Fig. 2 that when $\tau \geq 4$ sec, the shielding channel for T for such reactors is unnecessary in all modes except start-up.

The data obtained allow us also to determine the preferable form of shielding action when the ES is actuated by a T^* signal. If we take into account that $\dot{\rho} t = \rho$, then for a given T^* the initial dependences may be presented in the form $\rho = \psi(\dot{\rho}, \tau)$, as we show, for example, for $T^* = 15$ sec in Fig. 3. Analyzing the curves in Fig. 3, we can conclude that, when the channel for shielding the neutron-density relative-increase rate has a higher response rate, the signal for shielding actuation appears at lower reactivity values. Consequently, it is unnecessary to introduce "heavy" ES absorbing rods into the reactor. It is sufficient to stop the reactivity increase by sending a signal prohibiting extraction of the absorbers, or, when necessary, to introduce a "lightened" group of emergency-shielding rods into the reactor.

LITERATURE CITED

1. V. I. Kazachkov and A. S. Alpeev, At. Énerg., 31, No. 6, 627 (1971).
2. G. Keepin et al., Phys. Rev., 107, 1044 (1957).

TEMPORAL STATISTICAL STRUCTURE OF GLOBAL RADIOACTIVE FALLOUT ON THE OCEAN

K. G. Vinogradova, O. S. Zudin, B. A. Nelepo, and A. G. Trusov

UDC 614.73:543.053

It is known that the fluxes of global radioactive fallout on various parts of the Earth's surface fluctuate considerably both in space and in time. Since the distribution of global fallout has been previously elucidated through a circulation scheme for the fallout of radioactive aerosols from the atmosphere, in so doing a geographic factor has been established in the density of the fallout [1], during the investigation of which special attention was directed to the distribution with respect to the seasons of maxima in the concentration of the contamination of the ground layers of the atmosphere in the Northern and Southern Hemispheres.

There are several hypotheses explaining the planetary distribution of radioactive fallout, among which, in our opinion, special interest attaches to a compromise theory of a weather–climatic approach to the process of the fallout of radioisotopes associated with atmospheric deposits [2, 3]. However, in connection with the lack of experimental data on the fallout of radioisotopes over the surface of the ocean, it was impossible to form conclusions regarding the features of this approach. At the present time, few works are known in which the density of the fallout upon the ocean would be evaluated. For a description of the processes occurring in layers of the atmosphere adjacent to water, it is impossible to employ the regularity of the fallout of radioactive deposits upon dry land because the assumption concerning their uniformity is not verified [1]. Utilization of radioisotopes as tracers allows one to predict these processes and to determine their intensity at the surface of the ocean.

American investigators at weather centers obtained representative time sequences of observations for the fallout of Sr^{90} [4]. The density of strontium fallout was measured at fixed stations in the Atlantic Ocean (No. 1: 56°30' N lat., 51° E long.; No. 2: 52°45' N lat., 35°30' E long.; No. 3: 44° N lat., 41° E long.; No. 4: 35° N lat., 48° E long.) in the period from the middle of 1965 until June, 1971. However, the preliminary analysis of the density of Sr^{90} fallout for the measurements conducted (about 500) presents some difficulties. Consequently, for the analysis of the density distribution of the fallout, the data obtained was subjected to a statistical treatment. The time sequences proved to be representative. On the basis of this data, distribution functions were plotted and the moments for the distribution of Sr^{90} fallout from the atmosphere were calculated. Data beginning with 1966, i.e., at the time when the level of the average annual fallout was stabilized, was considered for the calculation of the fallout distribution functions [2, 3].

The arithmetic mean values $\bar{f}$, the root-mean-square deviations σ and σ_{unbi} (biased and unbiased estimate), the asymmetries A and A_{unbi}, the excesses E and E_{unbi}, and the statistical errors in their determination (m_{av}, m_σ, m_A, and m_E, respectively) are presented in Table 1.

Besides the statistical errors, it is necessary to take into account the errors in the measurements typical of the experimental data being used. Since the data contains only two significant figures after the decimal point, this error must not be less than ±0.005. The distribution function obtained at station No. 3 is shown in Fig. 1. The significant spread in the results is connected, obviously, with errors in the original data. Fairly accurate agreement is obtained by the comparison of a smoothed-out density function with the empirical density function of a normal distribution truncated at the point 0. The normal truncated distribution is characterized by two parameters of the original normal distribution and two truncation points:

Translated from Atomnaya Énergiya, Vol. 35, No. 2, pp. 136-138, August, 1973. Original letter submitted March 5, 1973.

TABLE 1. Results of Mathematical Treatment at Four Stations

Station No.	Observation time	Station coordinates: N lat.	Station coordinates: E long.	No. of measurements	$\bar{f}$	m_{av}	σ	σ_{unbi}	m_σ	A	A_{unbi}	m_A	E	E_{unbi}	m_E	f_0	σ_n	$\hat{f}$	σ^*
1	January 1966-April 1971	56°30′	51°00′	85	0,032	0,03	0,027	0,027	0,0017	1,48	1,49	0,02	2,49	2,65	0,04	0,02	0,025	0,03	0,018
2	January 1966-April 1971	52°45′	35°30′	84	0,044	0,005	0,042	0,042	0,0027	2,08	2,09	0,02	5,22	5,48	0,05	0,02	0,04	0,04	0,03
3	January 1966-February 1971	44°00′	41°00′	82	0,052	0,006	0,054	0,054	0,0034	3,12	3,14	0,03	12,85	13,4	0,05	0,02	0,05	0,05	0,03
4	January 1966-March 1971	35°00°	48°00′	80	0,048	0,06	0,053	0,054	0,0035	3,46	3,48	0,03	15,7	16,5	0,05	0,02	0,04	0,04	0,03

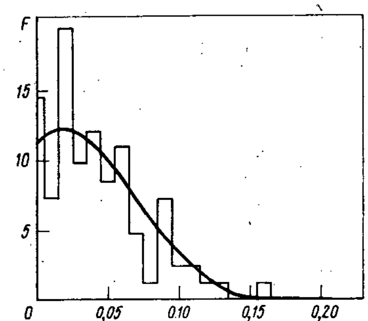

Fig. 1

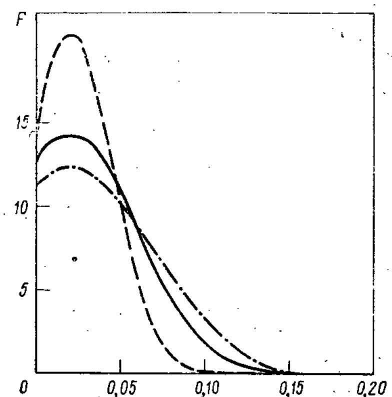

Fig. 2

Fig. 1. Histogram and distribution function for the density of Sr^{90} fallout for station No. 3.

Fig. 2. Density distribution functions for Sr^{90} fallout: – – –) station No. 1; ———) Nos. 2 and 3; – · –) No. 3.

$$F(f,\ f_0,\ \sigma_n)=\frac{A}{\sigma_n\sqrt{2\pi}}\ e^{\frac{f-f_0}{2\sigma_n^2}}\ \text{when}\ f\geqslant 0,$$

where $A=\frac{1}{0.5+\Phi_0(f_0/\sigma_n)}$; Φ is a probability integral; $\Phi_0(x)=\frac{1}{\sqrt{2\pi}}\int_0^x e^{-t^2/2}\,dt$. The quantity f_0 corresponds to the mode of the histogram for the probability distribution density; it equals 0.02 μCi/km² for all stations (Fig. 2). The parameter σ_n is close to the value of the root-mean-square deviation calculated from the original sequence. The mathematical expectation F and the root-mean-square deviation σ^* for a truncated normal distribution were calculated from the equations:

$$\hat{f}=f+B\sigma_n;$$

$$\sigma^{*2}=\sigma_n^2\left[1-B^2-\frac{f_0}{\sigma_n}A\varphi\left(\frac{f_0}{\sigma_n}\right)\right],$$

where $B=\frac{\varphi\left(\frac{f_0}{\sigma_n}\right)}{0,5+\Phi_0\left(\frac{f_0}{\sigma_n}\right)}$; $\varphi(f)=\frac{1}{\sqrt{2\pi}}e^{-f^2/2}$ is the normalized density for a normal distribution. The calculated values of the parameters are presented in Table 1, from which it is seen that the average values

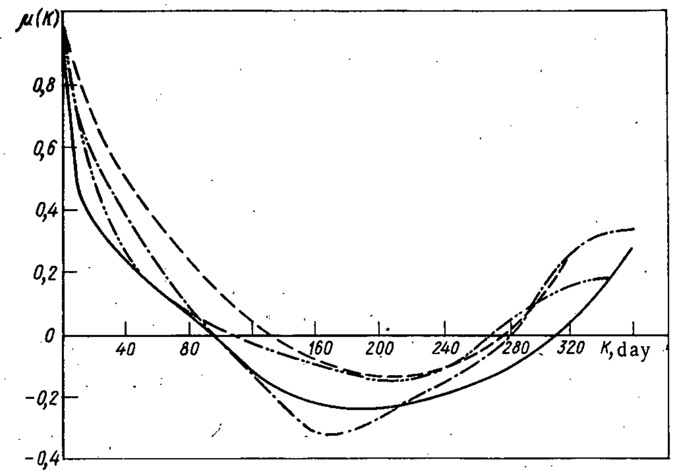

Fig. 3. Normalized autocorrelation density functions for Sr^{90} fallout: ——) station No. 1; – · –) No. 2; – ·· –) No. 3; – – –) No. 4.

obtained during the processing of the sequences agree well with the $\hat{f}$ for all stations. The root-mean-square deviations agree somewhat less, but are found, apparently, within the limits of admissible error.

Since the available data on the fallout density is obtained at different periods of the observations, we assumed for the calculation of the correlation functions that, within the limits of a single time interval, the fallout density remained at the average level. Using the data of the sequence cited, the fallout correlation functions were calculated from the equation

$$\mu_{f,f_k} = \frac{\Sigma f_r f_{r+k}}{\sqrt{\Sigma f_r^2 \Sigma f_{r+k}^2}}.$$

Normalized autocorrelation functions for the stations indicated are shown in Fig. 3. The correlation functions for all four sequences possess a similar kind of attenuated harmonic oscillations. It is easily seen that the period of the fundamental harmonic is approximately equal to one year. Thus, a characteristic alternation of summer maxima and winter minima in the fallout of artificial radioisotopes is observed upon the ocean as well as upon dry land. An increase in the number of fallout observation stations permits a more thorough statistical analysis, including the development of correlated coupling.

LITERATURE CITED

1. V. N. Lavrenchik, Global Fallout of Nuclear Detonation Products [in Russian], Atomizdat, Moscow (1965).
2. B. A. Nelepo, Nuclear Hydrophysics [in Russian], Atomizdat, Moscow (1970).
3. I. L. Karol', Radioactive Isotopes and Global Transport in the Atmosphere [in Russian], Gidrometeoizdat, Moscow (1972).
4. Fallout Program HASL-245 (1971).

SCIENTIFIC COOPERATION BETWEEN SOVIET AND AMERICAN PHYSICISTS

V. A. Vasil'ev

In November, 1970, a report was signed authorizing the undertaking of joint studies in the field of high-energy physics at the accelerators of the Institute of High-Energy Physics at Serpukhov, USSR, and at the National Accelerator Laboratory at Batavia, Illinois, USA. The report was signed by the authorized representatives of the State Committee on the Uses of Atomic Energy of the USSR, and the Atomic Energy Commission of the USA. At the same time, a group of American scientists and specialists had already been to Serpukhov and had participated, together with scientists from the Joint Institute for Nuclear Research, in an experiment on the investigation of the process of $\pi - e$ scattering and the structure of a π-meson on a large Soviet proton synchrotron. The construction of the US accelerator is nearing completion.

In February, 1972, the accelerator at Batavia attained an energy of 200 GeV, and in March of the same year a group of Soviet scientists and specialists arrived at the National Accelerator Laboratory to participate in a second joint Soviet–American experiment. The aim of the experiment was to study the process of elastic scattering of protons by protons at small angles over a wide energy range. There is much interest in studying the elastic scattering of high-energy particles because such experiments enable us to verify directly the fundamental postulates of quantum field theory (relativistic invariance and microcausality) and shed light on the dynamics of strong interactions (the analytical properties of the scattering amplitude). It was tempting to verify the energy dependence of the width of the diffraction cone and the real part of the scattering amplitude right up to the highest energies. In order to determine these quantities we had to measure the differential cross section of elastic scattering in the region of small angles with an accuracy of 1-2%. As an example we can note that for an energy of the initial proton beam of 20 GeV the scattering angles applicable for the measurement, in the laboratory system, fall within the range 0.1-0.05° [0.05° corresponds to the square of the transmitted impulse $t = -0.0005$ $(\mathrm{GeV/c})^2$].

Progress in this experiment depended, to a considerable extent, on the use of an original method, first proposed and used in accelerator experiments by a group of physicists from the High-Energy Laboratory of the Joint Institute for Nuclear Research (V. D. Bartenev, V. A. Nikitin, Yu. K. Pilipenko, V. A. Sviridov, K. D. Tolstov, et al.). It was proposed that we use as a target a thin (0.5 μ) polyethylene film or that we inject directly into the vacuum chamber of the accelerator a supersonic jet of condensed hydrogen, and then record the recoil protons formed in multiple collisions of the primary accelerated protons with the target.

The special experimental apparatus, including the hydrogen (or deuterium) gas jet target, the semiconductor detectors for recording the slow recoil protons with the necessary electronics, control devices, and the cryogenic system, were fabricated at the shops of the Joint Institute for Nuclear Research, and successful tests were carried out in experiments at the Serpukhov accelerator. The experience obtained in these experiments enabled the group of Soviet specialists, after arriving in Batavia, quickly to assemble and prepare for operation the apparatus that they had brought with them, and to install it on the American accelerator. From July, 1972 until March, 1973 in the experiment valuable scientific information was obtained on elastic proton–proton scattering with small transmitted momentum in the primary-proton energy range 20–400 GeV. The first preliminary results were reported in August, 1972 at the International Conference on the Physics of High-Energy Particles, at Chicago, Illinois, USA. A high opinion of the Soviet experimental apparatus and the results of the joint Soviet–American experiment was expressed at the

Translated from Atomnaya Énergiya, Vol. 35, No. 2, pp. 139-140, August, 1973.

meeting of the American Physical Society in New York. At this conference papers were presented by the scientific leaders of the joint experiment, V. A. Nikitin and Yu. K. Pilipenko.

After a brief break in April, 1973, the group of Soviet physicists again returned to Batavia in order to complete the experiment and to process the large amount of scientific information that had been obtained. The final results of this experiment are awaited with great anticipation. The point of interest is that in the region 150-300 GeV a deviation of the experimental points from the theoretical prediction has been detected, although there is good agreement at lower energies. If the preliminary data in the indicated energy range confirm this result, it will be an important new contribution to the further development of the theory of nuclear forces.

A reliably operating device using a gas jet as a pure hydrogen or deuterium target was of interest to many physicists who are carrying out or planning accelerator experiments. At present this target is simultaneously in use by four scientific groups. There is a preliminary agreement between the Joint Institute for Nuclear Research and the National Accelerator Laboratory concerning cooperation in the creation of a second similar installation and the carrying out of a joint experiment on the study of the process of proton–deuteron scattering on the accelerator at Batavia.

Soviet–American cooperation in the area of high-energy physics has been developing successfully. It is not limited to the examples presented above, but is taking new forms and broadening its boundaries. Recently the scientific council of the National Accelerator Laboratory approved a proposal on still another joint experiment on the investigation of the interaction of high-energy antineutrinos with nucleons using a large 15-foot (~457 cm) bubble chamber with neon–hydrogen filling. A group of Soviet physicists will be in Batavia and will participate in the preparation and carrying out of this experiment. Simultaneously at the Institute of High-Energy Physics and the Institute of Theoretical and Experimental Physics preparations will be made for the processing of the film information, which will be obtained in the experiment and sent from Batavia.

The establishment of closer, more intimate contacts between Soviet and American physicists not only promotes the more rapid generation of important scientific results, and exchange and mutually profitable use of the newest technical achievements, but at the same time contributes to better mutual understanding between our nations, to peace, and to progress.

SESSION OF THE SCIENTIFIC COUNCIL ON PLASMA PHYSICS

M. S. Rabinovich

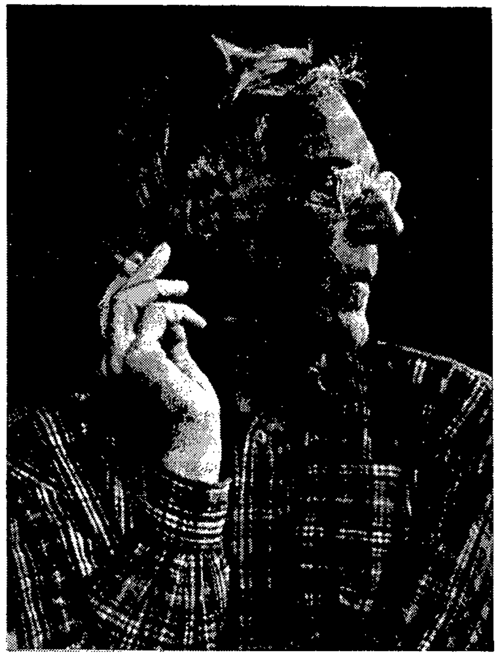

Academician M. A. Leontovich.

The annual session of the Scientific Council on Plasma Physics of the Academy of Sciences of the USSR is a scientific conference of a new type. For three days only review papers are presented. This year (March 5-9), they were dedicated to the stellarator program, the interaction of ultrahigh frequency waves with plasma, the interaction of relativistic electron beams with plasma, and the interaction of flowing plasma with a surface.

The meeting on March 9 was dedicated to the 70-year-old Academician M. A. Leontovich. B. B. Kadomtsev, who noted the outstanding contribution of M. A. Leontovich to the creation of a Soviet school of plasma theory in the development of controlled thermonuclear research (CTR), presided over the session. M. A. Leontovich's students – B. B. Kadomtsev, R. Z. Sagdeev, E. P. Velikhov, and V. D. Shafronov – gave scientific reports on MHD theory of plasma, turbulence of plasma and fluids, artificial plasma formation in the Earth's magnetosphere, and fast processes. A. M. Prokhorov reported on the latest achievements in the study of gasdynamic lasers. I. M. Fabelinskii discussed the propagation of hypersound in condensed matter. The latest attainments in this field, obtained by the use of lasers, confirm the theory developed by M. A. Leontovich over 30 years ago.

N. G. Basov, Director of the P. N. Lebedev Physical Institute of the Academy of Sciences of the USSR, and R. V. Khokhlov, Rector of the Moscow State University, congratulated M. A. Leontovich on his 70th birthday and wished him further creative success.

Translated from Atomnaya Énergiya, Vol. 35, No. 2, pp. 140-142, August, 1973.

As in the past, works on the physics of hot plasmas were the most fundamental and significant. Considerable achievements have been attained in the Tokamak program. The main trends in this area of research are listed below.

1. The conviction that tokamaks possibly do not have optimum geometry, and that it is possible to obtain better results by altering the shape of the cross section, is growing stronger. The so-called "ring-shaped" tokamaks will apparently begin operation in the near future.
2. New fundamental results can be obtained from the next generation of tokamaks. Therefore, the construction of the T-10 tokamak takes on special significance.
3. The first results on nonohmic heating methods have been obtained; these results may have considerable significance for the solution of the heating problem.
4. As is well known, the neoclassical theory has played a decisive role in the current representations of plasma confinement and heating. Recently many data have appeared which indicate the influence of other, nonneoclassical phenomena. In this context, the unsatisfactory position of electron transport processes should be noted. The best agreement with neoclassical theory is found in the "plateau" region. Transition to the hydrodynamic and collisionless regions leads to a large discrepancy between theory and experiment. The electron balance mechanism has not yet been elucidated. In short, the questions of diffusion and stability in toroidal systems require further detailed consideration. Several conclusions of the theory of local stability are very interesting, in particular, the observation that, at finite β, the flutes are stabilized because of an increase in the magnetic well depth.

Work on the stellarator program is being conducted at the Physics Institute of the Academy of Sciences of the USSR and at the Physicotechnical Institute of the Academy of Sciences of the Ukrainian SSR. V. T. Tolok and I. S. Shpigel' discussed this research in detail. The development of the stellarator program depends on the introduction of a new generation of stellarators (which have dimensions similar to the T-3 tokamak). Stellarator results correspond to tokamak results, if the size factor is taken into account. As with tokamaks, there are increasing indications of a departure from neoclassical diffusion.

Work on magnetic traps forms an important part of the CTR program. Significant results have been obtained on the PR-6 device, in which a plasma with density $2 \cdot 10^{12}$ cm^{-3} and ion temperature 200-300 eV is stable for the first 0.2-0.3 msec indicating that loss cone instability has a weak role. However, an instability subsequently develops, accompanied by electron heating and an increase of plasma potential.

The suppression of instabilities by feedback stabilization on the LIN-5 device is also of interst.

In 1972 there was increasing interest in pulsed processes. This is primarily due to laser fusion. If laser efficiency is ignored and only physical controlled thermonuclear reactions are of interest, then, according to calculation, a laser of 10^4 J is sufficient, or a laser of 10^5 J without complex programming of the laser pulse. Lasers with such pulsed energies will be produced in the near future. Having attained a physical CTR, from $4 \cdot 10^{16}$ to $4 \cdot 10^{17}$ neutrons will be obtained per pulse. Obviously, laser fusion has recently drawn our attention more and more.

Interest in high-current electron beams is growing. These beams have great possibilities for plasma heating and rf power generation. Micropinch studies in the USA merit attention. Interest in theta pinches has increased with the suggestion of using an imploding liner.

This indicates an increased or renewed interest in fast processes; this interest is sustained by calculations showing that the efficiency of transforming fusion energy into electrical energy will be significantly higher in pulsed processes than in steady-state processes. Thus, two main directions can be taken towards the solution of the CTR problem, but within each the resources must be concentrated on the most promising research. The confinement by plasma by multiple mirrors, suggested in the Institute of Nuclear Physics of the Siberian Branch of the Academy of Sciences of the USSR, should also be noted.

Research on rf plasma heating has achieved great success. The method of nonlinear wave transformation together with the methods of linear transformation, developed in the A. F. Ioffe Physicotechnical Institute of the Academy of Sciences of the USSR and in the Physics Institute of the Academy of Sciences must clearly be one of the most promising means of plasma heating.

The decay and parametric instabilities are important for understanding the processes occurring in a laser-produced plasma, in the ionosphere, and elsewhere. The induced Mandel'shtam–Brillouin scattering, first observed in the uhf frequency range at the Physics Institute of the Academy of Sciences, should be noted. Plasma heating near the ion–ion hybrid resonance in a plasma with two different ion components is also of interest (Physicotechnical Institute of the Academy of Sciences of the Ukrainian SSR). A deuterium–hydrogen plasma in the Omega toroidal device was heated near this resonance to a temperature of 200 eV at a density of about 10^{14} cm^{-3}.

Many interesting studies of the beam–plasma interaction have been conducted. A large efficiency of heating has been demonstrated when the beam is modulated at the lower hybrid resonance. The possibility of effective plasma heating by the anomalous transformation of high-frequency waves into low-frequency waves has also been shown. The theory of beam deceleration in a plasma has been developed in great detail. The spectrum of the Langmuir oscillations which arise during continuous beam injection into a plasma, when the level of the excited oscillations is limited by their induced scattering on plasma ions, has been determined.

The study of strongly nonlinear waves will obviously play an increasing role. A theory of two-dimensional Langmuir solitons has been developed in the Physicotechnical Institute of the Academy of Sciences of the Ukrainian SSR, and their acceleration by an electron beam has been accomplished.

As is well known, electric fields of up to GV/cm can be induced in strongly turbulent plasma. Such fields effectively retard and randomize any directed motion, such as an electron beam. Strong fields in a plasma can be utilized if they are synchronous and coherent.

The most significant result of the past year in the plasma accelerator field is the design of the engine on the satellite Meteor and its power supply. This engine worked for about 200 h and propelled the Meteor to a so-called conditionally synchronous orbit, during which time the orbit of the satellite changed in radius by 17 km.

Successes in the development of stationary plasma accelerators should also be noted. The problem now is to create a plasma injector for CTR on a new basis. And, finally, an era of ever broader applications of plasma accelerators in technological projects has arrived.

Research on the physics of electron and atomic collisions has been conducted in a number of institutions and organizations. A new technique for forming highly excited particles and ions has been developed. This technique is based on the high efficiency of the transformation of certain excited molecules into negative ions. New data on the excitation cross sections of particles by atomic and electron collisions have been obtained.

Numerical calculations of cross sections for excitation and ionization by electrons and photons have also been performed. Computer calculations are making significant progress.

The study of the formation of multiply charged ions has continued. The volume of research in this field has grown strongly, as was clear from the increase in the number of reports presented at the All-Union Conference (over 300 papers).

The next annual session of the Scientific Council on Plasma Physics will take place on February 25-28, 1974.

FRANCOSOVIET COLLOQUIUM ON FAST-REACTOR TECHNOLOGY

A. A. Rineiskii

A colloqiuium on fast-reactor technology was held on March 19-23, 1973 at the V. I. Lenin Scientific-Research Institute of Atomic Reactors (NIIAR), in Dimitrovgrad.

The following topics were on the agenda of this bilateral meeting:

1) sodium-coolant technology;

2) operating experience with engineering reactors (BOR-60, Rhapsodie), experience in the design, startup, and adjustment of power reactors (BN-350, Phoenix);

3) the construction of 1000-1500 MW(e) fast reactors for future nuclear power stations.

With a large number of sodium facilities being put into service, the problem of the reutilization of equipment that has been overhauled and repaired becomes more prominent. Sodium and sodium compounds must be completely removed from such process equipment. The French specialists reported on a method which they are using to eliminate sodium from reactor components withdrawn from the loop, without impairing the properties of the materials, and without disturbing the geometric configuration of the structures. The most effective method, in the opinion of the French specialists, is to use a jet of cold water mixed with air in the cleaning process. The water is fed in from special spray nozzles under ~7 kgf/cm^2 pressure. The reaction products, principally hydrogen (in amounts that must not exceed 2%), are eliminated from the flushing chamber. Since the processes take place at low temperatures (below 100°C), the formation of alkali is eliminated (the formation of alkali has been observed when using steam to wash out the sodium). This is one of the outstanding merits of the method. It was stressed that the components of the parts to be reused must be taken apart completely and thoroughly dried, and that fasteners (bolts, pins, etc.) should be replaced.

The Rhapsodie experimental reactor, redesigned in January, 1971, for ratings from 24 (design ratings) to 40 MW, has been operated successfully. The reactor operates stably on power, and responds readily to control.

The operation of sodium systems does not present any difficulties. Slight adjustments are needed with the rotation of plugs (reactor refueling systems). Sodium vapor condensed in the clearance between the fixed and moving parts, hindering the rotation of the plugs. Blowing the clearance with helium made it possible to smooth out the temperature field in the clearance and to increase the pressure there, effectively eliminating any precipitation of sodium vapor in the clearance.

Assembly work on the Phoenix fast reactor [~250 MW(e)] was completed in late 1972, and work started on adjustment operations. In late 1972 and early 1973 the reactor was filled with sodium (800 tons); because of the heat given off by the pumps, the temperature in the primary loop was raised from 200 to 350°C in March, 1973. Loading of fuel assembles and rise to criticality are scheduled for June, and the reactor is scheduled to go on power in the third quarter of 1973. The results of investigations that have already been completed are of interest. Vibration tests on the primary loop were carried out with the aid of 60 vibration pickups, 40 of which were mounted on equipment located within the reactor pressure vessel. There was virtually no vibration of the components, because of the low flow velocity of the sodium stream. A major mishap occurred in the startup and adjustment phase of the work when ~30 liters of oil from fans of the primary loop gas heating system got into the reactor, and a delay in the work resulted. The reactor

Translated from Atomnaya Énergiya, Vol. 35, No. 2, pp. 142-143, August, 1973.

was cooled down, some of the components were disassembled, and repair crews were allowed into the reactor when conditions permitted. It was assumed that ~5 liters of oil remained within the reactor after the cleanup operation. It was then seen to be necessary to provide for access to all of the cavities and components within the reactor pressure vessel and also to provide for the pouring off of sodium and the cooling of the pressure tank.

The large complex of experimental research projects undertaken to substantiate the design work is noteworthy; the coolant velocity distribution was measured on scaled-up models (scales 1/4 to 1/25) at all important points in the interior of the pressure vessel, including the distribution due to natural convection; the coolant flow-rate distribution when the primary loop operates symmetrically (balanced) or asymmetrically (with part of the loop equipment shut off) was also investigated and measured; surges in the coolant stream flow and vibrations caused by the surges were studied; damage resulting in core melt-down as the result of an explosion was simulated on a 1/25 scale model of the reactor pressure vessel.

Work on the design of a fast sodium-cooled reactor with electrical output ratings of 1200 MW (the Superphoenix) has been pursued on a large scale. The power ratings were arrived at on the basis of operating experience with the power station built around the Phoenix reactor and also on the basis of power equipment manufactured by industry for commercial sales (turbogenerator sets with ratings of 600 MW per unit). As in the case of the Phoenix reactor and its power plant, a monolithic format was decided upon for the primary loop. There were some slight differences in design. For instance, the flat cooled top cover was replaced by a top load-bearing cover plate on which all of the primary-loop equipment was mounted in a fixed position. In that respect the Superphoenix reactor is reminiscent of the British PFR reactor prototype. Four fuel filaments are employed in order to achieve thermal and hydraulic symmetry – two for each turbine.

Close attention is being given to the design of reliable equipment for a once-through-type drumless steam generator. Despite the general, factually sketchy stage of development which the nuclear power plant as a whole has reached, fabrication of scaled-up metal models of steam generators (thermal power ratings of the models 40 to 60 MW) is already underway. At the same time, the possibility of utilizing two basically different designs of steam generators is being examined: one would be a pressure-vessel type (one steam generator per heat-removing loop) and the other a modular type (several, say eight to 12, steam generators per subloop). The feasibility of building steam generators with spiral welded tubes, one of which would accommodate preheating, evaporative, and steam superheat intervals, and also with straight tubes, when the intervals in question are to be accommodated in separate vessels, is also under study.

All of the reports will be included in the proceedings of the colloquium, to be published by NIIAR.

At the concluding session, the leader of the Soviet delegation N. M. Sinev pointed out that the bilateral meeting of French and Soviet specialists had been a fruitful one, and that such meetings are to be welcomed in the future.

IAEA INTERNATIONAL SYMPOSIUM ON THE APPLICATIONS OF NUCLEAR DATA IN SCIENCE AND TECHNOLOGY

G. B. Yan'kov

An IAEA symposium devoted to the applications of nuclear data in science and technology was held on March 12-16, 1973, in Paris. This was the first organized meeting of those making use of, estimating, and measuring all nuclear data, whether neutron or nonneutron. The basic problem on the agenda of the symposium was the elucidation and discussion of nuclear data needs. These needs were discussed not only in the traditional area of fission chain reactors, but also within the framework of systems of safeguards, investigations of nuclear fusion and thermonuclear reactors, accelerators, activation analysis, experiments in outer space, biology and medicine, the use of radioisotopes in chemistry, etc. The interactions between the users and producers of nuclear data also came under discussion.

The symposium was attended by over 200 representatives of various countries and international agencies, and about 80 reports were presented.

The papers submitted showed that in addition to neutron data a generous quantity of nuclear spectroscopy information of a nonneutron nature is required for applied purposes. This refers primarily to information on the γ-ray spectra and structure of nuclei, nuclear data on fission fragments, cross sections of reactions involving charged particles, decay parameters of nuclei, and so forth.

Seven sessions out of 16 were devoted to discussions of the nuclear data used in the discussion, planning, investigations, monitoring, and operation of various types of reactor systems, especially fast reactors and thermal reactors, and also for models of thermonuclear reactors, and design plans for nuclear power facilities burning ^{238}Pu and a plasma uranium reactor. Nuclear data requirements for existing systems and for systems being set up were discussed from the point of view of calculating the basic reactor parameters to a high degree of accuracy, monitoring the fuel content in fuel elements and in wastes, in order to determine radiation damage and to dispose of radioactive wastes by burial, and also in order to estimate the feasibility and viability of competing design proposals. Two of the sessions were opened by Soviet papers which analyzed the effect of errors in nuclear data on the fuel breeding ratio in fast reactors and in thermonuclear reactors, and provided recommendations for ascertaining nuclear data. Some of the reports emphasized the major role played by integral experiments in the physics of fast reactors and thermal reactors, and in refining nuclear data. The comparative analysis of files of estimated data available in libraries and of different computational techniques was also carried out; in particular, it was shown that discrepancies in the K_{eff} values for a specific model of a fast reactor attained the level of 5%, when files from the ENDF/BIII library and KEDAK files were used. Close attention was also given to nuclear data on fission fragments; but, as previously, data on the capture cross section and inelastic scattering cross section of neutrons interacting with fission fragments are scarce.

The use of radioisotopes in medicine and in biology sometimes calls for nuclear structural information of high accuracy, as well as data on short-lived isotopes for the analysis of living specimens. It has been shown, specifically, that the accuracy of the information available on energy losses along the track of a fast particle (particularly multiply charged ions and negative π-mesons) is not sufficient to permit a tumor in a living organism to be reliably dealt with. The preparation of specially pure ^{238}Pu for use in a living organism was also among the problems discussed.

The nuclear data utilized in the interpretation of the chemical processes of hot atoms are very unusual. Here we refer specifically to the characteristics of the γ-radiation emitted by nuclides with lifetimes longer than 10^{-15} sec, electron–neutrino angular correlation in β decay, etc.

Translated from Atomnaya Énergiya, Vol. 35, No. 2, pp. 143-145, August, 1973.

TABLE 1. Areas of Application of Nuclear Data and Demands for Nuclear Data

Area of application	Use in this area	Basic needs	Level of acquaintance with nuclear physics required of user
Electric power	Fission reactors (design, radioactive wastes, control, environment, fuel-element monitoring including a system of safeguards)	Neutron data, fission data, data on radioactive decay and on the structure of the nucleus	High
	Radioisotope batteries	Data on radioactive decay	Low
	Controlled thermonuclear fusion	Reactions involving charged particles and neutrons	High
Biology and medicine	Diagnostic studies	Data on radioactive decay (some data on reactions)	Medium to low
	Therapy, research	Data on radioactive decay; reactions involving charged particles (protons, π-mesons, heavy ions)	Medium to high
Agriculture	Preservation of foodstuffs, genetic studies, plant studies	Data on radioactive decay	Low
Geology, archeology, forensics	Activation analysis	Data on radioactive decay, neutron capture, x-ray luminescence using charged particles and ν-photons	Medium to low
Industry	Leak detection; thickness and density gages; different modes of monitoring; fire-alarm and detection devices; filters; processing of materials; semiconductor devices; analysis of materials; radiography	Various of the types of data mentioned above, depending on the specific applications	Medium to low
Physical sciences	Nuclear physics; astrophysics; solid-state physics; chemistry	—	High to low, depending on specific features of the area of application

It is interesting to note that numerous specific requirements imposed on nuclear data have arisen in the design of instruments intended for the study of the properties of planetary surfaces and atmospheres, and in the design of high-precision high-energy accelerators (the TRIUMPH machine in Canada; meson-factory-type neutron sources in the USA).

Various techniques of activation analysis and their related nuclear data needs, not only as regards thermal neutrons and epithermal neutrons, but also where the participation of charged particles and γ-photons is involved, were discussed in detail. A discussion of the errors in the utilization of absolute methods revealed that the greatest contribution to error in the analysis is by the uncertainty that exists in the nuclear data. For example, the error in half-lives, decay schemes, and activation cross sections in the determination of the composition of matter leads to errors of 2-10%, 2-50%, and 5-30%, respectively. The process of automatic extraction from the complex γ-ray spectra of data on the content of isotopes in the samples studied requires nuclear data of high quality. This is a result of the high sensitivity to uncertainties in the decay schemes. There was also a discussion of the use of nuclear data for more specific problems: analysis of certain elements, the determination of the depth at which impurities are lodged, neutron metrology, the design of instruments for the prospecting and mining of minerals, etc.

The range of application of nuclear data and requirements for nuclear data are presented in general outline in Table 1 (based on data compiled by D. Horen and A. Weinberg, USA). Note that several fields, for example, agriculture, archeology, and forensics, were not discussed at the symposium.

The interaction between the users and producers of nuclear data is also of great importance. The basic link in this interaction, of course, as far as neutron data are concerned, is formed by the nuclear data centers (for example, the Nuclear Data Center at the Power Physics Institute in Obninsk, USSR), which have the responsibility not only of responding to inquiries and requests, but also of collecting, systematizing, processing, and storing neutron data, and organizing the evaluation and exchange of neutron data. The experience accumulated at the Brookhaven center (USA) was discussed at the symposium. Three reports dealing with nonneutron data centers were presented at the symposium: one on the Oak Ridge data center in the USA, the others on two data centers in the USSR (the data center of the I. V. Kurchatov Institute of Atomic Energy and the Leningrad Institute of Nuclear Physics).

With the marked increase in the demand for nuclear data in applied areas, the Advisory Committee on Neutron Cross Sections in the USA was expanded and transformed into the US Nuclear Data Committee; a special report was presented on these changes.

The past decade has been characterized by a pronounced increase in the volume of experimental information. Under these conditions, it is not possible to overestimate the significance of the work of compiling reviews and critical surveys. Such reviews and surveys not only satisfy the demand for information, but also permit experimental physicists to concentrate their efforts in areas where data are still lacking, or in areas where wide discrepancies in the data are evident. A. Weinberg (USA), in his introductory report discussing criteria for selecting topics where compilations are high in priority, advanced an estimate indicating that the cost of one item of numerical data in such compilations is less than 1% the cost of one item of numerical data in experimental research. The selection of topics and areas for compilations and reviews is also of the utmost importance, in view of the limited possibilities and resources available. Here national and international nuclear data committees can render valuable assistance in selecting and developing priority hierarchies and organizing and expediting inquiries.

Compilations of large volumes of data were taken up in some reports, such as: "Data compilation on γ-rays accompanying neutron capture" (G. Bartholomew, Canada), "Intensities of electromagnetic transitions in nuclides $A > 40$" (F. Bertrand et al., France), "Data file on various γ-emitters" (F. Dier and L. Boyt, USA), "Catalog of γ-ray spectra, data reference for users" (R. Heath, USA).

Compilations oriented to applications included excitation functions for reactions involving charged particles (M. Münsel et al., West Germany; published in 1973), an estimate of parameters of decay schemes (B. Greenberg team, in France, Netherlands, and Belgium), a compilation of nuclear data for use in medicine and biology (L. Dilman et al., USA), and work on the computer compilation of nuclear data in the form of tables of nuclides (C. Lederer and Y. Hollander, USA).

At the last session, following a concluding report by Lewis (Canada), there was a brief discussion on the future of nuclear data. A remarkable increase in the demand for nuclear data was acknowledged, as well as difficulties accompanying processing and systematization of a large volume of experimental information; confidence was expressed that these problems can be resolved successfully on the basis of international cooperation.

The excellent work done in organizing and running the conference deserves special mention. The obligatory procedure for duplicating the texts of reports enabled each participant of the symposium to obtain the full set of submitted papers prior to publication of the symposium proceedings. These sets of publications have been made available at our three centers (at Obninsk, Moscow, and Gatchina). IAEA expects to publish the symposium proceedings in 1973.

THE INTERNATIONAL CONFERENCE ON PHOTONUCLEAR REACTIONS AND APPLICATIONS

B. S. Dolbilkin, P. V. Sorokin,
and B. A. Tulupov

The International Conference on Photonuclear Reactions and Applications was held in the United States (Asilomar, California) on March 26-30, 1973. Its purpose was to discuss a wide range of important problems in this area of nuclear physics, to establish their relation to other trends in the physics of the nucleus, and to determine the directions to be followed in future investigations. An important place in the program of the Conference was occupied by the applications of photonuclear reactions in various fields of science and technology and to questions involved in the development of new types of experimental equipment.

Participants in the Conference included 408 persons from 24 countries. A total of 73 survey reports and 195 original communications were presented.

Many of the reports were devoted to research on the electromagnetic interactions of nuclei at low energies. Considerable attention was also devoted to the study of nuclear structure by means of high-energy photons and electrons. A number of meetings was devoted to studies on the status of experimental methods and problems of improving electron accelerators and the possibilities of using photonuclear reactions in medicine (for the treatment of cancer), solid-state physics, chemistry, the food industry, etc. However, no specific details on such applications were reported at the conference.

In the physics of low-energy photonuclear reactions the greatest attention was given to studies on giant resonances using quasimonochromatic photons, the study of the intermediate structure in photoabsorption cross sections, the disintegrations of excited states along various channels, and isospin effects. Such investigations, which make it possible to obtain more complete and valuable information on the structure of the nucleus, became possible as a result of substantial improvements in experimental methodology.

In the intermediate energy range the most interesting studies were those on deep-lying nuclear shells, the distributions of electrical and magnetic charges in nuclei, and the transition densities of charges.

The information presented included interesting data characterizing the level and rates of expansion of photonuclear-reaction physics. Throughout the world, about 120 papers are published on this subject each year; this number has remained approximately the same for the last 10 years. The USSR publishes about 30 papers a year.

Discussions of the experimental methods used in the study of new scientific and applications problems emphasized repeatedly the need for improving present-day accelerators and constructing new ones, with a view to increasing the duty cycle and improving the energy resolution. The most promising directions from this point of view seem to be the use of accelerating structures with a standing wave, rings of beam accumulators and stretchers, techniques for beam recirculation, and superconductive linear accelerators. The use of accelerators of new types together with improvements in the parameters of analyzing systems, the use of modern high-resolution detectors, and the automation of the processing of experimental data would make it possible to investigate new fields in the physics of photonuclear reactions.

Translated from Atomnaya Énergiya, Vol. 35, No. 2, p. 145, August, 1973.

THE EIGHTH SESSION OF THE INTERNATIONAL LIAISON GROUP ON THE THERMIONIC METHOD OF ELECTRIC POWER GENERATION

D. V. Karetnikov

The eighth session of the liaison group on thermionic conversion (TC) met in Vienna on March 22, 1973. Reports were heard from representatives of member-nations of the liaison group on the work done on TC during the time elapsed since the third international conference (Julich, 1972).

Considerable success has been achieved in the development of work on TC in the USSR. Tests have been carried out on the Topaz-3 thermionic reactor with the aim of achieving longer operating times and higher efficiency than those achieved earlier with the Topaz-1 and Topaz-2 thermionic reactors. The new reactor has been in service for about 3000 h at an electric power output level of 5 to 7 kW and an efficiency 30% higher than in the earlier reactors. In addition to tests run on the reactor as a whole, in order to develop the design of the electric-power-generating channels (EPGC) three tests for protracted service life were carried out on isolated five-element EPGC. One of them had worked for over 3000 h at an average power output level of 1.7 W/cm^2 by the beginning of March. A six-element EPGC with an enhanced power output rating and with an emitter made of tungsten–rhenium alloy and a collector made of niobium was also tested. The tests lasted 2670 h with an average power output level of 7 W/cm^2 at the outset of the tests. New results were obtained on the physics of direct conversion, specifically in investigations of the non-steady-state properties of cesium plasma.

Developmental work on an experimental prototype of a 20 kW(e) submarine reactor is continuing in France. Very serious attention is being given to radiation safety problems and to the problem of the compatibility of the reactor with the marine environment and with the underwater biosphere. Intermediate stages of this project will include two group reactor tests on systems of three-element EPGC with a total electric power rating of 10 kW for each system. The fabrication of EPGC for the first experiment has been begun. Reactor tests on an emitter with cermet nuclear fuel (60% uranium dioxide and 40% molybdenum) have demonstrated the excellent geometrical stability of the emitter in service for 3600 h at twice the rated heat-output. In the field of fundamental research, the major interest centers on comparative measurements of the work function of metal–oxygen–alkali metal systems, with a simultaneous analysis according to the shift of the Auger peaks of the formation of chemical compounds, where this occurs. The following results have been obtained for the minimum work function, eV:

Alkali metal	Pure metal	In the presence of oxygen
Cesium	1.6	0.9
Strontium	2.4	1.7-1.8
Barium	2.1	1.2

These results (obtained by utilizing the latest achievements of high-temperature ultrahigh-vacuum technology) are of unquestioned interest and can serve as a basis for the development of low-temperature TC in which the emitter temperature will not be greater than, say, 1200°C, while the collector temperature will correspond to the minimum work function. This approach is currently under analysis also in West Germany, where a portable thermionic power facility for nonspace applications is being developed

Translated from Atomnaya Énergiya, Vol. 35, No. 2, pp. 145-146, August, 1973.

for an output rating of 1-2 kW (work in West Germany on the design of a thermionic reactor for space applications has been halted for the time being because of difficulties in justifying the project). Such facilities, using liquefied gases for example, may find wide applications under field conditions. Preliminary results obtained using a cermet emitter (tungsten and uranium dioxide) and a collector made from a mixture of barium tungstenate and calcium tungstenate appear quite promising.

The international liaison group on TC has been operating for five years now. In the discussion of the report on its activities, it was pointed out that the liaison group is making an active contribution to the establishment of contacts and the exchange of information on TC between specialists of different countries. International conferences on TC were successfully prepared and held in 1968 and in 1972. Improvements in mutual understanding between specialists have been facilitated by work of major scientific value on the compilation of a glossary, now to be published in Russian. The liaison group considers that the development of the thermionic method of power conversion has now attained a level at which the basic parameters of the converters (power output, service life, efficiency) can be approximately doubled within the next five years.

US NATIONAL CONFERENCE ON ENGINEERING PROBLEMS OF CHARGED-PARTICLE ACCELERATORS

V. P. Sarantsev and I. N. Semenyushkin

The US national conference on charged-particle accelerators was one of the most representative conferences of its kind, and perhaps the only conference to encompass all types of accelerators. The conference was held in San Francisco on March 5-7, 1973. Over 600 specialists participated in the deliberations.

The morning session of March 5 and the evening session of March 7 were plenary sessions. They were scheduled to include reports on the design of new accelerator complexes, the PEP, the Isabella, and the 300-GeV CERN accelerator, and also on some possible applications of accelerators in radiotherapy and in technology. Of greatest interest was a report on a proton–electron–positron accelerator–storage complex (the PEP). This facility is designed to produce beams of 15-GeV electrons and ~150-GeV protons. Provision is made in it for the collision of these electron and proton beams at very high luminosity ($\sim10^{32}$ $cm^{-2} \cdot sec^{-1}$).

The remaining time was scheduled for three parallel panels on various accelerator topics. There were 12 such panel sessions in all: on superconducting resonator cavities, heavy-ion accelerators, improvements in existing accelerators, collective accelerators and high-current electron beams, injection and power supplies, beam transport and beam extraction, control and monitoring systems, superconducting magnets, storage rings, dynamics, linear accelerators, and applications of accelerators.

The extensive work being undertaken on existing accelerators to step up the intensity of the accelerated beam must be mentioned. The principal directions in this work are the replacement of existing injectors with high-energy high-intensity injectors, or the use of booster accelerators featuring high reproducibility of the acceleration cycle. These changes in injection systems will make it possible, over the coming years, to convert basic accelerators to intensities of 10^{13} particles per cycle. Capture conditions will also be improved in the largest (400-GeV) accelerator built near Chicago.

There was a separate report on the Berkeley 6-GeV accelerator. This accelerator is also being proposed for future use in the accleration of heavy ions. The injector will be a Superhilac heavy-ion linear accelerator. The accelerated ions are to be used in nuclear physics research, radiobiological research, and for various other purposes (such as calibration of nuclear instrumentation for artificial satellites).

A major result reported at the conference is a new technology for fabricating superconducting resonators. At the present time, record results have been achieved in work with these resonators: Q factor 10^{10}, field intensity 300 kV/cm; these resonators are not subject to deterioration in vacuum. Thus it is currently possible to use superconducting resonators widely in accelerator technology. There already exist about 15 designs of different electron, proton, and heavy-ion accelerators utilizing superconductivity.

The most interesting reports on storage rings dealt with the CERN proton–proton colliding-beam facilities, where the limiting design parameters (proton current in storage ring 12 A) have been achieved in practice, and also the Stanford electron–positron colliding-beam machine (luminosity 10^{32} $cm^{-2} \cdot sec^{-1}$ for colliding electron beams).

In recent years great progress has been made in particle-beam diagnostic systems for accelerators, and also in the computerization of accelerator control and monitoring functions. All recent accelerators

Translated from Atomnaya Énergiya, Vol. 35, No. 2, pp. 146-147, August, 1973.

built in the USA are equipped with semiautomatic control systems making use of standard electronic equipment and computers.

Reports on new high-precision electron-beam facilities were made for the first time in such a broad conference. An account was given of the performance of the Aurora and Hydra facilities. The Aurora yields an electron beam with electron energies of 15 MeV and pulse current $1.6 \cdot 10^6$ A. The Hydra has lower parameters. These machines are apparently being used only for applied purposes as sources of very-high-power γ-radiation. There is a program for the use of these machines to achieve controlled thermonuclear reactions.

Developmental work on pulsed superconducting magnets for storage-ring accelerators in the ultra-high-energy range, and for dc superconducting magnets in particle-beam transport applications occupies a major place in accelerator development and research plans in the USA. Investigations are also in progress on the possibility of building NbTi-based magnets with fast (5-10 sec) and slow (30 sec or longer) field growth to 40-50 kG. It is expected that in 1973 the reproducibility of the field characteristics of two identical magnets will be established. This will inevitably determine to a considerable extent the program for the future utilization of pulsed superconducting magnets.

Close attention is being given to applications of accelerators in medicine, particularly in cancer treatment. At the present time, facilities useful for the precise localization of tumors are being designed; undoubtedly, this will lead to the more effective utilization of accelerators in the treatment of internal malignancies.

EXPERIMENTAL NUCLEAR-PHYSICS RESEARCH FACILITIES IN THE SCIENTIFIC-RESEARCH INSTITUTE OF NUCLEAR PHYSICS, ELECTRONICS, AND AUTOMATIC CONTROL AT TOMSK POLYTECHNIC INSTITUTE

A. N. Didenko

Research in nuclear physics and the physics of elementary particles at Tomsk Polytechnic Institute (TPI) began in 1947, when one of the first betatrons in the Soviet Union was commissioned and put into service there. In 1958, the Scientific-Research Institute of Nuclear Physics, Electronics, and Automatic Control at Tomsk Polytechnic Institute (NII YaFÉA TPI) was established. At the present time, this institute has 4-6 MeV miniature betratrons, 25 MeV high-current betatrons, a 6 MeV microtron and a 10 MeV microtron, 10 MeV and 30 MeV waveguide synchrotrons, a 1.5 GeV electron synchrotron, a cyclotron with 120 cm polepiece diameter, a 2 MeV nanosecond accelerator, an ÉSG-2.5 electrostatic generator, and the IRT nuclear reactor. These accelerators and other nuclear research facilities are used by the staff of the scientific-research institutes and by the various departments of TPI in research on the physics of elementary particles, nuclear physics, radioactivation analysis, radiation physics, radiation chemistry, and nondestructive testing. Below, we cite the characteristics of the various facilities of this type.

1.5 GeV Electron Synchrotron. In late 1957, TPI was entrusted with the task of developing, building, and putting into service the Sirius 1.5 GeV electron synchrotron. The basic work in the design, fabrication, and starting of the accelerator was done at NII YaFÉA TPI. In early 1964, the accelerator was prepared for the comprehensive startup adjustment work. In January, 1965, the machine was put into operation under mild operating conditions, and in 1966 electrons were accelerated to 1.36 GeV at an intensity of $\sim 5 \cdot 10^9$ particles/pulse. The accelerator (Fig. 1) is distinguished by the following special features which are dictated, on the one hand, by the scientific problems for which the machine was designed and, on the other hand, by the practical realization of the concepts entertained in the design and building of the synchrotron:

1. In weak focusing, the synchrotron provides high energy; this in addition to the long acceleration cycle, makes it possible to investigate the effect of quantum fluctuations on the motion of particles in cyclic accelerators.
2. The microtron was selected as the most suitable injector for the synchrotron. At present, an electron energy of 6.4 MeV is obtained in this machine.
3. It was decided to use injection on the curved portion of the path. It was shown that difficulties associated with the passage of the beam through the stray magnetic field can be overcome; the high voltage across the injector can be reduced by a factor of three in comparison with that necessary in injection on the rectilinear portion of the path. This result will be decisive when the injection energy is increased. In particular, the injection energy can be increased to 12-15 MeV without bringing about any changes in the input device.

In 1966, the Sirius machine began to work in a physics research experiment. It was kept in operation for a period lasting over 15,000 h. Work on the modernization of the accelerator was carried out at the same time, specifically on the RF system, the injector, and the power supply to the electromagnet. As a result of that work, the intensity of particles in a pulse was increased to $2 \cdot 10^{10}$, and the cycle repetition

Translated from Atomnaya Énergiya, Vol. 35, No. 2, pp. 147-151, August, 1973.

TABLE 1. Technical Data on High-Current Induction Accelerators

Accelerator	Characteristics: type of construction	range of applications	energy of accelerated electrons, MeV	number of electrons accelerated in one cycle	pulse cycle repetition frequency, Hz	bremsstrahlung dose rate, r/min (at distance of 1 m from radiation source)
SBS-3-25	Stereo, twin-chamber	Pulsed x-ray diffraction	25	10^{12}	0,25	—
BS-1-25	Single-chamber	Radioactivation analysis, radiation chemistry, biology	25	$3 \cdot 10^{11}$	50	1600
SBS-4-25	Stereo, twin-chamber	Radiographic nondestructive testing of outsize industrial parts	15	10^{11}	50	400

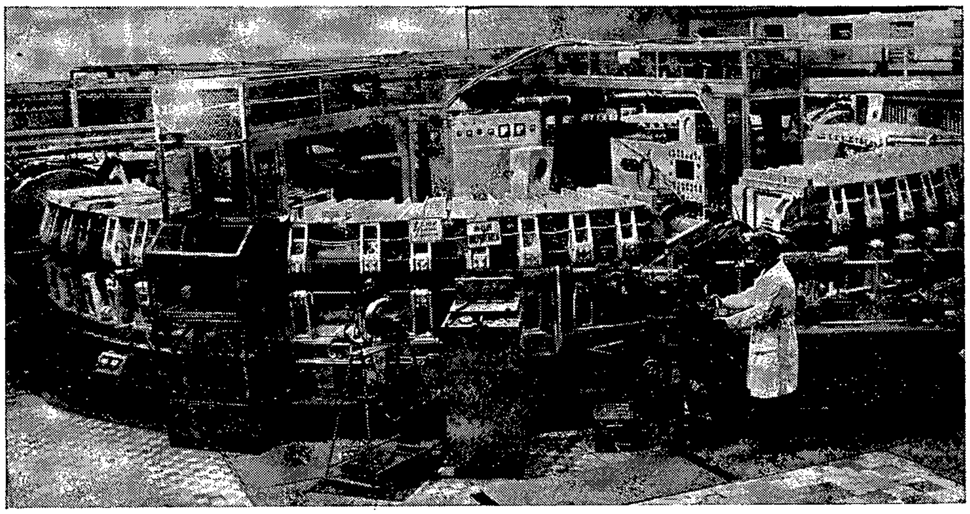

Fig. 1. General view of the Sirius 1.5 GeV electron synchrotron.

frequency was increased from 1 Hz to 4 Hz. At the present time, work is underway on the creation of a flat portion of the magnetic field and on the extraction of electrons from the synchrotron.

One of the first experiments performed on the Sirius was an investigation of the effect of quantum fluctuations on the motion of particles in cyclic accelerators. It was found that quantum fluctuations in synchrotron radiation cause the excitation of synchrotron and radial betatron oscillations. The "instantaneous" electron distribution was measured in both transverse and longitudinal directions, and an estimate was made of the limiting energy beyond which quantum excitation requires an appreciable increase in the width of the vacuum chamber.

Waveguide Synchrotrons. The purpose of the work with waveguide synchrotrons was to verify the possibility of using bent, closed waveguides, either fitted with an iris or smooth, placed in the pole gap of cyclic accelerators, as the accelerating system of a synchrotron. The electrodynamics of closed-loop waveguide systems has been developed fairly thoroughly at the institute. Calculations revealed that waveguide systems are much more economical, in terms of the RF power required, than separate or coupled resonator cavities, and that they make it possible to achieve large energy increments in a single revolution, while also compensating more simply for the effect of quantum fluctuations on particle motion.

A 10 MeV waveguide synchrotron having, as its accelerating system, a bent, closed waveguide with an iris was fabricated and put into service in 1963, in order to test and confirm the fundamental theoretical points, whilst in 1965 a 10 MeV waveguide synchrotron having, as its accelerating system, a smooth, bent, closed waveguide was built and put into service.

Work has now begun on the construction of a 30 MeV waveguide synchrotron. In recent years, in conjunction with the Radio-Engineering Institute of the Academy of Sciences of the USSR and the Erevan Physics Institute, work has been undertaken to confirm the prospects for the application of waveguide accelerating sections in the acceleration of protons and electrons to high energies.

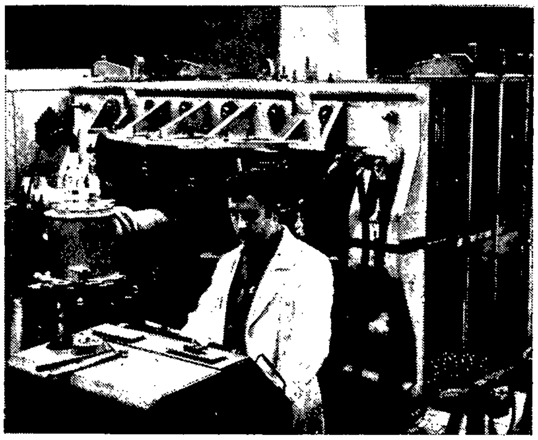

Fig. 2. View of the 25 MeV high-precision betatron.

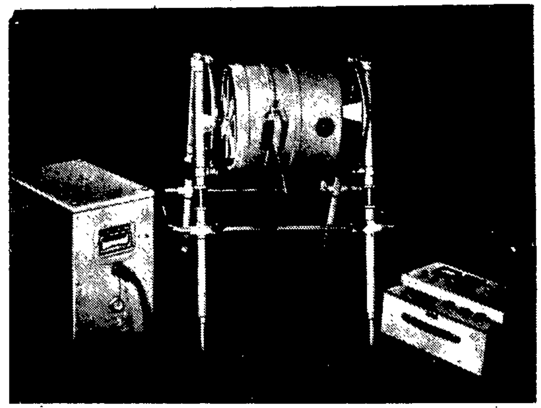

Fig. 3. Miniature portable PMB-6 betatron.

Microtrons. The problem of the construction of microtrons arose in 1954 in connection with the choice of an injector for the Sirius electron synchrotron. As a result of research and development work done at the institute, microtrons with energies in the range 5-10 MeV and pulse currents on the last orbit of up to 100 mA were built. The beam extraction ratio is 0.9 to 1.0; nonmonoenergeticity is not greater than 0.6%. A 10-20 MeV microtron with a microwave oscillator rated at 10 MW output is being prepared.

Induction Accelerators. In the investigation of the physical processes in the acceleration of electrons in betatrons, careful attention is being given to the construction of a theory to explain the mechanism of injection. The capture of electrons in acceleration is considered as a process of collective interaction. It has been shown that the principal factor affecting the capture process is the resonance attenuation of oscillations on inhomogeneities in the azimuthal distribution of the space-charge concentration generated by the beam of electrons emerging from the injector. A functional relationship between the intensity of the betatron radiation and the injection current has been confirmed experimentally.

Close attention is also being given to the development of betatrons with high radiation intensity and of miniature betatrons. In recent years, research and development work has been done on high-precision betatrons with accelerated-electron energies from 10 to 25 MeV. Technical data on some high-precision betatrons at TPI are listed in Table 1.

High-intensity beams of bremsstrahlung from high-precision betatrons used in nondestructive testing applications have enabled investigators to inspect layers of steel 510 mm thick in 40 min, at 25 MeV accelerated-electron energy. The excellent quality of the resulting x-ray plates is accounted for by the small size of the focal spot (2 to 5 mm^2).

For the stereoscopic inspection of parts and materials, a twin-chamber stereobetatron generating two intersecting beams of bremsstrahlung has been developed. The large dose produced by the stereobetatron (much larger than that produced by a twin-beam single-chamber betatron) at a high bremsstrahlung intensity in each beam greatly simplifies the irradiation technology and raises the productivity of inspection of large-size parts and materials. A high-precision 25 MeV betatron is shown in Fig. 2. The scientific and engineering principles underlying the design and fabrication of portable 3-6 MeV miniature betatrons capable of competing successfully with radioactive sources of radiation have also been established. These portable miniature betatrons are designed for the nondestructive testing of metallic and nonmetallic industrial parts and weldings by transmission radiography, in the laboratory, in the production department, and at the construction site. In addition, this type of accelerator can be used in training laboratories and in scientific-research laboratories for work involving pulsed x-radiation. In Fig. 3 a PMB-6 portable miniature betatron is shown. This machine comes in three modules: a radiator, a power-supply package, and a control panel. When in operation, the three modules are interconnected by flexible cabling. The dimensions and weights of the modules are such as to allow them to be carried by hand to the object to be inspected and facilitate inspection in areas that are not readily accessible in repair and maintenance operations. Below, we cite the basic characteristics of the PMB-6 betatron:

Declassified and Approved For Release 2013/01/22 : CIA-RDP10-02196R000400020002-7

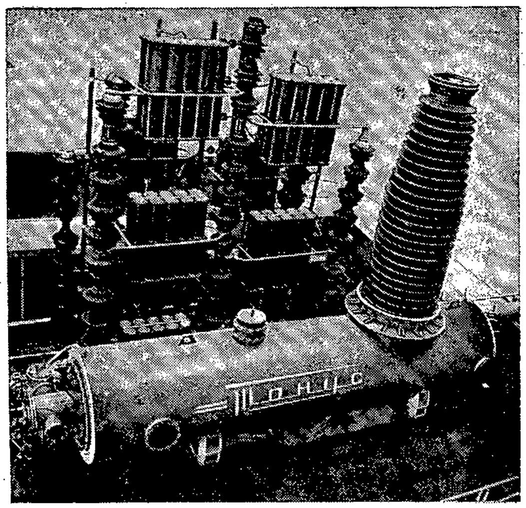

Fig. 4. General view of the high-power 2 MeV nanosecond electron accelerator.

Maximum energy of accelerated electrons, MeV. .	6
Permitted energy adjustments (in 1 MeV steps), MeV	2-6
Guaranteed exposure dose rate at 1 m, mR/sec . .	5
Power drain from a commercial 50 Hz, 220 V, single-phase line, kW	1.8
Length of continuous operation, h.	6
Weight of modules, kg:	
radiator.	100
control panel	15
power-supply package	65
Dimensions of facility, mm:	
radiator.	520 × 400 × 400
control panel	315 × 420 × 230
power-supply package	510 × 514 × 400

The PMB-6 betatron may be used to inspect steel parts up to 250 mm in thickness, or concrete structures up to 800 mm thick. Power adjustments facilitate a high degree (1-2%) of flaw discernability over a broad range of thicknesses inspected.

Small-batch production of PMB-6 betatrons has been organized at a factory in Tomsk for deliveries of these machines to scientific-research institutes and industrial enterprises in the Soviet Union, and for export to France, Finland, Czechoslovakia, Hungary, and elsewhere.

At the present time, an intensive search for new and improved models of miniature betatrons is in progress. One possibility that is being studied is a betatron with three-dimensional variation of the control magnetic field, which permits a reduction in the weight of the electromagnet, improvement in the heat conditions, and increase in the number of electrons accelerated. Research is continuing into the design of miniature converters based on thyristors: these would allow a considerable increase in the repetition frequency of the acceleration cycle, while at the same time increasing the mean intensity of the betatron radiation.

High-voltage miniature injection systems are being developed, and research on enhancing the reliability and stability of operation of the betatron is in progress.

Research and Development Work on High-Power Nanosecond Accelerators. The development of the technology of generating high voltages and of shaping high-voltage nanosecond pulses (300 to 500 kV; $3 \cdot 10^{-9}$ to 10^{-8} sec) and the development of vacuum electronics have provided the prerequisites for the construction of low-energy high-current nanosecond accelerators. The purpose of such accelerators is to investigate the properties of powerful electron beams. An experimental accelerator built in 1969 has the

TABLE 2. Control Range for the Energy of the Accelerated Particles, MeV

State of cyclotron	Acceleration at fundamental frequency				Accln. at 3rd harmonic		
	p	d	He^4	He^3	O^{16}	O^{14}	O^{12}
Prior to redesign of cyclotron	6,7	13,4	27	—	—	—	—
After redesign of cyclotron	4,5·10	9—14,5	18—29	14—30	21	18	15

following parameters: U = 400 kV, I = 5 kA; $\tau = 3 \cdot 10^{-8}$ sec. This machine uses a plasma cathode based on the generation of plasma in the arcing of a dielectric in vacuo.

A 2 MeV accelerator with current 30-60 kA and pulse duration 50 nsec has now been built. This accelerator consists of a pulsed voltage generator based on an Arkad'ev–Marks circuit, a double pulse-shaping circuit, a discharge gap switch, and an electron gun. The voltage rating of the pulsed voltage generator with charging at both ends is 2.2 MV, the shock capacitance 11,000 pF; the pulsed voltage generator uses IM 110/0.022 capacitors and a modular assembly design in which ONSh-35-2000-type insulators are employed.

The diameter of the outer cylinder of the double pulse shaper is 1200 mm, the length 5 m, the characteristic impedance 25Ω. Transformer oil is used as an insulator in the double-pulse-shaper module, and the porcelain cover of a PTN-220T current transformer with test voltage 1650 kV also serves as an insulator.

The cathode in the electron gun is a multiple-tip field-emission cathode. An extensive program of research work on interactions between strong electron beams and plasma, the generation of microwave oscillations, and the investigation of collective modes of acceleration of charged particles has been planned for the accelerator. A general view of the accelerator is shown in Fig. 4.

Cyclotron. In 1959, a cyclotron of pole gap 120 cm was put into service at the institute. Considerable work has been undertaken to improve many of the accelerator modules at this cyclotron facility while it has been in service, with the object of improving the reliability and improving the parameters of the beam of accelerated particles. As of 1971, deuterons have been accelerated to 13.6 MeV in this cyclotron, α-particles have been accelerated to 27 MeV, and protons to 6.5 MeV. The parameters of the accelerated beam of deuterons are as follows: maximum current 120 μA, mean current 50 μA, angular dispersion 1°. The cyclotron is used in experimental work for more than 6000 h each year.

Work on converting cyclotrons to He^3 acceleration and to acceleration modes with energy adjustment was carried out in 1971 in response to the needs of experimental physicists. This necessitated a huge volume of work in replacing some of the parts of the resonant system and of the RF generator, retuning the frequency of the RF system from 9 MHz to 14 MHz, correcting the magnetic field in the 9-15 kOe range, developing a stabilization system for the electromagnet supply currents, and designing a gas-recycling system.

Table 2 lists data on the range over which the energy of particles accelerated can be controlled.

The 2.5 MeV Electrostatic Generator. The 2.5 MeV electrostatic generator is capable of accelerating either electrons or protons. A beam of accelerated electrons can be extracted from irradiating objects of any kind.

The accelerator control system allows continuous monitoring of the energy of accelerated particles and the smooth variation of this energy from 0.8 MeV to 2.5 MeV, the measurement and variation of the currents of extracted electrons, and the determination of the nonuniformity of the current with respect to area. A 5 mm diameter beam of particles at a current of 250 μA can be extracted from the machine. Preparations are now underway for converting the accelerator to He^3 acceleration.

Nuclear Reactor. The IRT thermal-neutron research reactor built at the institute supports a broad range of research projects dealing with solid-state radiation physics, radiobiology, activation analysis, and radiation chemistry carried out by different institutions in Tomsk. At the present time the reactor is operating at a level of 2.5 MW. It has 10 horizontal channels and 18 vertical channels, so it is possible simultaneously for work to be carried out independently by different groups of experimental physicists at each of the channels. Thermal neutrons in the nine horizontal channels are cut off by means of cadmium filters. A three-crystal TK SN-400 neutron spectrometer was installed at one of the horizontal 100 mm diameter channels. The other horizontal channel, of the same diameter, is equipped with a pneumatic shuttle of diameter 16 mm and 40 mm. Reloading devices making it possible to load test specimens in the channel while the reactor is on full power were installed at six horizontal channels 100 mm in diameter and at one such channel 150 mm in diameter.

The reactor features a radiation indium–gallium–tin loop constituting a source of "pure" γ-radiation. Any desired form can be imparted to the loop irradiator according to the requirements of the experiment. The peak activity attained in the loop amounts to 75 kg-equivalents Ra/MW (reactor power output level).

The dose rate is determined by the size and shape of the irradiator. Consequently, in a cylindrical hollow irradiator standing 400 mm, with an inner diameter of 80 mm and an outer diameter of 120 mm, the dose rate at the geometric center is 1000 R/sec · MW, and the nonuniformity of the dose field over the internal channel of the irradiator does not exceed 15-20% on the average, while it amounts to 5-7% in the zone adjacent to the geometric center extending to 10 cm on both sides of the axis.

Large objects (up to 1 m across) can be irradiated either in a special irradiator or in the external field. The size of the working chamber where the irradiator is installed makes it possible to carry out the irradiation of such objects. The energy of the γ-photons runs from 0.4 to 2.2 MeV. The effective energy is not greater than 1.3 to 1.5 MeV.

A hot chamber for work at activity levels up to 30 kg-equivalents radium is included in the reactor.

Declassified and Approved For Release 2013/01/22 : CIA-RDP10-02196R000400020002-7

N. G. Gusev,* L. R. Kimel',
V. P. Mashkovich, B. G. Pologikh,
and A. P. Suvorov

PROTECTION AGAINST IONIZING RADIATIONS. VOL. I. PHYSICAL PRINCIPLES OF THE PROTECTION AGAINST IONIZING RADIATIONS†

Reviewed by S. G. Tsypin

This manual was written by qualified specialists in the field who have taken an active part in developing radiation-protection measures in our country. They are well acquainted with the theoretical and practical achievements and problems in this field of applied nuclear physics, and have extensive experience in publishing scientific literature. All this contributes to the high qualities of this manual, which is the first of its kind in the Soviet or foreign literature. The second volume of the manual, Radiation Protection of Nuclear-Engineering Facilities, is scheduled for publication by Atomizdat in 1973.

The publication of this manual must be considered timely, since the broad development of work on nuclear power, on nuclear physics, and on the utilization of nuclear processes and radiation processes in science and in industry, as envisaged in the resolutions of the Twenty-Fourth Congress of the Communist Party of the Soviet Union, is closely related to the problem of radiation protection.

In this book, which consists of eight chapters, all the fundamental problems of the protection against ionizing radiations are considered.

The first (and introductory) chapter deals with radioactivity units and units of ionizing radiations, as well as basic concepts and terminology. It will be especially useful to those readers studying protection against radiation who have no prior acquaintance with the contents of a course on radiation dosimetry. The second chapter validates and calculates the limiting tolerance levels for ionizing radiations. Chapters three to five cover the theoretical principles of radiation protection. These chapters discuss the basic elementary events in the interaction between ionizing radiations and matter, the radiation-transport equation, numerical methods, analytical methods, and semiempirical methods for radiation calculations. The sixth chapter analyzes the radiation field of point sources and extended sources on the other side of shielding (no shielding is treated as a special case), taking into account the geometry of the problem and self-absorption. Protection against γ-photons and against neutrons is treated in the last two chapters, where a discussion of the physical laws of the propagation of radiation through a medium shares space with a discussion of practical methods for calculating shielding and means of protection for the most important cases. Here the albedo of radiations is considered together with the shape of the spectral and angular distributions of radiation on the far side of shielding.

We see then that the text of the manual discusses all of the principal divisions of the physical principles of radiation protection knowledge of which is necessary for the solution of practical problems.

*Editor.
† Atomizdat, Moscow (1969).

Translated from Atomnaya Énergiya, Vol. 35, No. 2, pp. 151-152, August, 1973.

In preparing the second edition of the book, the authors should take note of the following points:

1. The theoretical fundamentals of radiation protection should be presented in a more readily accessible form, considering that the book serves as a training text; the Monte Carlo method which is used so extensively should be discussed in greater detail.

2. The second chapter should take into account the NRB-69 new norms and standards of radiation safety.

3. The section on radiation albedo should be set aside as a separate chapter.

4. The book should be expanded to include sections on protection against α- and β-radiations, and on the radiation field at the earth–air interface.

5. The section dealing with buildup factors in heterogeneous media should be revised in the light of new data in the literature.

The book is an excellent training text for students in engineering and physics departments and applied physics departments of higher educational institutions. Experience in working with the text has shown that it is also useful to research and staff scientists, to graduate students, engineers, designers, and other workers concerned with protection and shielding when various sources of ionizing radiations are in use.

I. P. Stakhanov, V. P. Pashchenko, A. S. Stepanov, and Yu. K. Gus'kov

PHYSICAL PRINCIPLES OF THERMIONIC ENERGY CONVERSION*

Reviewed by B. A. Ushakov

The demand for new efficient sources of electric power has stimulated the development of promising techniques for the direct conversion of thermal energy to electrical energy, including the thermionic conversion method. This necessitated an exhaustive study of the physical processes at work in a thermionic converter. Numerous papers that have appeared in recent years both in the Soviet Union and elsewhere attest to the great progress achieved in this field. It is now necessary to systematize and analyze the results obtained and to formulate the problems that require further study.

The authors of this monograph have successfully undertaken such a task.

The monograph consists of eight chapters, in which the processes exerting decisive influences on the performance of thermionic converters are discussed in turn.

The first chapter deals with electrode phenomena. The structure of the electrode sheath, the virtual cathode, the Schottky effect, and special features of the charged-particle distribution function are discussed in detail, leading to the formulation of the boundary conditions necessary for the solution of the transport equation – one of the most complex and important problems in the theory of a confined nonequilibrium low-temperature plasma.

The discussion of that problem is the principal part of the following chapters. The solution of the problem makes it possible to ascertain the electrical characteristics of a thermionic converter which are needed in practice.

The authors deduce transport equations for a three-component plasma in the presence of a magnetic field, as well as expressions for the kinetic coefficients. Detailed analytical calculations of the electrical

* Atomizdat, Moscow (1973).

characteristics in the various possible operating modes of the thermionic converter permit the basic features of those operating modes to be determined. The bulk ionization mode is that of greatest practical interest.

On the basis of a solution of the kinetic equation for fast free electrons and of a system of equations for the occupation numbers of excited levels of the cesium atom, a discussion of nonequilibrium bulk ionization is undertaken.

The influence of the Schottky effect and of the virtual cathode on the voltage–current characteristics of the converter in the bulk ionization mode is analyzed, together with the conditions for the ignition and quenching of a low-voltage discharge.

The experimental characteristics of thermionic converters are dealt with in a separate chapter which discusses in detail the experimental procedure, typical measuring arrangements and laboratory facilities, and also experimental results for the various operating modes of the converters.